

©[2018]

Monika Kazancioglu

ALL RIGHTS RESERVED

INORGANIC POLYMERS MADE DIRECTLY FROM MINERALS

by

MONIKA KAZANCIOGLU

A dissertation submitted to the

School of Graduate Studies

Rutgers, The State University of New Jersey

In partial fulfillment of the requirements

For the degree of

Doctor of Philosophy

Graduate Program in Chemical and Biochemical Engineering

Written under the direction of

Masanori Hara

And approved by

New Brunswick, New Jersey

October, 2018

ABSTRACT OF THE DISSERTATION

Inorganic Polymers Made Directly from Minerals

By MONIKA KAZANCIOGLU

Dissertation Director:

Masanori Hara

This work seeks to develop the scientific knowledge by which conventional organic polymers can be replaced with their inorganic counterparts. It is aimed to synthesize silicate-based inorganic polymers directly from minerals, such as silica, which are readily available in nature (e.g., sands and rocks). Inorganic polymers decrease the dependence on crude oil and promise chemically more stable compounds than organic polymers. Having silicate as the backbone, the need for recycling is eliminated and the new materials are likely to be non-flammable and non-toxic. Specifically, we are developing a new class of polymers in which the backbone is comprised of ionic (primary) and secondary bonds. The high processing temperature of silica is first decreased via addition of metal ions (from a modifier, such as strontium oxide, rubidium oxide, calcium oxide, or potassium oxide) that serve to reduce the interchain bond strength, hence lowering the glass transition temperature (T_g); and providing additional free volume for the subsequent insertion of new moieties (i.e., ionic liquid). During this process, highly crosslinked structure can be converted to one-dimensional and two-dimensional structures commonly seen for organic polymers. Subsequently, addition of ionic liquid allows “plasticization” of silicate glass, and results in further reduction in bond strength and T_g ; materials behave as polymers. Results show that T_g of modified silicate glass can be decreased from 410 °C to 155 °C

by addition of ionic liquid; i.e., by plasticization with ionic liquid. The properties and reaction mechanism of synthesized inorganic polymers are investigated by various characterization methods, such as DSC, FTIR, XRD, XPS, SEM, and TEM, in addition to mechanical testing.

Acknowledgements

I would like to express my very great appreciation to my advisor, Professor Masanori Hara, for his continuous support, motivation, and immense knowledge. Our discussions during the meetings helped me to reach this point. I would also like to express my sincere gratitude to Professor Richard Lehman for always showing me another point of view and making me think as a Material Scientist. This dissertation would not be possible without their help and guidance. I am very grateful to my committee members, Dr. Nina Shapley and Dr. Meenakshi Dutt, for their time and effort.

I would like to thank B. Krishnamurthi and C. Tabezki for teaching me the lab experiments in the first place. S. Saran, Z. Lin, S. Snyder, S. Mueller, E. Mikhaylova, N. Haruna, M. Hernandez, K. Chi, M. Albarracin, D. Ramphal, and J. Perona are appreciated for their contributions to the work.

Additionally, I would like to thank Dr. George Tsilomelekis for his help on FTIR measurements; Professor Frederic Cosandey and Dr. Pinaki Mukherjee for teaching me TEM; Professor Eric Garfunkel and Aleksandra Biedron for XPS measurements; Dr. Robert Horvarth for teaching me DSC and the help for glass making; Arya Tewatia for taking SEM pictures; and Dr. Thomas Emge for XRD measurements.

I would like to thank my family, especially my uncle, Nebil Kazancioglu; and dedicate this dissertation to my parents Sonya and Nedim Kazancioglu, and my sister and brother, Selena and Andy. Thank you for the love, support, and constant encouragement over the years. Finally, to Gur Gursoy for always being there for me.

Table of Contents

ABSTRACT OF THE DISSERTATION.....	ii
Acknowledgements	iv
Table of Contents.....	v
List of Tables	vii
List of Figures.....	ix
Chapter 1	1
INTRODUCTION	1
Chapter 2	5
RESEARCH METHODOLOGY	5
2.1. Synthesis of Inorganic Polymers	5
2.2. Characterization of Inorganic Polymers	6
Chapter 3	8
EXPERIMENTAL PROCEDURE	8
3.1. Materials	8
3.2. Sample Preparation	11
3.3. Monovalent System	12
3.4. Divalent/Monovalent System: CaKSiO_2	17
3.5. Divalent/Monovalent System: SrRbSiO_2	23
3.6. Instrumentation and Characterization	28
Chapter 4	35

RESULTS: MONOVALENT SYSTEM	35
4.1. Effect of Ionic Liquid Addition on Glass Transition Temperature, T_g	35
4.2. Mechanical Properties of NaSiO ₂ -based Inorganic Polymers	39
Chapter 5	42
RESULTS: DIVALENT/MONOVALENT SYSTEM (CaKSiO₂)	42
5.1. Effect of Ionic Liquid Addition on Glass Transition Temperature, T_g	42
5.2. Investigation of Reaction Mechanism via FTIR	52
5.3. Mechanical Properties of CaKSiO ₂ -based Inorganic Polymers.....	65
5.4. TEM / SEM.....	69
Chapter 6	72
RESULTS: DIVALENT/MONOVALENT SYSTEM (SrRbSiO₂).....	72
6.1. Effect of Ionic Liquid Addition on Glass Transition Temperature, T_g	72
6.2. Effect of Water on Inorganic Polymer Properties	80
6.3. Investigation of Reaction Mechanism via XPS	84
6.4. Inorganic Polymers Aged in Desiccator	87
CONCLUSION.....	88
FUTURE WORK.....	90
Appendix A	92
Appendix B.....	96
REFERENCES.....	99

List of Tables

Table 3.1 List of ionic liquids	9
Table 3.2 Ionic liquid structures used in this work	10
Table 3.3 Specifications for synthesized monovalent ion silicate glasses along with their names.....	13
Table 3.4 Inorganic polymer synthesis conditions for monovalent system used in this work.....	16
Table 3.5 Specifications for synthesized divalent/monovalent silicate glasses (CaKSiO ₂) along with their names.....	19
Table 3.6 T _g values of potassium silicate glasses with different concentrations of CaO.	20
Table 3.7 Inorganic polymer synthesis conditions for divalent/monovalent system (CaKSiO ₂) used in this work.....	22
Table 3.8 Specifications for synthesized divalent/monovalent silicate glasses (SrRbSiO ₂) along with their names.....	24
Table 3.9 T _g values of rubidium silicate glass with different concentrations of SrO. 24	
Table 3.10 Inorganic polymer synthesis conditions for divalent/monovalent system (SrRbSiO ₂) used in this work.....	27

Table 4.1 T_g of inorganic polymers made of rubidium silicate (0.78) and different concentrations of EMIM ES.	36
Table 4.2 Compressive mechanical properties of NaSiO ₂ -based inorganic polymers.	40
Table 5.1 T_g of inorganic polymers made of KSiO ₂ or 10 % CaKSiO ₂ with different concentrations of EMIM TF.	45
Table 5.2 Absorption bands and peak assignments of NaSiO ₂ ([Na ₂ O]/[SiO ₂]= 0.8) and 10 % CaKSiO ₂ glasses.....	53
Table 5.3 Absorption bands and peak assignments of inorganic polymers (e.g., 10 % CaKSiO ₂ +EMIM TF).	54
Table 5.4 Compressive mechanical properties of SiO ₂ -based inorganic polymers ...	67
Table 6.1 T_g of inorganic polymers made of 10 % SrRbSiO ₂ and 1/12 EMIM TF, compression molded under 1500 psi and at different temperatures.....	79
Table 6.2 T_g of samples made of 10 % SrRbSiO ₂ and different concentrations of water.	82

List of Figures

Figure 1.1 Plasticization of an organic polymer.	1
Figure 2.1 An overview for the synthesis of inorganic polymers starting from silica. 6	
Figure 3.1 Alkali modified glass preparation.....	11
Figure 3.2 A flow diagram for sample preparation (left) and a set-up for compression molding (right).	11
Figure 3.3 Glass formation mechanism for silicate glasses of monovalent-ion system. [29].	12
Figure 3.4 DSC heating curves for silicate glasses modified with Rb ⁺ (black) and K ⁺ (red) ions. [R ₂ O]/[SiO ₂]=0.78. T _g for RbSiO ₂ and KSiO ₂ glasses are 307.1 °C and 403.6 °C, respectively.	14
Figure 3.5 Effect of alkali ion ratio on T _g : DSC thermograms of KSiO ₂ glasses with different alkali ion ratios. The values in parenthesis represent alkali ion ratios.....	15
Figure 3.6 A picture of an inorganic polymer synthesized for monovalent system. The diameter is 10 mm and height is 20 mm.....	16
Figure 3.7 Suggested structures for monovalent-ion inorganic polymers. KSiO ₂ (1.0) glass with EMIM TF (left) and RbSiO ₂ (0.78) glass with EMIM ES (right).	17
Figure 3.8 Glass formation mechanism for silicate glasses of divalent/monovalent system.	18

Figure 3.9 Effect of divalent ion concentration: DSC second heating curves for 0 %, 5 %, 10 %, and 15 % CaKSiO ₂ (1.0) glasses. Note that 0 % CaKSiO ₂ (1.0) is equivalent to KSiO ₂ (1.0).	20
Figure 3.10 Effect of divalent ion (Ca ²⁺) concentration on T _g	21
Figure 3.11 A picture of an inorganic polymer synthesized for divalent/monovalent system.	22
Figure 3.12 Representation of proposed inorganic polymer prepared with CaKSiO ₂ and EMIM TF.....	23
Figure 3.13 Effect of divalent ion (Sr ²⁺) concentration on T _g	25
Figure 3.14 Effect of divalent ion concentration: DSC second heating curves for 0 %, 10 %, 18 %, 30 %, and 50 % SrRbSiO ₂ (0.78) glasses. Note that 0 % SrRbSiO ₂ (0.78) is equivalent to RbSiO ₂ (0.78).	26
Figure 3.15 Stoichiometric representation of proposed inorganic polymer prepared with 30 % SrRbSiO ₂ and 1/8 EMIM TF.....	28
Figure 3.16 TA Instruments DSC Q20 (left); possible phase transitions in DSC analysis (right) [38].....	29
Figure 3.17 Nicolet™ iS50 FTIR Spectrometer (Thermo Fisher Scientific).	30
Figure 3.18 Compression test of a cylindrical sample (left), a typical stress strain curve for brittle materials (right).	34
Figure 4.1 Effect of the amount of ionic liquid: DSC second heating curves for inorganic polymers made of RbSiO ₂ glass (0.78) and EMIM ES. The amounts of EMIM	

ES are 1/4 (black curve), 1/8 (red curve), and 1/16 (blue curve) as compared with pure RbSiO ₂ (0.78) (green curve) used as a reference.	35
Figure 4.2 Effect of the amount of ionic liquid on T _g for RbSiO ₂ (0.78) glass.	36
Figure 4.3 Effect of processing conditions on T _g : DSC thermograms of inorganic polymers made of KSiO ₂ and 1/6 EMIM TF (compressed to 1500 psi at room temperature) (black) and KSiO ₂ and 1/8 EMIM TF (gradually compressed to 1500 psi as the sample is heated up to 180 °C) (red).	37
Figure 4.4 Effect of processing conditions on T _g : one-time compression to 1500 psi at room temperature decreases the plasticization power of ionic liquid (red). Gradual increase in compression to 1500 psi as the sample is heated up increases the plasticization of silicate glass by ionic liquid (black).	38
Figure 4.5 Compressive stress-strain curves for samples made of NaSiO ₂ and 1/8 EMIM TF (compression molded at 200 °C and 1500 psi).	40
Figure 5.1 Effect of ionic liquid addition on T _g : DSC thermograms of 10 % CaKSiO ₂ glass (red) and inorganic polymer made of 10 % CaKSiO ₂ and 1/8 EMIM TF (black).	43
Figure 5.2 Effect of silicate structure on T _g : DSC thermograms of inorganic polymers made of 1/8 mole ratio of EMIM TF and different silicate glasses; KSiO ₂ (black) and 10 % CaKSiO ₂ (red).	44
Figure 5.3 Effect of the amount of ionic liquid on T _g : DSC thermograms of inorganic polymers made of 10 % CaKSiO ₂ and 1/4 (black), 1/6 (red), and 1/8 (blue) mole ratios of EMIM TF.....	45

Figure 5.4 Effect of silicate structure and amount of ionic liquid on T_g : inorganic polymers made of 10 % CaKSiO ₂ (red) and KSiO ₂ (black).....	46
Figure 5.5 Effect of silicate structure on T_g : change in T_g as a function of ionic liquid amount for inorganic polymers made of EMIM TF and silicate glasses of RbSiO ₂ (0.78) (blue), KSiO ₂ (1.0) (black), and 10 % CaKSiO ₂ (1.0) (red).....	47
Figure 5.6 Effect of ionic liquid cation on T_g : DSC thermograms of inorganic polymers made of 10 % CaKSiO ₂ and 1/8 mole ratio of BMIM TF (black) and EMIM TF (red).	49
Figure 5.7 Effect of ionic liquid anion on T_g : DSC thermograms of inorganic polymers made of 10 % CaKSiO ₂ and 1/8 mole ratio of BMIM PF ₆ (black) and BMIM TF (red).	50
Figure 5.8 Effect of processing conditions on T_g : DSC thermograms of inorganic polymers made of 10 % CaKSiO ₂ and 1/6 mole ratio of EMIM TF; compressed to 1500 psi at room temperature (black) and gradually compressed to 1500 psi as the sample is heated to 180 °C (red).....	51
Figure 5.9 Effect of processing conditions on T_g : one-time compression to 1500 psi at room temperature decreases the plasticization power of ionic liquid (red). Gradual compression to 1500 psi as the sample is heated increases the plasticization of silicate glass with ionic liquid (black).....	52
Figure 5.10 Room temperature FTIR spectra of 10 % CaKSiO ₂ glass (red) and inorganic polymers made of 10 % CaKSiO ₂ and EMIM TF with mole ratios of 1/8 (blue) and 1/6 (green).....	55

Figure 5.11 A simplified illustration of the reaction mechanism of EMIM TF with KSiO ₂ (left) and 10 % CaKSiO ₂ (right) glasses.....	56
Figure 5.12 Room temperature FTIR spectra of inorganic polymers made of 10 % CaKSiO ₂ and 1/8 mole ratios of different ionic liquids: EMIM TF (blue), BMIM TF (red), EMIM PF ₆ (black).	57
Figure 5.13 Effect of ionic liquid amount (left): room temperature FTIR spectra of 10 % CaKSiO ₂ glass (red) and inorganic polymers made of 10 % CaKSiO ₂ and EMIM TF with mole ratios of 1/8 (blue) and 1/6 (green). Effect of ionic liquid type (right): room temperature FTIR spectra of 10 % CaKSiO ₂ glass (black) and inorganic polymer made of 10 % CaKSiO ₂ and 1/8 mole ratio of EMIM PF ₆ (red).....	58
Figure 5.14 FTIR spectra of 10 % CaKSiO ₂ glass at room temperature (red) and 100 °C (black) compared with that of inorganic polymer made of 10 % CaKSiO ₂ and 1/8 mole ratio of EMIM TF at room temperature (blue) and 100 °C (green).	59
Figure 5.15 FTIR spectra of inorganic polymer made of KSiO ₂ and 1/8 mole ratio of EMIM TF at room temperature (red), 50 °C (black), and 100 °C (blue).	61
Figure 5.16 FTIR spectra of inorganic polymer made of KSiO ₂ and 1/8 mole ratio of EMIM TF at room temperature (red), 50 °C (black), and 100 °C (blue).	63
Figure 5.17 FTIR spectra of inorganic polymer made of 10 % CaKSiO ₂ and 1/8 mole ratio of EMIM PF ₆ at room temperature (black), 50 °C (blue), and 100 °C (red).....	64
Figure 5.18 FTIR spectra of inorganic polymers made of 10 % CaKSiO ₂ and 1/8 mole ratios of EMIM TF (black) and EMIM PF ₆ (red) at 100 °C.....	65

Figure 5.19 Compressive stress-strain curves for samples made of 5 % CaKSiO_2 and 1/8 mole ratio of EMIM TF (compression molded at 180 °C and 1500 psi).	66
Figure 5.20 Compressive stress-strain curves for samples made of 1/8 mole ratio of EMIM TF and 5 % CaKSiO_2 (black and red) and NaSiO_2 (green and blue).	66
Figure 5.21 Electron diffraction pattern (left) and TEM picture of inorganic polymer made of 10 % CaKSiO_2 and 1/10 mole ratio of EMIM TF (right).	70
Figure 5.22 TEM pictures of inorganic polymer made of 10 % CaKSiO_2 and 1/10 mole ratio of EMIM TF.....	70
Figure 5.23 SEM (left) and EDS (right) images of the sample prepared with 30 % SrRbSiO_2 and 1/8 mole ratio EMIM TF compression molded at 95 °C and 1000 psi.	71
Figure 6.1 Effect of divalent ion ratio: DSC thermograms of inorganic polymers made of 1/12 mole ratio of EMIM TF and 10 % SrRbSiO_2 (black) and 30 % SrRbSiO_2 (red).	73
Figure 6.2 Effect of the type of ionic liquid: DSC thermograms of inorganic polymers made of 30 % SrRbSiO_2 and 1/12 mole ratio of EMIM TF (red), EMIM ES (blue), and EMIM BF_4 (green).	74
Figure 6.3 DSC second heating curves for samples made of 10 % SrRbSiO_2 glass and 1/12 EMIM TF. Compression molding conditions are 150 °C and 1500 psi (black curve) and 1000 psi (red curve).	76
Figure 6.4 First cooling and second heating DSC curves for samples made of 10 % SrRbSiO_2 glass and 1/12 EMIM TF. Compression molding temperature is kept at 150	

°C but pressure is changed. The first sample (black) is prepared at zero pressure. The second sample (red) is compression molded at a pressure of 1000 psi..... 77

Figure 6.5 XRD data for the sample made of 50 % SrRbSiO₂ glass and 1/12 EMIM TF. Literature data for RbTF (red curve) matches the sample data (black curve) very well. 77

Figure 6.6 Effect of heating: DSC second heating curves for inorganic polymers made of 10 % SrRbSiO₂ and 1/12 EMIM TF under 1500 psi. The compression molding temperatures are 300 °C (black), 250 °C (red), 150 °C (blue) and room temperature (green)..... 78

Figure 6.7 Effect of compression molding temperature on T_g for the inorganic polymer made of 10 % SrRbSiO₂ and 1/12 mole ratio of EMIM TF. 79

Figure 6.8 Water absorption of samples made of 18 % and 30 % SrRbSiO₂ + 1/3 mole ratio of EMIM TF..... 80

Figure 6.9 Effect of water concentration on T_g: DSC thermograms of samples made of 10 % SrRbSiO₂ with different mole ratios of water; 1/4 (black), 1/6 (red), 1/12 (blue). Compressed 10 % SrRbSiO₂ is used as a reference (green)..... 81

Figure 6.10 The change in T_g as a function of water concentration..... 83

Figure 6.11 Effect of water and ionic liquid: DSC thermograms of inorganic polymers made of 30 % SrRbSiO₂ and 1/24 EMIM TF together with 1/6 water (black), 1/12 EMIM TF (red). Inorganic polymers are compared to the compressed 30 % SrRbSiO₂ glass as a reference. 83

Figure 6.12 High-resolution XPS spectra at N1s orbital binding energy for: (i) BMIM PF ₆ ; (ii) inorganic polymer made of 30 % SrRbSiO ₂ glass and 1/3 BMIM PF ₆ compression molded at 150 °C and 1000 psi; (iii) 30 % SrRbSiO ₂ glass.	85
Figure 6.13 High-resolution XPS spectra at O1s orbital binding energy for: (i) BMIM PF ₆ ; (ii) inorganic polymer made of 30 % SrRbSiO ₂ glass and 1/3 BMIM PF ₆ , compression molded at 150 °C and 1000 psi; (iii) 30 % SrRbSiO ₂ glass.	86
Figure 6.14 Synthesized inorganic polymers showing characteristics of conventional polymers: bending (left), fibril formation (middle), and flow (right).	87
Figure A.1 Set-ups for ball mixing (left) and melt mixing (right).	92
Figure A.2 Effect of mixing: DSC thermograms of samples made of 5 % CaKSiO ₂ and 1/10 mole ratio of EMIM TF. The samples were prepared by different mixing methods, but not compression molded.	94
Figure A.3 Effect of mixing: DSC thermograms of samples made of 5 % CaKSiO ₂ and 1/10 mole ratio of EMIM TF. The samples, prepared by different mixing methods, were compression molded at 180 °C and 1500 psi.	94
Figure A.4 Pictures of samples prepared by ball mixing (left) and simple mixing (middle). The samples are made of 5 % CaKSiO ₂ and 1/10 mole ratio of EMIM TF. Ball-mixed sample showing thin film formation is given on the right.	95
Figure B.1 Plasticization of NaSiO ₂ with DOP. Pure NaSiO ₂ is shown on the left and the compression molded sample is shown on the right.	96

Figure B.2 DSC thermograms of NaSiO₂ glasses plasticized with 10 wt.% (red) and 22 wt.% (blue) DOP. DSC thermogram of NaSiO₂ glass is given as a reference (black).

..... 97

Figure B.3 DSC thermograms of samples made of 5 % CaKSiO₂ and 5 wt.% (black), 10 wt.% (red), and 20 wt.% (blue) DOP. 98

Chapter 1

INTRODUCTION

Polymers belong to one of the major material groups, in addition to metals and ceramics, and are found in a vast array of commercial and industrial applications. Besides technical limitations, such as their tendency to degrade at moderate temperatures, and even to a significant extent under ambient conditions, these petroleum-based products consume increasing scarce petrochemicals. Starting from this point, this graduate work seeks to develop the scientific knowledge by which conventional organic polymers can be replaced with their inorganic counterparts.

The basic idea behind this work is based on traditional softening method of plastics, i.e. plasticization. Main constituents of organic polymers are plasticizers which enable polymers to gain elasticity, durability and flexibility. A well-known industrial example of plasticized organic polymer is poly(vinyl chloride) (PVC) with dioctylphthalate (DOP). Plasticizers incorporated into the structure of organic polymers break the intermolecular bonds and increase chain mobility. The resulting effect is a decrease in glass transition temperature, T_g .

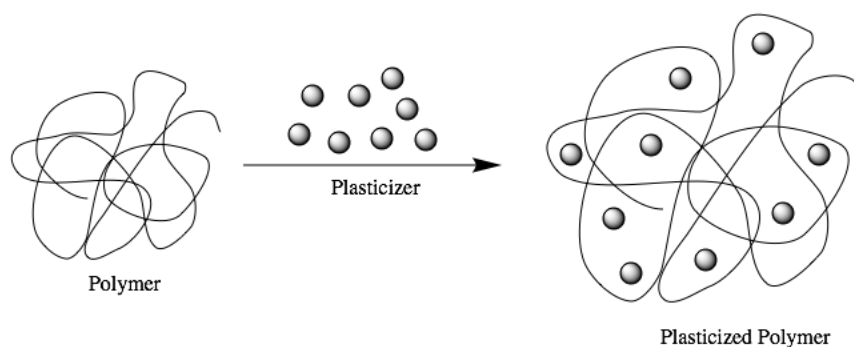


Figure 1.1 Plasticization of an organic polymer.

In this work, ionic liquids are envisaged as a plasticizer for inorganic polymers. It is hypothesized that charged sites of ionic liquids attack ionic aggregates and ionic crosslinking in minerals, lowering the T_g and hence softening the material.

It is proposed to develop and study a new class of low temperature polymers in which the backbone is formed from silicate ($-\text{SiO}_2-$) units and the interchain bonds are comprised of a novel mixture of ionic (primary) and secondary bonds. To successfully synthesize these novel inorganic polymers, high processing temperature of silicate cluster is first decreased via addition of metal ions (from a modifier, such as strontium oxide and rubidium oxide, or calcium oxide and potassium oxide) that serve to reduce the interchain bond strength, hence lowering the glass transition temperature (T_g); and providing additional free volume for the subsequent insertion of new moieties (i.e., ionic liquids). During this process, highly crosslinked structure can be converted to one-dimensional and two-dimensional structures commonly seen for organic polymers. Subsequently, addition of ionic liquid allows further reduction in bond strength and T_g ; materials behave as polymers. The expected result is interchain bonding that retains a weak ionic character, supplemented by various secondary bonds.

The choice of silicate-chain as the backbone relies on its structural similarities with the carbon (C)-chain. They both possess tetrahedral orientation in their most stable form and are capable of forming polymeric chains, where silicate (Si-O) bonds are thermodynamically even more stable than C-C bonds [1, 2]. Another advantage of using silicate is the abundances of silicon (Si) and oxygen (O). They are the most abundant elements on the earth's crust: Si with 28 % and O with 47 %, whereas C is only 0.03 % [3]. Certainly, the high abundances of these elements do not solely justify their use and, in fact, silicon and oxygen are refined for many uses. However, in this work, inorganic polymers are synthesized directly from minerals, such as silica sands or rocks, which

are readily available in nature. This top-down approach is unique and economical than the bottom-up approach by which polymers, such as poly(dimethyl siloxane) (PDMS), are made from basic elements [4]. In addition, PDMS is a hybrid polymer made of organic and inorganic components; thus, inherent weakness of organic polymers cannot be eliminated.

Ionic liquids, the other constituent of the proposed inorganic polymers, are molten salts whose melting temperatures are below 100 °C and are usually in liquid form at room temperature. Room-temperature ionic liquid structures consist of a pair of poorly coordinated organic cation and inorganic or organic anion [5]. The unique properties of ionic liquids stem from the fact that, according to the application purposes, the anion and the cation can be tailored [6]. Additionally, they are non-toxic and have low vapor pressure [7]. In this respect, having silicate and ionic liquid in their structure, inorganic polymers decrease the dependence on crude oil and promise chemically more stable compound for industrial usage. They do not need to be recycled and are likely to be non-flammable and non-toxic.

It should be stressed that the idea and approach used in this work are novel such that there are no references available about silicate/ionic liquid combinations despite some papers available for silica/ionic liquid systems. Silica is very stable due to its highly crosslinked structure (“closed” structure) and thus used as an inert structure for supporting/containing ionic liquids when porous structure is formed [8-10]. On the contrary, silicates are less stable (or more reactive) due to their more “open” structure arising from disruption of many Si-O bonds (and thus formation of ionic groups, such as $\text{O}^- \cdots \text{K}^+$, which can interact with various materials). We take advantage of such “reactivity” of silicates to make new types of inorganic materials that behave as polymers. Recently, patent was issued based on the idea described above [11], but no

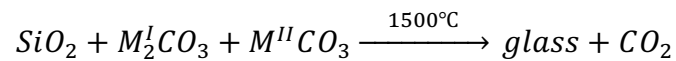
papers are available. Naturally, it takes longer time to find proper processing conditions to make even a prototype of sample for one type of experiment - many trial and errors were needed - since little relevant information is available in literature.

Chapter 2

RESEARCH METHODOLOGY

2.1. Synthesis of Inorganic Polymers

The synthesis of proposed inorganic polymers consists of two steps. First, silicate glasses are prepared with large alkali and alkaline earth ions (M^I and M^{II} , respectively), since incorporation of large metal ions leads to lower processing temperatures: corresponding alkali and alkaline earth carbonates ($M^I_2CO_3$ and $M^{II}CO_3$) are mixed with silica (SiO_2) and melted at above 1500 °C. During the reaction between silica and carbonates, CO_2 leaves the reaction system and remaining oxides (M^I_2O and $M^{II}O$) contribute to the glass structure [12].



In the second step of the synthesis, prepared alkali (and/or alkaline earth) modified silicate glass is ground into a powder form, followed by simple mixing with ionic liquid using a pestle and mortar. The ionic liquid content is determined based on the total number of positive charges in the glass. The concentrations of single-charged alkali ion $[M^{I+}]$ and double-charged alkaline ion $[M^{II2+}]$ are added by considering the number of moles of each ion that comes from their corresponding oxides. Thus, the ionic liquid to metal ion ratio is calculated as follows:

$$\text{Ionic liquid ratio} = \frac{[IL]}{[M^{I+}] + 2[M^{II2+}]} = \frac{[IL]}{2([M^I_2O] + [M^{II}O])} \quad (3)$$

Ionic liquids with different anions and cations were used in this work. These ionic liquids were chosen based on their melting and decomposition temperatures, reactivity, tendency to crystallization, and availability of literature data.

In the final step, the mixture of alkali modified silicate glass and ionic liquid is compression molded either between two foils (such as aluminum, Teflon, or Kapton film) or in a mold (rectangular or cylindrical) at different temperatures and pressures.

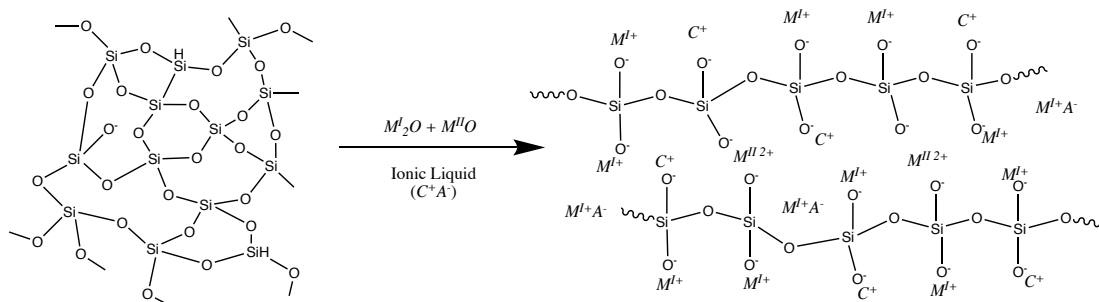


Figure 2.1 An overview for the synthesis of inorganic polymers starting from silica.

Both large alkali ions and ionic liquid weaken the interchain bonds, which provide flexibility to the inorganic polymers and also contribute to reduce covalent silicate clustering. The new materials have lower T_g values and can be compression molded, or even injection molded. During this thermal forming stage, the materials are further processed into their final shapes.

2.2. Characterization of Inorganic Polymers

To understand the reaction mechanism, structure, and properties of the inorganic polymers, various characterization methods are used. Differential Scanning Calorimetry (DSC) measures the changes in heat flow rate as the temperature of the sample is increased or decreased at a given rate [13]. It is used to determine glass

transition temperature (T_g) of the amorphous inorganic polymer, and melting and crystallization temperatures (T_m and T_c) of possible crystals in the polymer structure formed during the synthesis. In case of crystal formation in the sample, crystals are identified by X-Ray Diffraction (XRD), which also provides information on unit cell dimensions [14].

X-Ray Photoelectron Spectroscopy (XPS) and Fourier Transform Infrared Spectroscopy (FTIR) are used to understand the surface and bulk properties, respectively. XPS is used to determine the atomic composition, oxidation state, and sometimes the structure of the examined compounds. The penetration depth of x-ray radiation is about 1 to 100 Å. This means only the surface of the compounds can be examined with this method [15]. FTIR is used to observe the vibrational and rotational spectra of the molecules. For that purpose, a specimen is exposed to infrared radiation, which is then transmitted and absorbed by the sample. The energy coming from the radiation causes vibrational and rotational movements of the molecules. The obtained spectrum is thereof molecular absorption and transmission spectrum of the sample, which is characteristic of molecular groups [16].

Microscopic techniques, such as Transmission Electron Microscopy (TEM) and Scanning Electron Microscopy (SEM), are used to identify the morphology of the inorganic polymer samples. SEM, coupled with Energy Dispersive X-Ray Spectroscopy (EDS), is used to observe the distribution of the elements in the sample. In these techniques, the sample surface is exposed to electron beam that generates signals containing information on topography and composition of the sample [17].

Finally, mechanical properties are determined through a series of experiments that follow ASTM standards (D695-15) [18]. Compressive testing was chosen to eliminate the effects of flaws and thus to focus on characteristics of the polymer [19].

Chapter 3

EXPERIMENTAL PROCEDURE

3.1. Materials

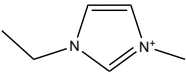
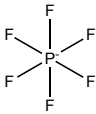
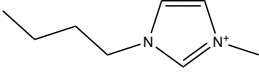
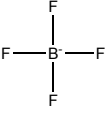
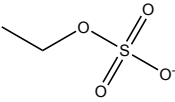
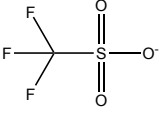
Ionic liquids, such as 1-ethyl-3-methylimidazolium trifluoromethane sulfonate (EMIM TF), 1-ethyl-3-methylimidazolium ethylsulfate (EMIM ES), 1-ethyl-3-methylimidazolium tetrafluoroborate (EMIM BF₄), and 1-butyl-3-methylimidazolium hexafluorophosphate (BMIM PF₆), were purchased from IoLiTec and used as received. The properties and structures of these ionic liquids are shown in Table 3.1 and Table 3.2, respectively.

Sodium metasilicate (Na₂SiO₃; denoted as NaSiO₂ in this thesis for consistency of notations) was purchased from Sigma Aldrich (CAS # 6834-92-0) and used as received. Other alkali modified silicate glasses were prepared in Corning Glass Laboratory in Material Science and Engineering Department at Rutgers University through the reaction of silica (SiO₂) and alkali carbonates. Silica was purchased from Spectrum (CAS # 14808-60-7) and used as received for all silicate glasses. Calcium carbonate (CaCO₃) and potassium carbonate (K₂CO₃) were purchased from Alfa Aesar (CAS # 471-34-1) and Fisher Chemical (CAS # 6381-79-9), respectively, for making CaKSiO₂ glasses. Strontium carbonate (SrCO₃; CAS# 1633-05-2) and rubidium carbonate (Rb₂CO₃; CAS# 584-09-8) were obtained from Sigma Aldrich for making SrRbSiO₂ glasses.

Table 3.1 List of ionic liquids

CAS #	Abbreviation	Full name	Formula	Molecular Weight (g/mol)	Melting Point (°C)	Decomposition Temperature (°C)
145022-44-2	EMIM TF	1-Ethyl-3-methylimidazolium triflate	$C_7H_{11}F_3N_2O_3S$	260.24	-9 [20]	440 [20]
342573-75-5	EMIM ES	1-Ethyl-3-methylimidazolium ethylsulfate	$C_8H_{16}N_2O_4S$	236.29	< -150 [24]	408 [21]
143314-16-3	EMIM BF ₄	1-Ethyl-3-methylimidazolium tetrafluoroborate	$C_6H_{11}BF_4N_2$	197.97	11 [22]	450 [22]
174501-64-5	BMIM PF ₆	1-Butyl-3-methylimidazolium hexafluorophosphate	$C_8H_{15}F_6N_2P$	284.18	-8 [25]	349 [23]

Table 3.2 Ionic liquid structures used in this work

Cation	Anion
 EMIM ⁺ (1-ethyl-3-methylimidazolium)	 PF ₆ ⁻ (hexafluorophosphate)
 BMIM ⁺ (1-butyl-3-methylimidazolium)	 BF ₄ ⁻ (tetrafluoroborate)
	 ES ⁻ (ethyl sulfate)
	 TF ⁻ (trifluoromethane sulfonate)

A common procedure was followed for the synthesis of all alkali modified silicate glasses [26-28]. Silica and corresponding alkali carbonates were mixed in specified ratios. Half of the mixture was poured in an alumina crucible and placed in preheated high temperature furnace at 1215 °C. The temperature was set to 1350 °C and 30 minutes later, the remaining mixture was added to the crucible in the furnace. Total melt time was determined as 1 hour 30 minutes. After the glass was melted, it was quenched in graphite mold. The silicate glass was then annealed at 500 °C for 30 minutes, followed by cooling down to 120 °C at a rate of 1 °C/min. The final glass was kept at 120 °C until pick-up and placed straight to a desiccator to avoid any water absorption.

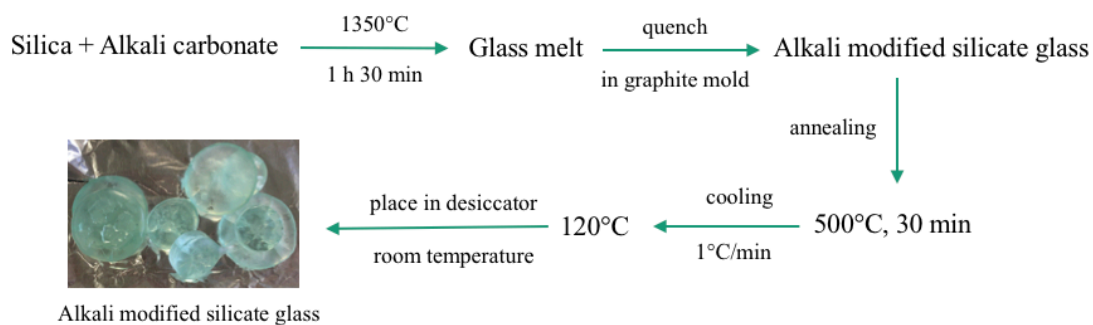


Figure 3.1 Alkali modified glass preparation.

3.2. Sample Preparation

Prepared silicate glasses were ground into a powder form with IKA A10 Analytical Mill for about 1 minute. Specified amount of ionic liquid was then mixed with ground silicate glass using a mortar and pestle. Once a homogeneous mixture was obtained, it was transferred into a mold (cylindrical or rectangular), or between aluminum foils for compression molding. The samples were compression molded with Carver Heated Hydraulic Press (Model C) under desired conditions. Once the samples were molded, they were ready for characterization.

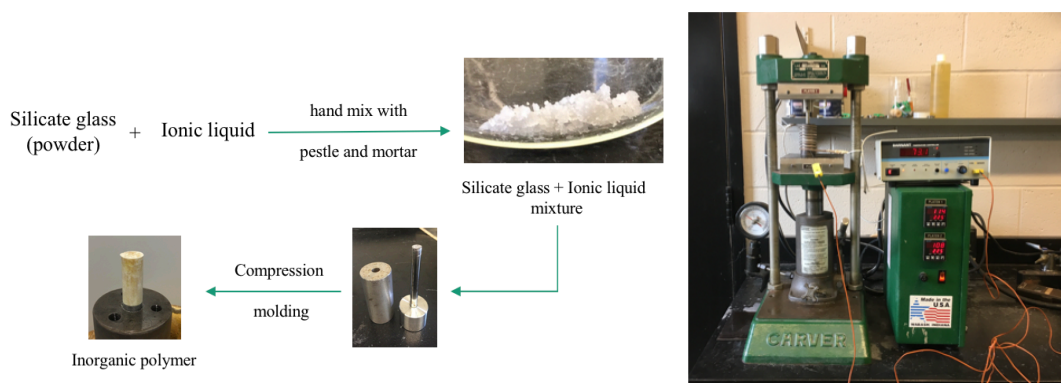


Figure 3.2 A flow diagram for sample preparation (left) and a set-up for compression molding (right).

3.3. Monovalent System

3.3.a. Synthesis of silicate glass

Rubidium silicate (RbSiO_2) and potassium silicate (KSiO_2) glasses were synthesized in different ratios for the experiments of monovalent-ion system. As mentioned earlier, modified silicate glasses were obtained through the reaction between silica and corresponding alkali carbonates.

At elevated temperatures, $\text{Si}-\text{O}-\text{Si}$ bonds in silica rupture due to the presence of alkali carbonates and increased vibrational energy. The resulting non-bridging oxygens (NBO) of $\text{Si}-\text{O}^-$ bonds are attacked by alkali carbonates forming an intermediate complex structure. This unstable state terminates as carbon dioxide (CO_2) leaves the complex structure and alkali modified silicate glass is formed (Figure 3.3).

1. Rupture of Si-O-Si bond



2. Formation of modified silicate glass

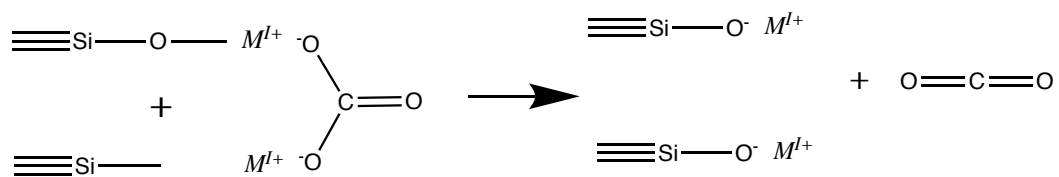
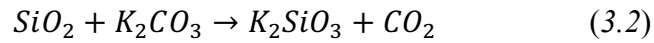
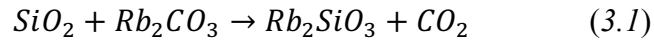


Figure 3.3 Glass formation mechanism for silicate glasses of monovalent-ion system. [29].

Based on the mechanism given above, rubidium silicate was synthesized with the reaction of silica and rubidium carbonate (3.1), whereas for potassium silicate the alkali ion is replaced with potassium carbonate (3.2).



Modifier to silica ratio was altered between 0.31 and 1.0 to observe the effects of alkali concentration on glass properties. The type and ratios of the alkali ions are given in Table 3.3 along with their names used in this thesis.

Table 3.3 Specifications for synthesized monovalent ion silicate glasses along with their names.

Alkali ion	$\frac{modifier}{SiO_2}$ ratio (mol/mol)	Glass name
Rb	0.78	RbSiO ₂ (0.78)
K	0.31	KSiO ₂ (0.31)
	0.56	KSiO ₂ (0.56)
	0.78	KSiO ₂ (0.78)
	1.0	KSiO ₂ (1.0)

3.3.b. Effect of modifier addition on glass transition temperature, T_g

It is well known that addition of modifiers decreases the T_g of silicate glass [30, 31]. For the same number of modifiers (equal number of NBOs created) in the glass, the larger is the modifier, the lower is the T_g due to homogeneous distribution of the modifier in the glass. Previous work in this laboratory on synthesis of inorganic

polymers showed that the T_g for RbSiO_2 glass ($307.1\text{ }^\circ\text{C}$) is lower than KSiO_2 glass ($403.6\text{ }^\circ\text{C}$) for a modifier to silicate ratio of 0.78 (Figure 3.4).

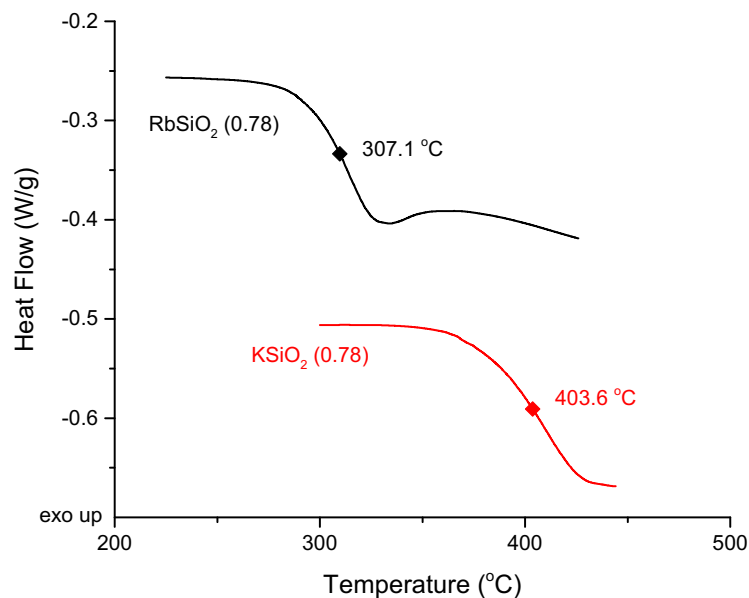


Figure 3.4 DSC heating curves for silicate glasses modified with Rb^+ (black) and K^+ (red) ions. $[\text{R}_2\text{O}]/[\text{SiO}_2]=0.78$. T_g for RbSiO_2 and KSiO_2 glasses are $307.1\text{ }^\circ\text{C}$ and $403.6\text{ }^\circ\text{C}$, respectively.

The size of the modifier in silicate glass affects the T_g . Increased diameter of the ion decreases the glass transition temperature [31]. In Figure 3.4, rubidium and potassium silicate glasses are compared with the same ratio. Rubidium and potassium ions have a diameter of 0.148 and 0.133 nm, respectively [32]. Having a larger diameter, rubidium decreases the glass transition temperature more than potassium.

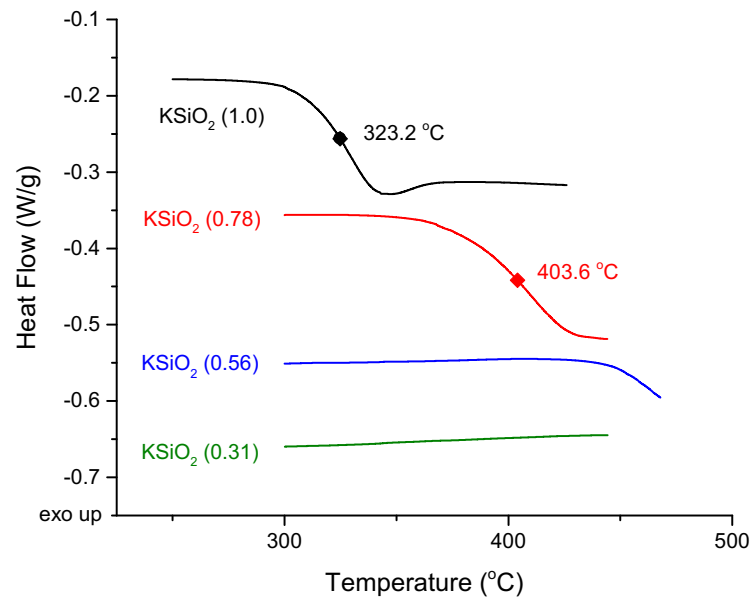


Figure 3.5 Effect of alkali ion ratio on T_g : DSC thermograms of KSiO_2 glasses with different alkali ion ratios. The values in parenthesis represent alkali ion ratios.

The alkali ion ratio ($[\text{modifier}]/[\text{SiO}_2]$) affects the structure of the silicate glass. Alkali ion breaks the Si-O bond and shapes the structure of silicate glass. A ratio smaller than 1 causes the silicate to have a crosslinked structure. Increased amount of alkali ions leads to increased breakage of the bonds and creates chain-like structures. As the number of Si-O-Si bond decreases, the glass transition temperature decreases. In Figure 3.5, silicate glasses with different potassium ratios are compared. Potassium amount increases from the bottom to the top. As seen in this figure, the glass transition temperature of potassium silicate glass decreases as the amount of potassium ion increases. Potassium in silica structure breaks the Si-O-Si bonds and causes a decrease in T_g .

3.3.c. Synthesis of inorganic polymer from $RbSiO_2$ and $KSiO_2$ glasses

$RbSiO_2$ and $KSiO_2$ based inorganic polymers were synthesized with the method explained earlier in section 3.2. The specific conditions for these inorganic polymers are listed in Table 3.4. The ionic liquid amount is determined based on the ratio of moles of ionic liquid to the moles of total positive ions in silicate glass.

Table 3.4 Inorganic polymer synthesis conditions for monovalent system used in this work.

Ionic liquid ratio (mol/mol)	Ionic liquid	Compression molding temperature ($^{\circ}C$)	Compression molding pressure (psi)
1/4	EMIM TF	150	1000
1/6	EMIM ES	180	1500
1/8			
1/16			



Figure 3.6 A picture of an inorganic polymer synthesized for monovalent system. The diameter is 10 mm and height is 20 mm.

It is expected that, upon addition of ionic liquid to silicate glass, cations of ionic liquid (i.e., $EMIM^+$) interact with negatively charged oxygen atoms (NBOs) in silicate structure, possibly leading to replacement of alkali ions with ionic liquid cations.

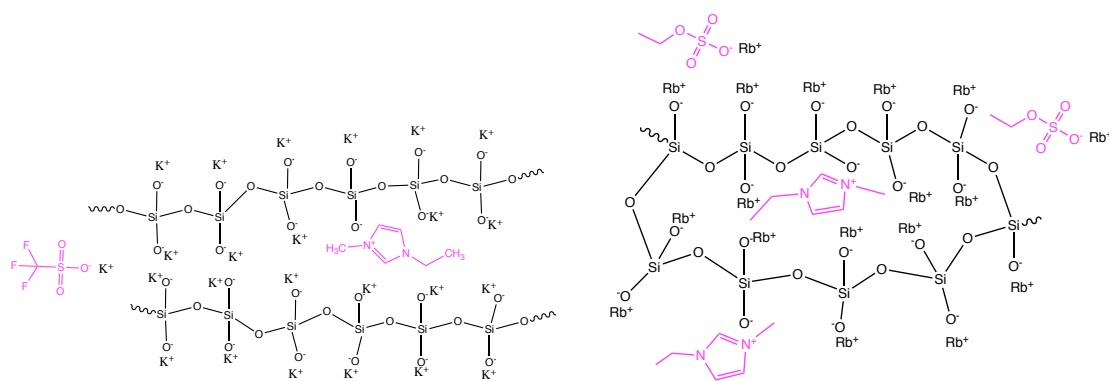


Figure 3.7 Suggested structures for monovalent-ion inorganic polymers. KSiO₂ (1.0) glass with EMIM TF (left) and RbSiO₂ (0.78) glass with EMIM ES (right).

A possible model of inorganic polymer structure is given in Figure 3.7. Based on the alkali ion concentration in silicate glass, it is expected that KSiO₂ (1.0) based inorganic polymers have a chain structure, whereas RbSiO₂ (0.78) based inorganic polymers have more crosslinked ring-structure. In both cases, alkali ions are replaced with cations of ionic liquids.

3.4. Divalent/Monovalent System: CaKSiO₂

3.4.a. Synthesis of CaKSiO₂ glass

Similar to monovalent system, during formation of alkali and alkaline earth modified silicate glass, Si–O–Si bonds are broken. NBOs, which are formed due to this rupture, interact with modifiers to form the silicate glass. A simple mechanism for this reaction is shown in Figure 3.8. In addition to NBO – M^{I+} interactions, as seen in monovalent system, NBO – M^{II+} interactions take place in divalent/monovalent systems.

1. Rupture of Si-O-Si bond



2. Formation of modified silicate glass

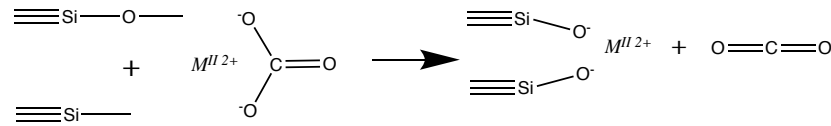
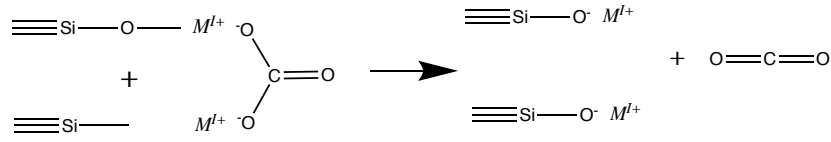
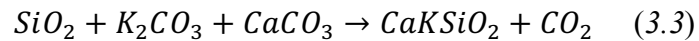


Figure 3.8 Glass formation mechanism for silicate glasses of divalent/monovalent system.

CaKSiO_2 glasses were prepared through the reaction of silica with calcium carbonate (CaCO_3) and potassium carbonate (K_2CO_3). As seen in the reaction below (3.3), CaKSiO_2 glass is formed as the main product and carbon dioxide (CO_2) as the side product.



The total alkali and alkaline earth oxide ratio to silica is kept constant at 1 (3.4). This provides CaKSiO_2 glass to have chain-like structure [33]. The amounts of $[\text{K}^+]$ and $[\text{Ca}^{2+}]$ ions are determined from the ratio of calcium oxide (CaO) to potassium oxide (K_2O) given in (3.5).

$$\text{Total ion (modifier) to silicate ratio} = \frac{[\text{K}_2\text{O}] + [\text{CaO}]}{[\text{SiO}_2]} = 1 \quad (3.4)$$

$$\text{Alkaline earth ions to alkali ions ratio} = \frac{[\text{CaO}]}{[\text{K}_2\text{O}]} \quad (3.5)$$

To observe the effect of concentration of divalent ions on silicate glass properties, different silicate glasses were synthesized with varying calcium ion (Ca^{2+}) concentrations. Table 3.5 lists the concentrations of Ca^{2+} used in this work along with their corresponding names.

Table 3.5 Specifications for synthesized divalent/monovalent silicate glasses (CaKSiO_2) along with their names.

Alkaline ion	Alkali ion	$\frac{\text{modifier}}{\text{SiO}_2}$	ratio	$\frac{\text{Alkaline}}{\text{Alkali}}$	ratio	Glass name
		(mol/mol)		$(\%)$		
Ca	K	1		5		5 % CaKSiO_2
				10		10 % CaKSiO_2
				15		15 % CaKSiO_2

3.4.b. Effect of calcium-ion addition on glass transition temperature, T_g

Different ratios of $[\text{CaO}]/[\text{K}_2\text{O}]$ are used, by keeping the total modifier amount at a ratio of 1, to explore the effects of divalent ions on the properties of inorganic polymers, including hygroscopicity. To obtain a general idea for the effect of Ca^{2+} on material properties, silicate glasses of 5, 10, and 15 % $[\text{CaO}]/[\text{K}_2\text{O}]$ are prepared. Then, DSC data are collected for these silicate glasses, which can also be used as a reference to discuss the DSC data on CaKSiO_2 with ionic liquids later.

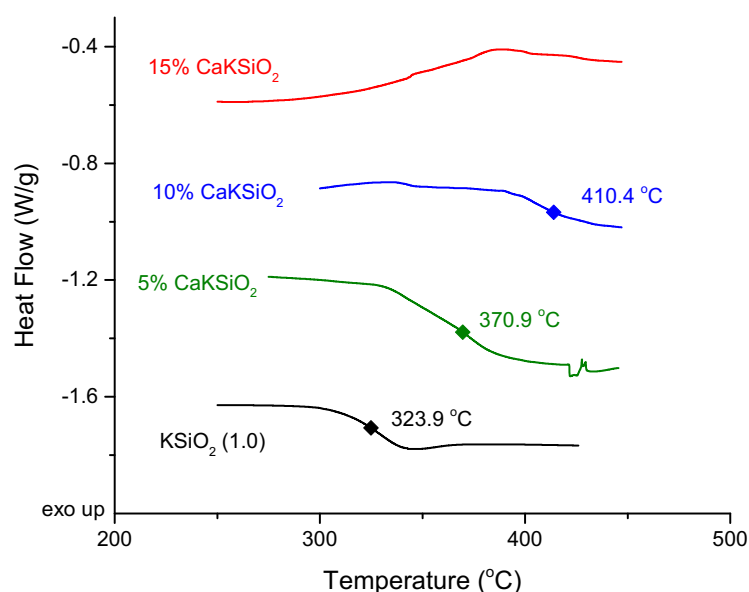


Figure 3.9 Effect of divalent ion concentration: DSC second heating curves for 0 %, 5 %, 10 %, and 15 % CaKSiO₂ (1.0) glasses. Note that 0 % CaKSiO₂ (1.0) is equivalent to KSiO₂ (1.0).

In DSC measurements, a heat/cool/heat cycle is adopted. In the first heating step, thermal stress and water that is possibly absorbed by the sample are released. Therefore, second heating curves are used for material characterization. The endothermic changes on heating curve may represent glass transition, melting, or decomposition [34]. In the light of this information, in Figure 3.9, the second heating curves for 0, 5, 10, and 15 % CaKSiO₂ (silicate) glasses are shown.

Table 3.6 T_g values of potassium silicate glasses with different concentrations of CaO.

[CaO]/[K ₂ O] ratio (%)	Glass transition temperature (°C)
0	323.9
5	370.9
10	410.4

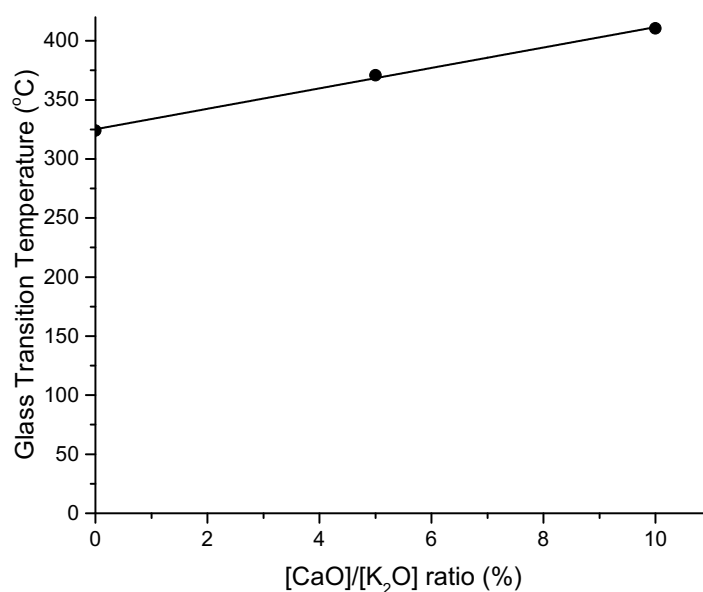


Figure 3.10 Effect of divalent ion (Ca^{2+}) concentration on T_g .

It is seen that the glass transition temperature increases with increasing divalent ion concentration, $[\text{Ca}^{2+}]$. KSiO_2 glass shows a T_g at 323.9°C , whereas for 5 % and 10 % CaKSiO_2 glasses T_g increases to 370.9°C and 410.4°C , respectively. 15 % CaKSiO_2 glass does not show a T_g up to 450°C , meaning T_g for this glass is above 450°C . This data shows the significant effect of Ca^{2+} ions on T_g . We have observed that introduction of alkaline earth (divalent) ions to the silicate glass structure helps to eliminate hygroscopicity significantly. However, at the same time, it increases T_g .

3.4.c. Synthesis of inorganic polymer with CaKSiO_2 glass

Powdered CaKSiO_2 glass is mixed with desired type and amount of ionic liquid for the synthesis of inorganic polymers, as explained in section 3.2. The amounts of ionic liquids and molding conditions used for the synthesis of CaKSiO_2 based inorganic polymers are given in Table 3.7.

Table 3.7 Inorganic polymer synthesis conditions for divalent/monovalent system (CaKSiO_2) used in this work.

Ionic ratio	liquid	Ionic liquid	Compression molding	Compression molding
			temperature ($^{\circ}\text{C}$)	pressure (psi)
1/4		EMIM TF	180	1500
1/6		BMIM TF	200	
1/8		BMIM PF_6		

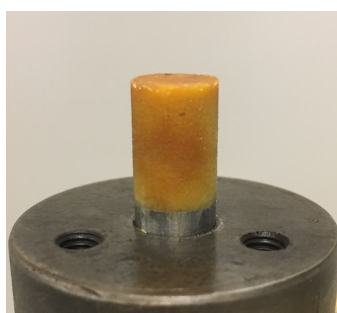


Figure 3.11 A picture of an inorganic polymer synthesized for divalent/monovalent system.

CaKSiO_2 glasses have chain structures due to the total modifier concentration in the structure. NBOs form an ionic bond with either monovalent ions (K^+) or divalent ions (Ca^{2+}). Upon addition of ionic liquid to silicate glass, alkali and alkaline earth ions are expected to be replaced by cations (EMIM^+ or BMIM^+) of ionic liquid. At this stage it is envisaged that EMIM^+ and BMIM^+ are mostly replacing monovalent ions (K^+) due to their lower bond strength with NBOs compared to divalent ions (Ca^{2+}). The possible mechanism for the reaction between CaKSiO_2 and EMIM TF is given in Figure 3.12.

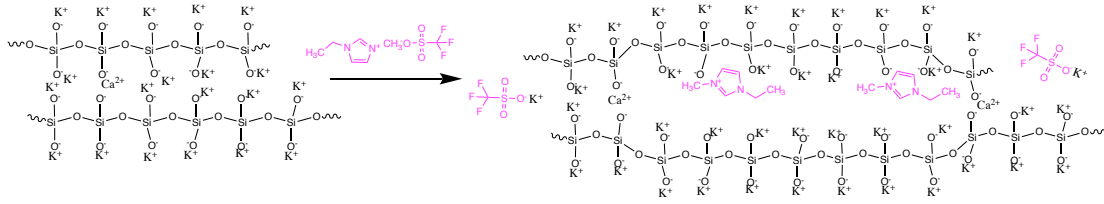
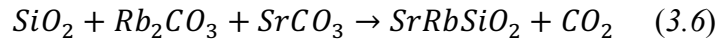


Figure 3.12 Representation of proposed inorganic polymer prepared with CaKSiO_2 and EMIM TF.

3.5. Divalent/Monovalent System: SrRbSiO_2

3.5.a. Synthesis of SrRbSiO_2 glass

The formation reaction of SrRbSiO_2 glass is given below. Specifically, silica (SiO_2) is reacted with rubidium carbonate (Rb_2CO_3) and strontium carbonate (SrCO_3) at elevated temperatures to form SrRbSiO_2 . Carbon dioxide (CO_2) is formed as a by-product.



In this reaction the total alkali and alkaline earth oxide ratio to silica is kept constant at 0.78 (3.7). This provides SrRbSiO_2 glass to have chain like structures with small amounts of crosslinking, i.e. leading to the formation of ring structures [33]. The amounts of $[\text{Rb}^+]$ and $[\text{Sr}^{2+}]$ ions are determined from the ratio of strontium oxide (SrO) to rubidium oxide (Rb_2O) given in (3.8).

$$\text{Total ion (modifier) to silicate ratio} = \frac{[\text{Rb}_2\text{O}] + [\text{SrO}]}{[\text{SiO}_2]} = 0.78 \quad (3.7)$$

$$\text{Alkaline earth ions to alkali ions ratio} = \frac{[\text{SrO}]}{[\text{Rb}_2\text{O}]} \quad (3.8)$$

As in the CaKSiO_2 system, divalent-to-monovalent ion ratio was altered to observe the effects of divalent ions (i.e., Sr^{2+}). Different ratios of glasses studied in this work are listed in Table 3.8 with their names.

Table 3.8 Specifications for synthesized divalent/monovalent silicate glasses (SrRbSiO_2) along with their names.

Alkaline earth ion	Alkali ion	$\frac{\text{modifier}}{\text{SiO}_2}$ ratio	$\frac{\text{Alkaline}}{\text{Alkali}}$ ratio	Glass name
		(mol/mol)	$(\%)$	
Sr	Rb	0.78	10	10 % SrRbSiO_2
			18	18 % SrRbSiO_2
			30	30 % SrRbSiO_2
			50	50 % SrRbSiO_2

3.5.b. Effect of strontium-ion addition on glass transition temperature, T_g

Different ratios of $[\text{SrO}]/[\text{Rb}_2\text{O}]$ are used by keeping the total modifier amount at a ratio of 0.78 to explore the effects of divalent ions on properties of inorganic polymers, including hygroscopicity. To obtain a general idea for the effect of Sr^{2+} on material properties, 10, 18, 30, and 50 % SrRbSiO_2 glasses are made.

Table 3.9 T_g values of rubidium silicate glass with different concentrations of SrO .

$[\text{SrO}]/[\text{Rb}_2\text{O}]$ ratio (%)	Glass transition temperature ($^{\circ}\text{C}$)
0	307.1
10	373.1
18	420.8

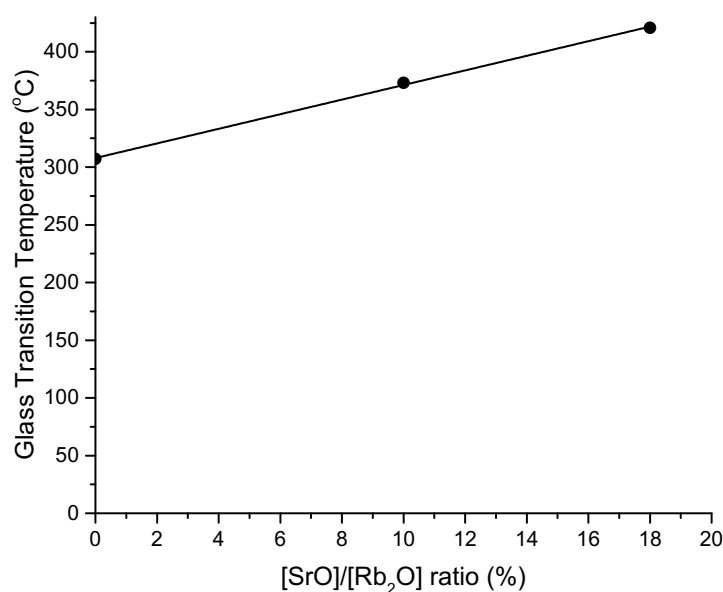


Figure 3.13 Effect of divalent ion (Sr^{2+}) concentration on T_g .

Addition of modifiers (oxides of alkali and alkaline earth ions) decreases the glass transition temperature due to breakage of Si-O-Si bonds. The decrease in T_g depends on size and charge of the modifier. As seen in Figure 3.13, rubidium silicate glass has a T_g of 307 °C, whereas addition of 10 % strontium ion (Sr^{2+}) increases the T_g to 372 °C. Addition of divalent ion, Sr^{2+} ion in this case, leads to stronger bonds and hence increases the T_g . Although in this work increase in glass transition temperature is an undesirable result, divalent ions should be added to the structure of inorganic polymers as they decrease the hygroscopicity of the material. The optimum divalent ion ratio should be determined based on desirable properties of the inorganic polymers.

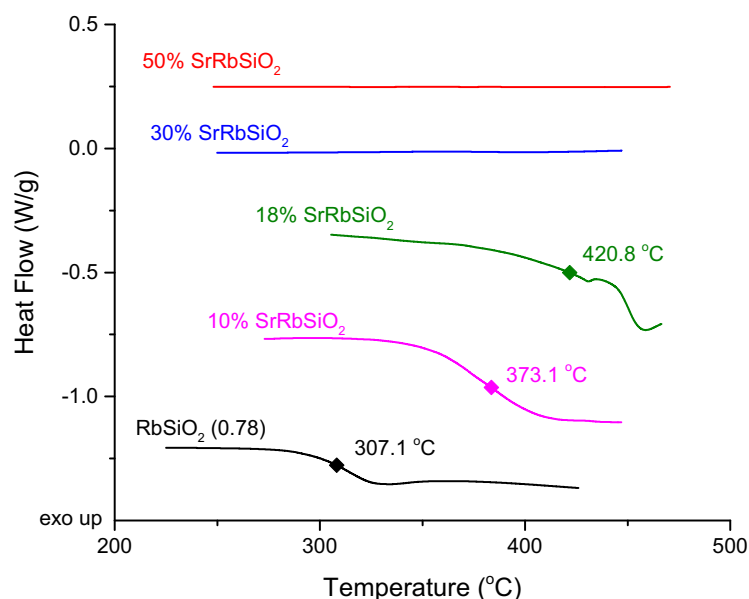


Figure 3.14 Effect of divalent ion concentration: DSC second heating curves for 0 %, 10 %, 18 %, 30 %, and 50 % SrRbSiO₂ (0.78) glasses. Note that 0 % SrRbSiO₂ (0.78) is equivalent to RbSiO₂ (0.78).

In Figure 3.14, the second heating curves for 10, 18, 30, and 50 % SrRbSiO₂ (silicate) glasses are shown. Only 10 % and 18 % SrRbSiO₂ glasses show T_g at 373.1 °C and 420.8 °C, respectively, up to 450 °C. The T_g values of 30 and 50 % SrRbSiO₂ glasses are higher than 450 °C and hence cannot be seen in the scan up to 450 °C. This data shows the significant effect of Sr²⁺ ions on T_g . It is observed that introduction of alkaline earth (divalent) ions to the silicate glass structure helps to eliminate hygroscopicity significantly. However, at the same time, it increases T_g (recall that T_g for RbSiO₂ (0.78) is 307.1°C) and causes higher tendency for crystallization in the polymer structure upon addition of ionic liquid.

3.5.c. Synthesis of inorganic polymer with SrRbSiO_2 glass

Synthesized silicate glasses are then ground to a powder form, followed by addition of ionic liquid based on the moles of positive charges in the silicate structure, as explained in section 3.2. The mixture of modified silicate glass and ionic liquid is then processed by compression molding as the final step. Table 3.10 summarizes the conditions and compositions used in this work to prepare inorganic polymers.

Table 3.10 Inorganic polymer synthesis conditions for divalent/monovalent system (SrRbSiO_2) used in this work.

Ionic Ratio	Liquid	Ionic Liquid	Compression Molding	Compression Molding
			Temperature ($^{\circ}\text{C}$)	Pressure (psi)
1/24		EMIM TF	150	1000
1/12		EMIM ES	250	1500
		EMIM BF_4	300	

Addition of modifiers to silica creates non-bridging oxygens (NBO) [35]. Positively charged alkali (i.e., monovalent) and alkaline earth (i.e., divalent) ions compensate the charges created around NBOs. Introducing ionic liquid to the structure, the cations of the ionic liquid are assumed to replace the positively charged ions from modifiers located around NBOs (e.g., Rb^+) expanding the structure further. The anions on the other hand, interact with free ions from modifiers in the structure.

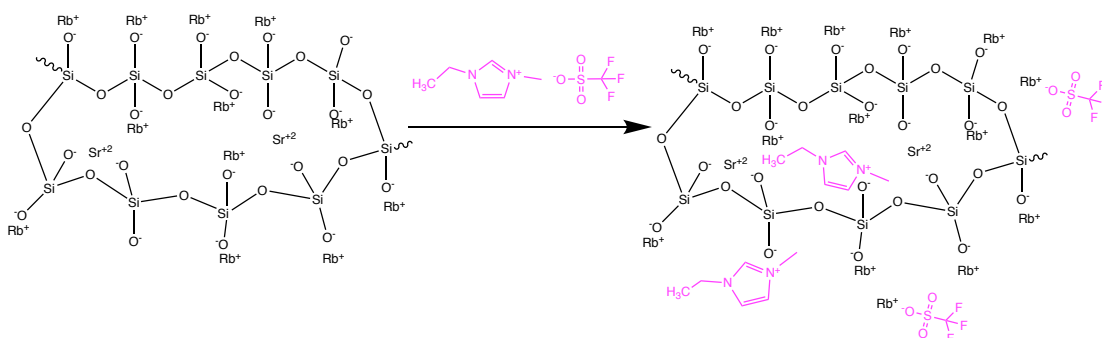


Figure 3.15 Stoichiometric representation of proposed inorganic polymer prepared with 30 % SrRbSiO_2 and 1/8 EMIM TF.

A suggested reaction mechanism for the synthesis of inorganic polymer is shown in Figure 3.15. Alkaline/alkali modified silicate glass (30 % SrRbSiO_2) has a ring structure due to the total alkaline/alkali ion to silica ratio of 0.78. Ionic liquid, in this case EMIM TF, possesses a cation and an anion reacting with NBOs and free alkali ions, respectively. Replacement of alkali ion with the cation of ionic liquid, i.e. EMIM^+ , expands the ring structure and provides additional free volume. This reduces the T_g and enables usage of silicate glasses as inorganic polymers.

3.6. Instrumentation and Characterization

3.6.a. Differential Scanning Calorimetry (DSC)

DSC is one of the useful thermal methods to determine material's melting, decomposition, crystallization, and glass transition temperatures, in addition to heat of reactions. Monitoring the heat required to keep the sample and the reference pans isothermal as temperature is changed is the basic principle of DSC [36]. Whenever the sample is undergoing an endothermic phase transition, such as glass transition, melting, or evaporation, more heat is required for the sample pan to keep the sample and

reference at the same temperature. Conversely, in the event of an exothermic phase transition, such as crystallization, oxidation, or decomposition, less heat is required for sample pan than for reference pan. Placing separate heating units for the sample and the reference pans, DSC can track the heat inputs, which is precisely equivalent to the energy absorbed or evolved [37].

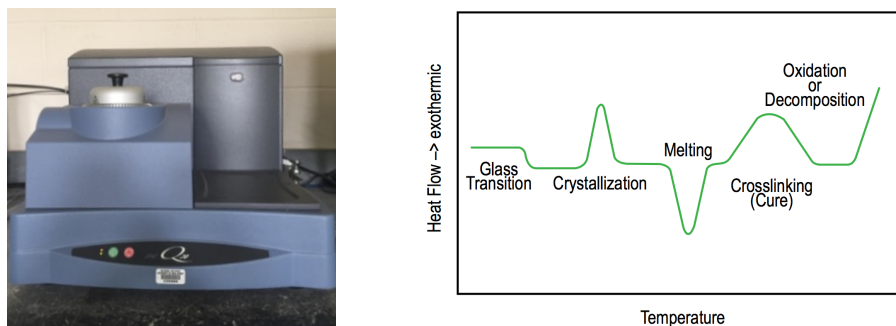


Figure 3.16 TA Instruments DSC Q20 (left); possible phase transitions in DSC analysis (right) [38].

The TA Instruments DSC Q20 was used to perform the thermal measurements of inorganic polymers (Figure 3.16, left). First, the samples were ground into fine powder to eliminate the effects of possible heterogeneity and then placed in Tzero Aluminum pan, followed by sealing. The sample mass was kept around 10 mg to obtain good sensitivity of the signals. Reference pan was prepared by sealing an empty Tzero Aluminum pan with its lid. Finally, the sample and the reference pans were placed into their corresponding ports and the experiment was started.

Custom heat/cool/heat cycle was adopted for all measurements. In the first heating cycle, samples were heated to 300 °C at a rate of 10 °C/min to remove the thermal history of the sample and then they were cooled down to 30 °C at a rate of 5 °C/min. In the final cycle, i.e., second heating, the samples were heated to 400 °C at a rate of 10 °C and the experiment was terminated. Thermal analysis of inorganic polymers was performed using the second heating cycle. After data was collected, heat

flow (W/g) was plotted against temperature (°C) and using Universal Analysis (TA Instruments) software, the phase transitions were determined. Figure 3.16 (right) gives possible phase transitions that can be observed in a Heat Flow vs. Temperature plot. For example, endothermic step changes, i.e., baseline shifts, were used to determine T_g .

3.6.b. Fourier-Transform Infrared Spectroscopy (FTIR)

FTIR is a powerful method used to obtain information about molecular structure and molecular bonds. The specimen is exposed to a broadband infrared radiation, which is then absorbed selectively by the sample [36]. The obtained spectrum is molecular absorption or transmission spectrum and is characteristic of molecular groups present in the structure [16]. The disadvantage of FTIR technique is that the infrared is only absorbed if the molecule's electric dipole moment changes during vibration or rotation. Thereof, not all types of molecules are detectable in FTIR. Usually, FTIR is coupled with other techniques, such as RAMAN spectroscopy, to obtain detailed information about the structure in question.

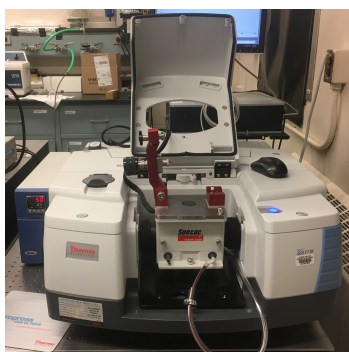


Figure 3.17 Nicolet™ iS50 FTIR Spectrometer (Thermo Fisher Scientific).

Nicolet™ iS50 FTIR Spectrometer was used to perform FTIR measurements. Before each measurement, sample was first ground into powder and then placed on a cleaned sample port. After each scan, the sample port was cleaned with distilled water.

3.6.c. X-Ray Photoelectron Spectroscopy (XPS)

X-Ray Photoelectron Spectroscopy is used to determine the atomic composition, oxidation state, and sometimes the structure of the examined compounds. In this technique, the sample is irradiated by X-rays, so that photons excite a core electron and eject it at a specific energy. This energy is called the binding energy and is specific for a given electron in a given element [37, 39]. During XPS measurement, the incoming X-ray energy is kept constant, so that the collected binding energy is directly related to the chemical environment of the species. Hence, any change in the chemical environment as a result of an interaction or a reaction can be detected from the shifts in the binding energies [39]. One of the disadvantages of this technique is that the penetration depth of x-ray radiation is about 1 to 100 Å. That means only the surface of the compounds can be examined with this method and bulky compounds cannot be analyzed [15]. In this work, K-Alpha X-ray Photoelectron Spectrometer (Thermo Fisher Scientific) was used for XPS measurements.

3.6.d. X-Ray Powder Diffraction (XRD)

XRD is a method used to identify the crystal structures in species. During the measurement, sample is exposed to x-rays, which are then diffracted from the sample elastically, i.e., without energy loss. Diffracted x-rays are collected and used for analysis [40]. A diffraction pattern contains information about the atomic arrangement within the crystal. Amorphous materials, such as glass, do not have a periodic array with long-range order, so they do not produce a diffraction pattern. This method also gives fingerprint XRD patterns for species. No two crystals are expected to possess identical spacing between the planes in all angular directions. Therefore, XRD patterns

give unique results for each specie [39]. In this work, Philips XPert Powder Diffractometer was used to identify the possible crystal structures in inorganic polymers.

3.6.e. Scanning Electron Microscopy (SEM) Coupled with Energy Dispersive X-Ray Spectroscopy (EDS)

SEM is a method used to image samples by focused electron beam. Signals are generated as a result of the high energy electron beam on the surface of the sample and converted into information for determination of morphology, chemical composition, crystalline structure, and the orientation of the sample. Two types of beams are included in the instrumentation: primary and secondary beams. Primary beam is the gun which sends electrons on the sample surface. The secondary beam on the other hand, consists of secondary-, backscattered-, and diffracted backscattered electrons, photons, and visible light. Secondary and backscattered electrons are used for imaging, whereas photons (x-ray) for elemental analysis [41]. Elemental analysis of the sample is performed by EDS, which is instrumented in SEM. By EDS method, signals are collected and plotted as energy as a function of x-ray counts. Analyzing the peaks, elemental composition can be determined. The advantage of SEM and EDS is that bulk specimens can be imaged and analyzed, whereas the disadvantage is that the measurements should be performed in high vacuum because the electrons sent from the primary beam may interact with the particles involved in the air. The need for high vacuum causes limitations with sampling, thus, samples that decompose in high vacuum, or liquids cannot be analyzed. Additionally, the sample surface must be electrically conductive and non-conductive samples should be coated with very thin conductive metals, such as gold [28, 42]. In this work, cylindrical samples of inorganic

polymers were imaged and analyzed with Zeiss Sigma Field Emission SEM coupled with Oxford EDS.

3.6.f. Transmission Electron Microscopy (TEM)

TEM is another useful imaging method used to identify sample's morphology. Similar to SEM method, in TEM imaging, the sample is exposed to electron beam, but unlike SEM, electron beam passes through the specimen and an image is obtained due to interactions between the sample and the electrons [28]. The advantage of TEM is that very high magnifications can be achieved (around $\times 1,000,000$), whereas the disadvantage is that the sample should be very thin, so that electron beams can pass through. In this work, TEM-Topcon 002B was used to obtain TEM images of inorganic polymers. The samples for imaging were prepared by dissolving synthesized inorganic polymers in water, with a concentration of 0.001 g/mL, followed by evaporation of 1-2 drops of solution on a copper grid (Holley Carbon-Cu, 200 mesh, 50 micron). The prepared copper grid was then inserted into the electron microscope to start imaging.

3.6.g. Mechanical Testing

In addition to characterization methods, mechanical properties are crucial to identify useful materials, especially the ones which are intended for industrial applications. Most significant properties include modulus, strength, and toughness (ductility). In this work, the procedure of ASTM D695-15, "Standard Test Method for Compressive Properties of Rigid Plastics," was adapted to perform mechanical testing [18]. The measurements were performed for cylindrical samples with 20 mm in length and 10 mm in diameter with Tinius Olsen H5KS Tester in EMSL Analytical, Inc.

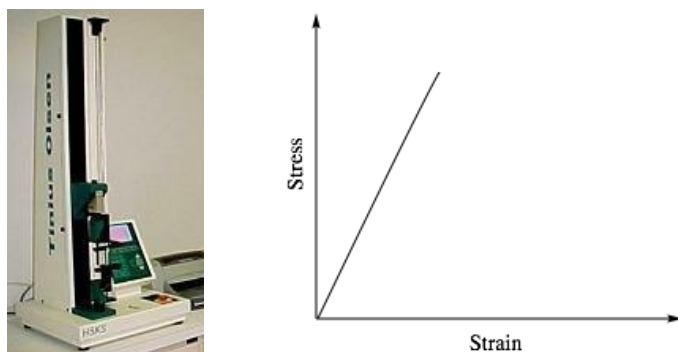


Figure 3.18 Compression test of a cylindrical sample (left), a typical stress strain curve for brittle materials (right).

All inorganic polymer samples were tested at a speed (rate of motion of the grip) of 1.3 mm/min. At the end of each measurement, a stress-strain curve was plotted, and the compressive data were calculated from this plot (Figure 3.18, right). Modulus is determined from the slope of the straight portion of the stress-strain curve. The maximum stress is used as the strength and the area under the stress-strain curve is used for the toughness [28, 43].

Chapter 4

RESULTS: MONOVALENT SYSTEM

4.1. Effect of Ionic Liquid Addition on Glass Transition Temperature, T_g

Addition of ionic liquid to RbSiO_2 and KSiO_2 glasses decreases T_g even further. However, the problem occurs due to highly hygroscopic nature of the modified silicate glasses. The hygroscopicity of these glasses is so high that it negatively affects their applications. As one of the purposes of this work, divalent ions (Sr^{2+} and Ca^{2+}) are added to silicate glass along with monovalent ions (Rb^+ and K^+ , respectively) to overcome the hygroscopicity problem without losing the processability. DSC results for aforementioned silicate glasses are given in results section.

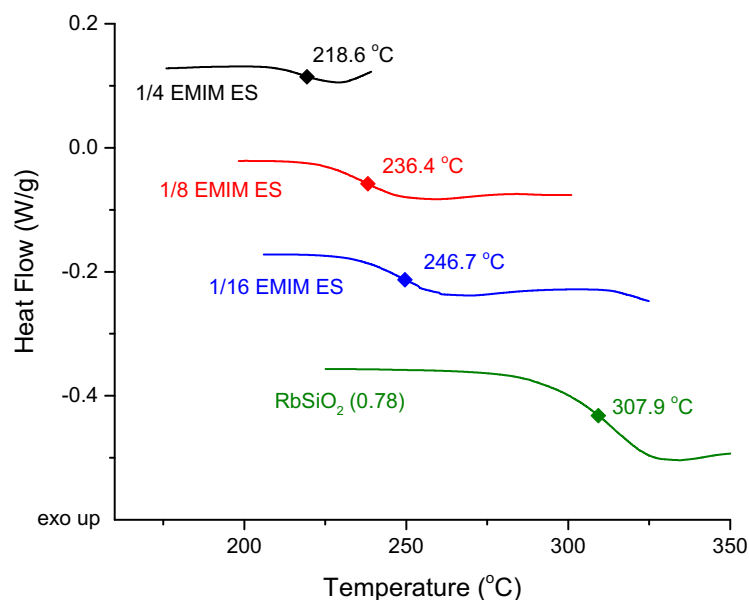


Figure 4.1 Effect of the amount of ionic liquid: DSC second heating curves for inorganic polymers made of RbSiO_2 glass (0.78) and EMIM ES. The amounts of EMIM ES are 1/4 (black curve), 1/8 (red curve), and 1/16 (blue curve) as compared with pure RbSiO_2 (0.78) (green curve) used as a reference.

Figure 4.1 compares the thermograms of inorganic polymers made of RbSiO_2 (0.78) and EMIM ES. The ionic liquid concentration was altered to study the effect of EMIM ES on T_g . Plasticization of RbSiO_2 (0.78) with the ionic liquid EMIM ES reduces the T_g from 307.9 °C to 246.9 °C, 236.4 °C, and 218.6 °C for the amounts 1/16, 1/8, and 1/4, respectively.

Table 4.1 T_g of inorganic polymers made of rubidium silicate (0.78) and different concentrations of EMIM ES.

EMIM ES ratio (mol/mol)	Glass transition temperature (°C)
0	307.9
1/16	247
1/8	236.4
1/4	218.6

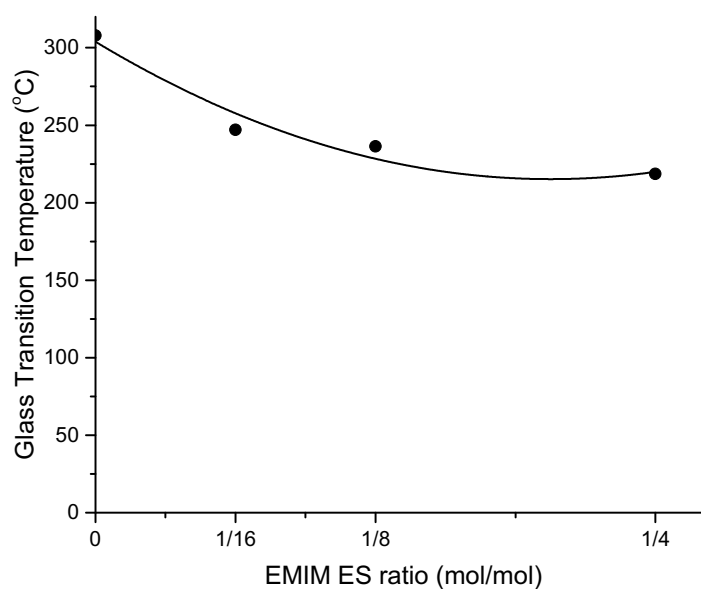


Figure 4.2 Effect of the amount of ionic liquid on T_g for RbSiO_2 (0.78) glass.

Plasticization of silicate glass was achieved by the addition of ionic liquid. It is observed that, in the beginning, T_g of RbSiO_2 drops significantly with the addition of a small amount of EMIM ES, i.e. 1/16 ratio. Once the plasticization of RbSiO_2 glass occurs, further addition of EMIM ES does not drop the T_g of the inorganic polymer as significantly as in the beginning. Such a change is widely observed for organic-polymer/plasticizer systems [44]. Increasing the ionic liquid concentration of inorganic polymers decreases the T_g until saturation point is reached.

KSiO_2 glass was also successfully plasticized by the addition of EMIM TF. The T_g of this modified silicate glass (inorganic polymer) was dropped by approximately 170 °C upon addition of 1/8 mole ratio of EMIM TF.

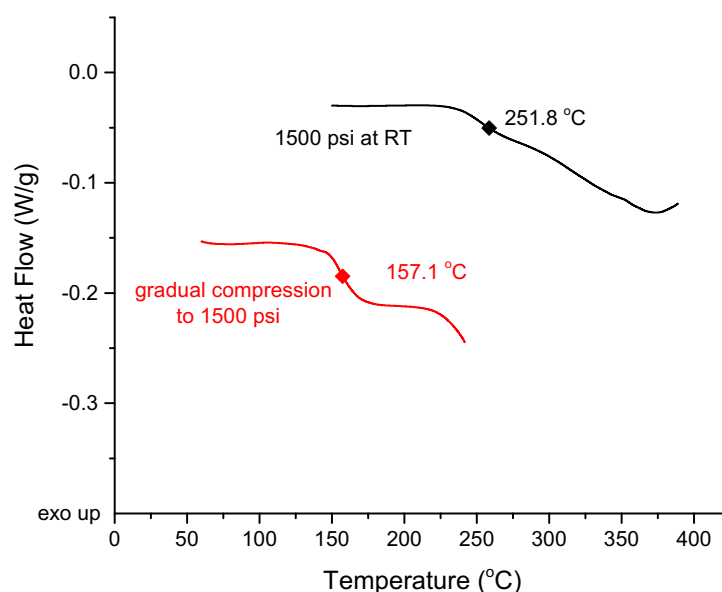


Figure 4.3 Effect of processing conditions on T_g : DSC thermograms of inorganic polymers made of KSiO_2 and 1/6 EMIM TF (compressed to 1500 psi at room temperature) (black) and KSiO_2 and 1/8 EMIM TF (gradually compressed to 1500 psi as the sample is heated up to 180 °C) (red).

Figure 4.3 gives the DSC thermogram of KSiO_2 -based inorganic polymers containing 1/6 and 1/8 mole ratios of EMIM TF. These two samples were prepared with different synthesis methods. In the light of the information obtained from RbSiO_2 system, it is expected that increasing the amount of ionic liquid decreases the T_g . However, in this case, higher concentration of EMIM TF led to higher T_g : inorganic polymers containing 1/6 and 1/8 mole ratios of EMIM TF show T_g values of 251.8 °C and 157.1 °C, respectively.

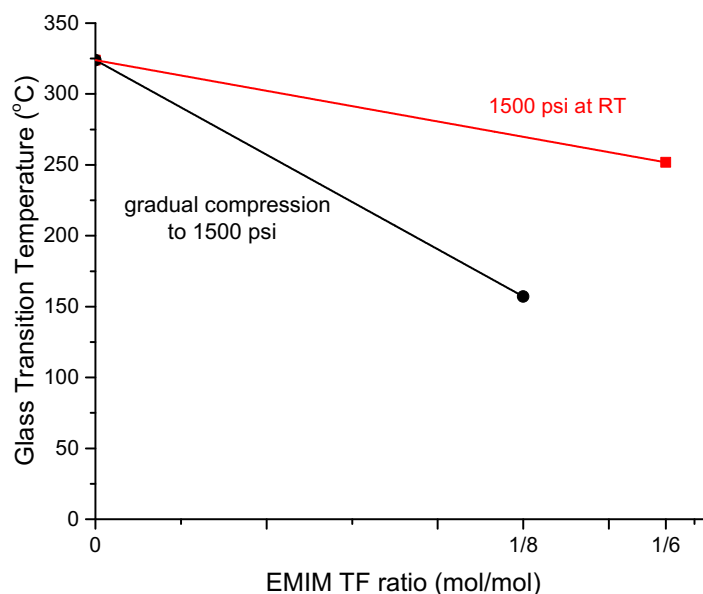


Figure 4.4 Effect of processing conditions on T_g : one-time compression to 1500 psi at room temperature decreases the plasticization power of ionic liquid (red). Gradual increase in compression to 1500 psi as the sample is heated up increases the plasticization of silicate glass by ionic liquid (black).

This outcome indicates the importance of synthesis conditions of inorganic polymers. The sample prepared with 1/6 mole ratio of EMIM TF was pressed to 1500 psi pressure at room temperature and gradually heated up to 180 °C. By contrast, the second sample was heated up to 100 °C without pressure. At 100 °C the pressure was increased to 1000 psi and eventually it was brought to 1500 psi at 180 °C. During the

synthesis of inorganic polymers, it was observed that applying pressure at room temperature resulted in leakage of the ionic liquid out of the mold. The leakage could be reduced for the second method, where the pressure was gradually increased at higher temperatures. In this case, more ionic liquid can be incorporated into the inorganic polymer structure and hence increases the plasticization. Therefore, in this example, the sample with less amount of EMIM TF, i.e. 1/8 mole ratio, gives a lower T_g than the sample with 1/6 mole ratio of EMIM TF (Figure 4.4).

4.2. Mechanical Properties of NaSiO₂-based Inorganic Polymers

Samples were made of NaSiO₂ glass and 1/8 mole ratio of EMIM TF to obtain preliminary data for mechanical properties of inorganic polymers. This silicate glass was chosen because of its wide availability and low hygroscopicity compared to many other silicate glasses prepared in this laboratory. Compression testing was chosen here because tensile tests are most sensitive to material flaws and microscopic cracks, while compression tests are less sensitive to these flaws and thus tend to be characteristic of the polymer [19].

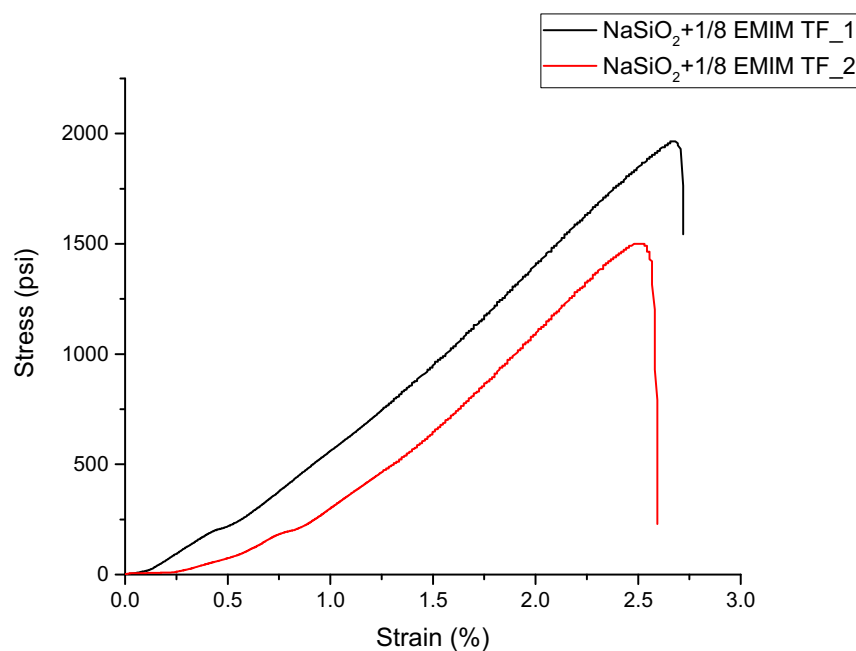


Figure 4.5 Compressive stress-strain curves for samples made of NaSiO₂ and 1/8 EMIM TF (compression molded at 200 °C and 1500 psi).

Table 4.2 Compressive mechanical properties of NaSiO₂-based inorganic polymers.

Sample	Modulus		Toughness		Compressive Strength	
	(psi)	(GPa)	(psi)	(MPa)	(psi)	(MPa)
1	85.8	0.59	24.3	0.17	1964	13.5
2	92.0	0.63	15.5	0.11	1500	10.3
Polystyrene (PS)*	91.7	0.63	541.7	3.73	9830	67.8

* measured values by using the PS sample of the same size and using the same instrument.

The stress-strain curves for compression testing are given in Figure 4.5. Modulus, toughness and compressive strength values are calculated from the plot and are shown in Table 4.2. Polystyrene (PS) sample was prepared using the same set-up for inorganic polymer and tested with the same instrument and same conditions. It is seen that modulus values of NaSiO_2 system are comparable to PS, whereas toughness and compressive strength values are much smaller. These results will be compared with 5 % CaKSiO_2 -based system and discussed in detail in section 5.3.

Chapter 5

RESULTS: DIVALENT/MONOVALENT SYSTEM

(CaKSiO₂)

5.1. Effect of Ionic Liquid Addition on Glass Transition Temperature, T_g

5.1.a. *Effect of silicate structure*

Ionic liquids are envisaged as a plasticizer for inorganic polymers. Hereby, addition of ionic liquids decreases the glass transition temperature of silicate glasses. In section 4.1, it was found that addition of 1/8 mole ratio of EMIM TF to KSiO₂ decreases the T_g by 167 °C (from 323.9 °C to 157.1 °C). To study the effect of divalent ions on T_g, CaKSiO₂-based inorganic polymers were synthesized. As is expected, addition of 1/8 mole ratio of EMIM TF to divalent/monovalent silicate glass, 10 % CaKSiO₂, decreases the T_g by 218 °C (from 410.4 °C to 192.5 °C) (Figure 5.1). Thus, the drop in T_g is larger for the divalent/monovalent system (CaKSiO₂) than for the monovalent system (KSiO₂). This can be a result of plasticization of divalent ions (Ca²⁺), in addition to the plasticization of monovalent ions (K⁺).

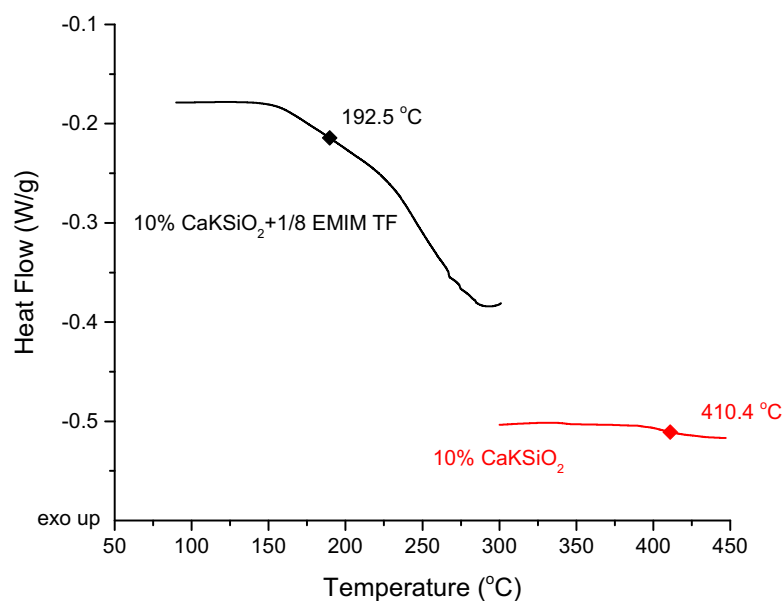


Figure 5.1 Effect of ionic liquid addition on T_g : DSC thermograms of 10 % CaKSiO₂ glass (red) and inorganic polymer made of 10 % CaKSiO₂ and 1/8 EMIM TF (black).

The T_g of inorganic polymer made of 10 % CaKSiO₂ and 1/8 mole ratio of EMIM TF was found to be 192.5 °C (Figure 5.2), compared to a T_g of 157.1 °C for KSiO₂ glass with 1/8 mole ratio of EMIM TF. As expected, the T_g increases significantly when divalent ions are incorporated into the structure. Divalent ions form stronger ionic bonds with NBOs, making the ionic liquid harder to decrease the bond strength and to be incorporated into the structure. Therefore, the T_g of divalent-ion containing inorganic polymers are higher than that of their monovalent counterparts.

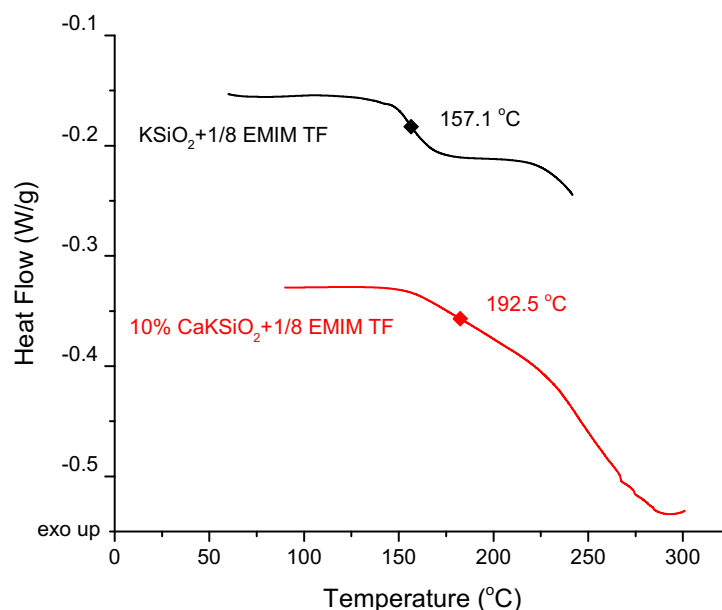


Figure 5.2 Effect of silicate structure on T_g : DSC thermograms of inorganic polymers made of 1/8 mole ratio of EMIM TF and different silicate glasses; KSiO_2 (black) and 10 % CaKSiO_2 (red).

Apart from the fact that the T_g values are higher for divalent/monovalent inorganic polymers, plasticization can be promoted by increasing the amount of ionic liquid in the structure. In Figure 5.3, DSC thermograms of 10 % CaKSiO_2 -based inorganic polymers are illustrated with different EMIM TF concentrations. It is observed that, comparable to monovalent system, increasing ionic liquid concentration decreases the T_g . Processing temperature of 10 % CaKSiO_2 glass can be decreased from 410.4 °C to 192.5 °C, 174.5 °C, and 154.7°C by addition of 1/8, 1/6, and 1/4 mole ratios of EMIM TF, respectively (see also Table 5.1).

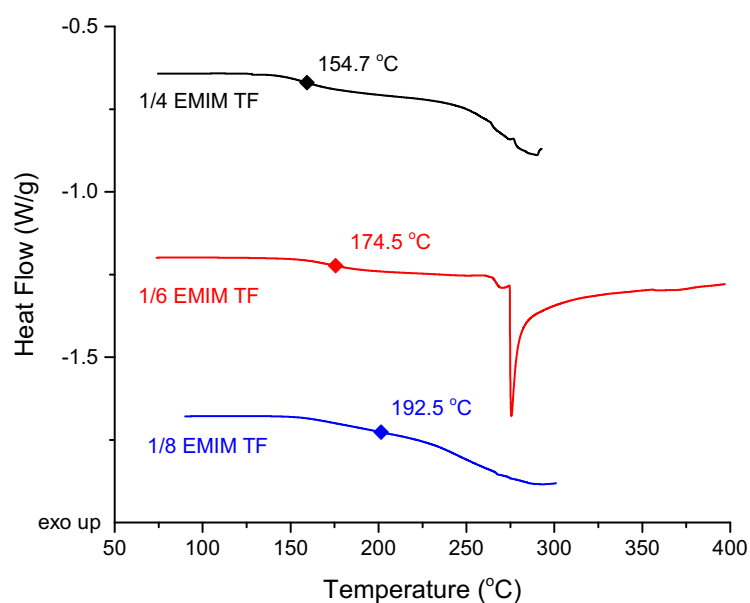


Figure 5.3 Effect of the amount of ionic liquid on T_g : DSC thermograms of inorganic polymers made of 10 % CaKSiO₂ and 1/4 (black), 1/6 (red), and 1/8 (blue) mole ratios of EMIM TF.

Table 5.1 T_g of inorganic polymers made of KSiO₂ or 10 % CaKSiO₂ with different concentrations of EMIM TF.

Type of silicate glass	EMIM TF concentration (mol/mol)	Glass transition temperature (°C)
KSiO ₂	0	323.9
	1/8	157.1
10 % CaKSiO ₂	0	410.4
	1/8	192.5
	1/6	174.5
	1/4	154.7

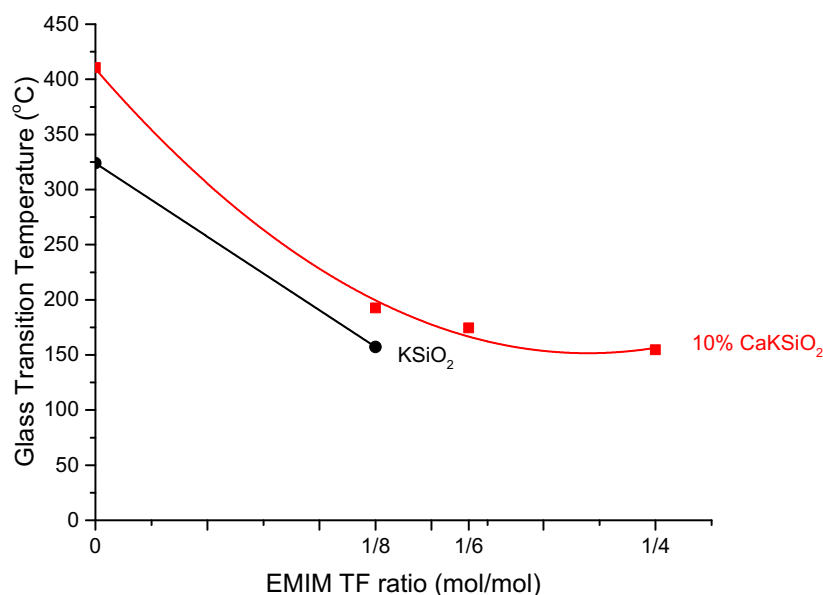


Figure 5.4 Effect of silicate structure and amount of ionic liquid on T_g : inorganic polymers made of 10 % CaKSiO_2 (red) and KSiO_2 (black).

Addition of small amount of EMIM TF, i.e. 1/8 mole ratio, to 10 % CaKSiO_2 glass decreases the processing temperature significantly. Similar to monovalent system, the T_g starts to level off as EMIM TF concentration is further increased (Figure 5.4). Monovalent and divalent/monovalent systems show a similar behavior towards ionic liquid addition. Processing temperature of both silicate glasses decrease with addition of ionic liquid. The slope for divalent/monovalent system (i.e., a mixture of Ca^{2+} and K^+) is steeper than for monovalent system (i.e., K^+ only), because in divalent/monovalent system some Ca^{2+} bonds are broken in addition to K^+ bonds. As Ca^{2+} bonds are stronger, the slope (i.e., drop rate) is steeper when they are broken. In addition, divalent/monovalent system has higher T_g than monovalent system. This is due to the stronger bonds formed between Ca^{2+} ions and NBOs, which is also responsible for lower hygroscopicity for Ca-containing inorganic polymers.

Nonetheless, the disadvantage of higher processing temperatures found for divalent/monovalent systems can be compensated by the addition of ionic liquid, so that the difference in processing temperature between the monovalent system and the divalent/monovalent system becomes insignificant. Coupled with our observation that inorganic polymers made of divalent/monovalent systems show lower hygroscopicity, divalent/monovalent systems provide better inorganic polymers for practical use.

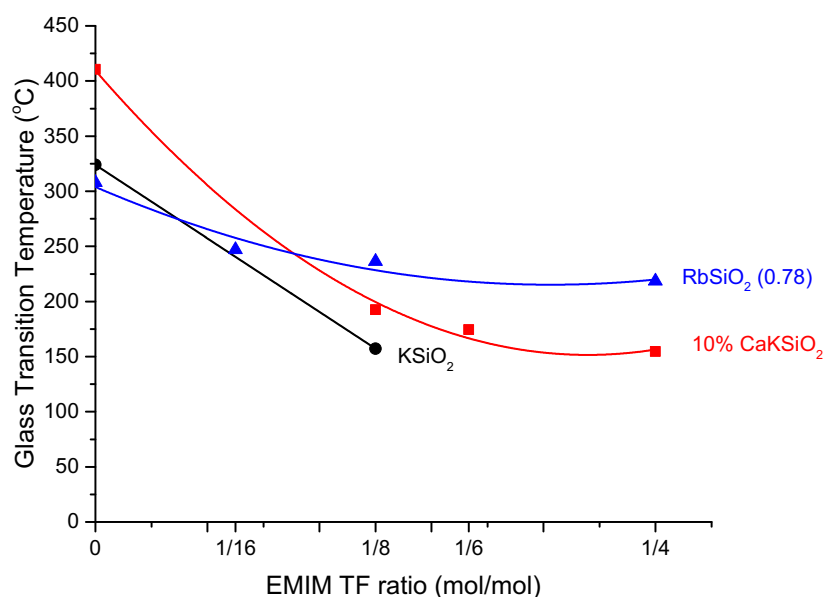


Figure 5.5 Effect of silicate structure on T_g : change in T_g as a function of ionic liquid amount for inorganic polymers made of EMIM TF and silicate glasses of RbSiO₂ (0.78) (blue), KSiO₂ (1.0) (black), and 10 % CaKSiO₂ (1.0) (red).

A similar observation was made for RbSiO₂ (0.78) monovalent-ion system with EMIM TF, as shown in Figure 5.5. After a significant drop of T_g in the beginning, the slope begins to level off, indicating a possible saturation of ionic liquid in inorganic polymer structure.

Despite the fact that the general trend is similar in all systems, one important difference stands out. It is seen in Figure 5.5 that KSiO_2 and 10 % CaKSiO_2 systems respond to ionic liquid addition better than RbSiO_2 (0.78). Starting with higher values of glass transition temperatures, the drop in T_g is steeper in the beginning for KSiO_2 and 10 % CaKSiO_2 systems so that they show lower T_g values in general. This observation can be related to the number of positive ions in the starting silicates. As explained earlier, KSiO_2 and 10 % CaKSiO_2 have chain structures ($\frac{\text{modifier}}{\text{SiO}_2} = 1$), whereas the structure of RbSiO_2 (0.78) is more crosslinked. The number of positive ions is calculated to be 1.75 times larger for these two K-containing systems than for RbSiO_2 (0.78) glass. This leads to the outcome that ionic liquids are more effective in decreasing the glass transition temperature when the silicate glass has higher number of positive ions. Thus, for divalent/monovalent systems, the disadvantage of having higher T_g values can be eliminated by increasing the number of positive ions, i.e. by increasing the amount of modifier amount. As a result, less hygroscopic polymers can be synthesized. Another reason for the larger drop in T_g for the KSiO_2 and CaKSiO_2 systems than for the RbSiO_2 system is that the former polymers are linear polymers that contain intermolecular ionic bonds and the latter polymer is lightly cross-linked polymer that also contains ionic bonds. Because Si-O-Si based cross-links are stronger than ionic bonds, breaking Si-O-Si bonds (cross-links) by ionic liquid is more difficult, thus leading to less drop in T_g .

5.1.b. Effect of ionic liquid type

In addition to the effect of silicate structure on inorganic polymers, the effect of ionic liquid type is studied by changing the anion and cation type one at a time. First

the cation is switched from EMIM⁺ to BMIM⁺, wherein inorganic polymer was synthesized from 10 % CaKSiO₂ and 1/8 mole ratio of BMIM TF. The synthesis conditions were kept constant and the DSC thermograms were compared (Figure 5.6). It is observed that changing the cation of ionic liquid to a bulkier counterpart (i.e., BMIM⁺) has a very small effect on T_g (only 8 °C drop).

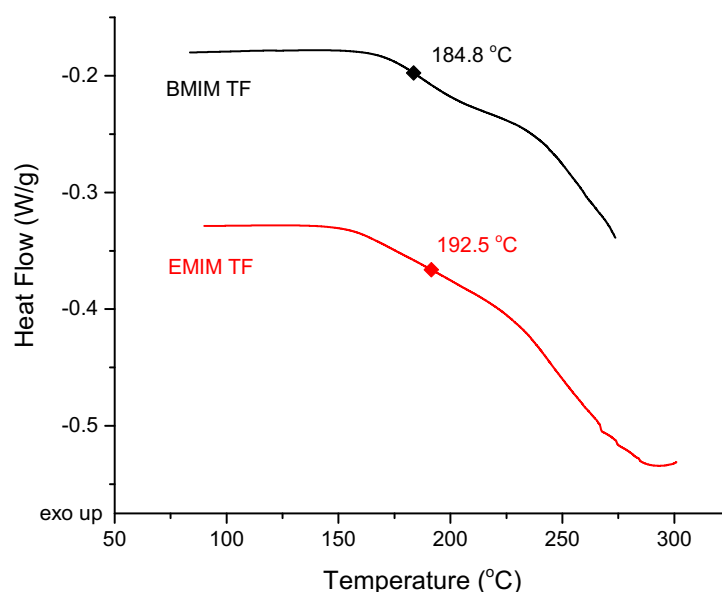


Figure 5.6 Effect of ionic liquid cation on T_g: DSC thermograms of inorganic polymers made of 10 % CaKSiO₂ and 1/8 mole ratio of BMIM TF (black) and EMIM TF (red).

Theoretically, it is expected that bulkier cation creates more free volume compared to smaller cation and thus decreases the T_g, but experimentally this expectation was not met by switching the cation from EMIM⁺ to BMIM⁺. It should be stressed that more distinct observation may still be possible by using bulkier cations than BMIM⁺, such as TOP⁺ (tetraoctylphosphonium⁺).

Regarding the effect of anion type on inorganic polymer properties, samples were prepared using the same cation (BMIM⁺) and different anions (PF₆⁻ and TF⁻). DSC thermograms of these samples show that anion type has a greater effect on thermal

properties than cation type does (Figure 5.7). The T_g of 10 % CaKSiO₂ glass decreases to 184.8 °C upon addition of 1/8 mole ratio BMIM TF, whereas it only drops to 229.3 °C when the same amount of BMIM PF₆ is added.

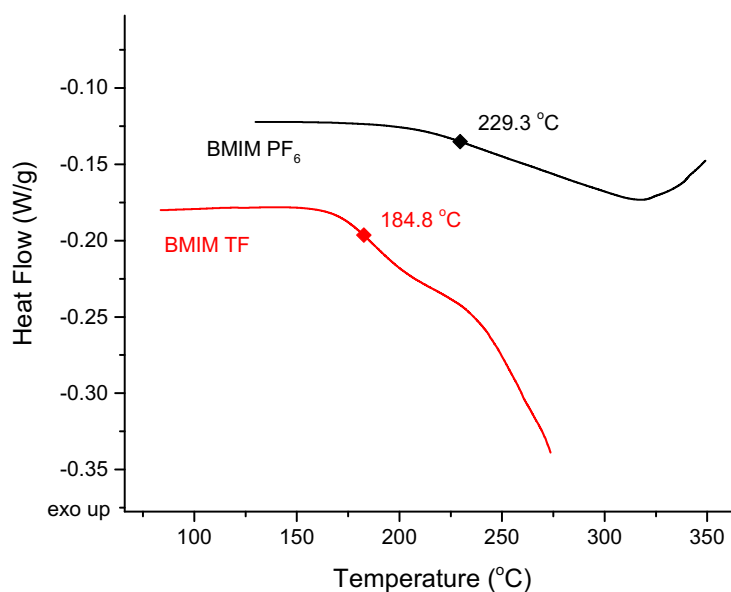


Figure 5.7 Effect of ionic liquid anion on T_g : DSC thermograms of inorganic polymers made of 10 % CaKSiO₂ and 1/8 mole ratio of BMIM PF₆ (black) and BMIM TF (red).

Although it is expected that anions are not incorporated into inorganic polymer structure, they show an indirect effect on thermal properties. Change in anion type changes the glass transition temperature by more than 40 °C (Figure 5.7). This outcome may be explained by the difference in the cation-anion interaction energy of the ionic liquids. Possessing higher cation-anion interaction energy than BMIM TF, BMIM PF₆ requires more energy to dissociate [45]. Consequently, BMIM⁺ cannot detach easily from PF₆⁻ and be incorporated into the inorganic polymer structure. Thus, the drop in T_g is smaller for BMIM PF₆ as compared to BMIM TF.

5.1.c. Effect of processing conditions

As mentioned earlier for monovalent system, processing method is crucial for thermal properties. Two identical samples were made of 10 % CaKSiO₂ and 1/6 mole ratio of EMIM TF, where the first sample was pressed to 1500 psi at room temperature and the second sample was gradually brought to 1500 psi as it was heated. A similar result was obtained for divalent/monovalent system (Figure 5.9). T_g drops to only 305.6 °C when high pressure is applied at room temperature. However, when the pressure is gradually increased, the T_g drops by an additional 130 °C and reaches to 174.5 °C. The mechanism for this difference was already discussed in section 4.1.

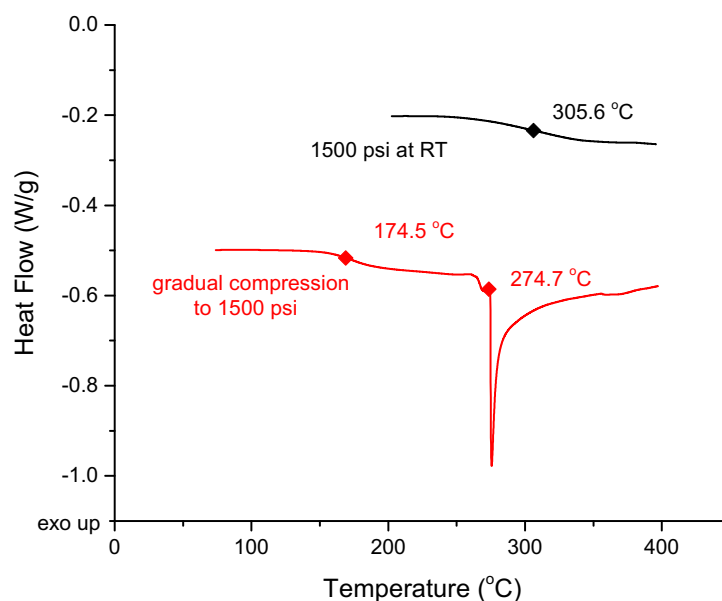


Figure 5.8 Effect of processing conditions on T_g : DSC thermograms of inorganic polymers made of 10 % CaKSiO₂ and 1/6 mole ratio of EMIM TF; compressed to 1500 psi at room temperature (black) and gradually compressed to 1500 psi as the sample is heated to 180 °C (red).

In addition, it was observed that the second sample, which was compressed gradually to 1500 psi, showed another T_g that is comparable to the first sample

(compressed to 1500 psi at room temperature). Formation of two T_g values may indicate that this specific inorganic polymer has an ionic liquid rich region (with lower T_g value) and an ionic liquid poor region (with higher T_g value). The plasticization is more effective in the ionic liquid rich region than in the ionic liquid poor region.

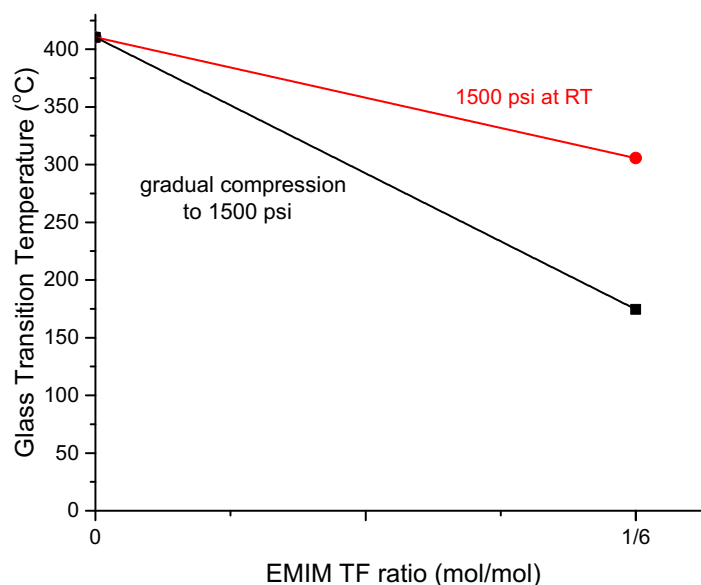


Figure 5.9 Effect of processing conditions on T_g : one-time compression to 1500 psi at room temperature decreases the plasticization power of ionic liquid (red). Gradual compression to 1500 psi as the sample is heated increases the plasticization of silicate glass with ionic liquid (black).

5.2. Investigation of Reaction Mechanism via FTIR

5.2.a. FTIR spectra at room temperature

FTIR measurements were performed to gain insights into interactions at molecular level. The normalized spectra are used in this section. Samples with 10 % CaKSiO_2 glass were prepared with ionic liquids of different types and ratios. These samples were compared to samples prepared with KSiO_2 to observe the effect of Ca^{2+} ions on plasticization mechanism.

Table 5.2 compares absorption bands for NaSiO₂ ([Na₂O]/[SiO₂]= 0.8) glass with that of 10 % CaKSiO₂. It is seen that the absorption bands are in close ranges for these two glasses, but specifically, the peak assignments show differences. Previously it has been reported that alkali ion type and concentration in silicate glasses have a great effect on the position of absorption peaks. The peaks at 730 and 935 cm⁻¹ decrease with increasing alkali ion concentration and appear at different positions for different alkali ions, whereas the peak at 468 cm⁻¹ remains the same [46, 47]. In the light of this information and other literature values, we assigned the peaks for synthesized silicate glasses and corresponding inorganic polymers by extrapolating the reported values for potassium metasilicate glasses. The vibrational wavenumbers and their assignments are summarized in Table 5.3.

Table 5.2 Absorption bands and peak assignments of NaSiO₂ ([Na₂O]/[SiO₂]= 0.8) and 10 % CaKSiO₂ glasses.

NaSiO ₂ ([Na ₂ O]/[SiO ₂]= 0.8) [46, 48]		10 % CaKSiO ₂	
Wavenumbers (cm ⁻¹)	Assignment	Wavenumbers (cm ⁻¹)	Assignment
468	Si-O-Si bending		
730	Si-O-Si stretching	703	Si-O bending [49]
935	Si-O ⁻ stretching (NBO)	908	Si-O ⁻ stretching [47]
		954	Si-O-Si vibration for Q ₂ [†] [50]
1040	Si-O stretching (BO)		

[†] Q_n stands for SiO₄ tetrahedra with n number of bridging oxygens (BO). Accordingly, Q₂ is SiO₄ tetrahedra with 2 BOs.

Table 5.3 Absorption bands and peak assignments of inorganic polymers (e.g., 10 % CaKSiO₂+EMIM TF).

Wavenumbers (cm ⁻¹)	Assignment
640	SO ₃ bending [51], C-H out-of-plane bending [51], O ⁻ ... ⁺ EMIM cation-motion vibration ‡
703	Si-O bending [49]
832	Isolated orthosilicate (SiO ₄ ⁴⁻) vibrations (Q ₀)§ [50]
908	Si-O ⁻ stretching [47]
954	Si-O-Si vibration for Q ₂ [50]
1164	R-SO stretching of TF ⁻ [51, 52]
1230	R-SO stretching of TF ⁻ [52, 53]
1259	R-SO stretching of TF ⁻ [52, 53]

FTIR plots in Figure 5.10 compares samples with different concentrations of EMIM TF with 10 % CaKSiO₂ glass. The absorbances at 703 and 954 cm⁻¹ are assigned to Si-O bending and Si-O-Si (Q₂) vibrations, respectively [49, 50]. These peaks remain approximately the same for all samples and are not affected by ionic liquid addition. Unlike these bands, peak formation occurs at 832 cm⁻¹ and peak intensities change at 640 and 908 cm⁻¹ upon addition of EMIM TF. Specifically, the peak intensity at 640 cm⁻¹ increases with addition of EMIM TF. This peak is reported to be SO₃ bending of TF⁻ anion and C-H out-of-plane bending of EMIM⁺ cation [51]. In this work, considering that EMIM⁺ interactions affect the peak at 640 cm⁻¹ and based on the data obtained for all samples, this peak is tentatively assigned to O⁻...⁺EMIM cation motion

‡ tentative assignment.

§ Q₀ stands for SiO₄ tetrahedra with no BOs, i.e., all oxygens bound to Si are non-bridging oxygens (NBO).

vibration. Once ionic liquid is introduced to 10 % CaKSiO₂ system, alkali ions are replaced by the cation (⁺EMIM) of ionic liquid^{**}, hence the peak intensity increases. By contrast, the band at 908 cm⁻¹ (Si-O⁻ stretching vibrations) decreases. This may be interpreted by the plasticization mechanism of modified silicate glass, in which K⁺ ions are replaced by EMIM⁺ cations of ionic liquid (Figure 5.11). As a result of ion replacement, the dipole moment change of Si-O⁻ decreases; so the peak intensity (908 cm⁻¹) decreases.

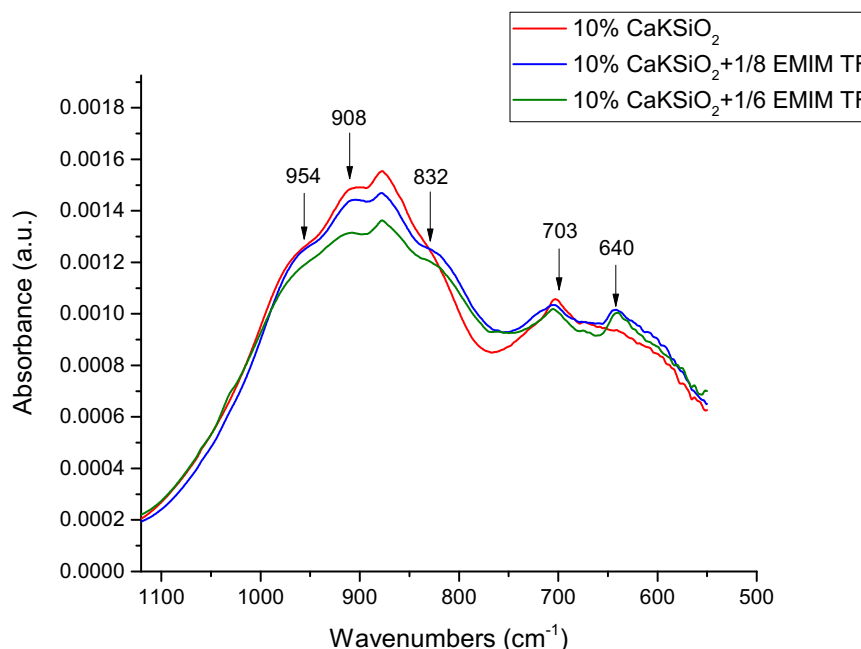


Figure 5.10 Room temperature FTIR spectra of 10 % CaKSiO₂ glass (red) and inorganic polymers made of 10 % CaKSiO₂ and EMIM TF with mole ratios of 1/8 (blue) and 1/6 (green).

^{**} This assumption is made based on the XRD data obtained in Figure 6.5.

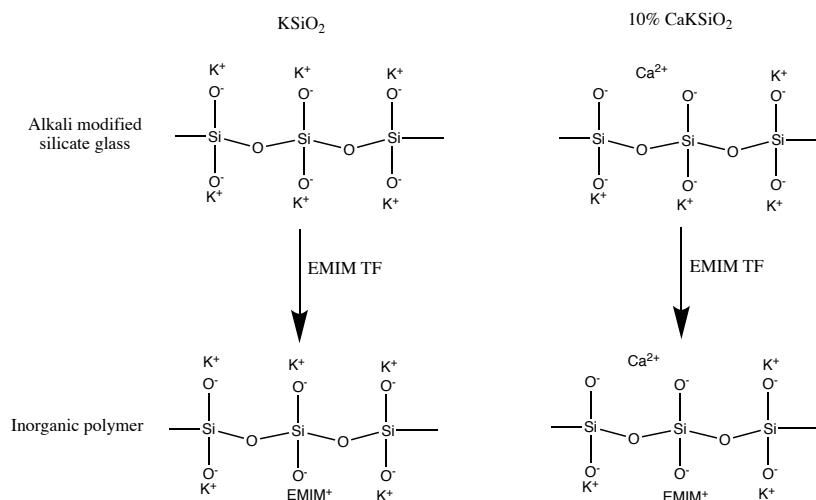


Figure 5.11 A simplified illustration of the reaction mechanism of EMIM TF with KSiO_2 (left) and 10 % CaKSiO_2 (right) glasses.

In Figure 5.10, it is also seen that the peak at 954 cm^{-1} slightly decreases for the EMIM TF ratio of 1/6 (highest concentration), while the peak at 832 cm^{-1} is formed. These bands are assigned to isolated Q_0 vibrations and Q_2 vibrations, respectively for 832 cm^{-1} and 954 cm^{-1} . This means, upon addition of EMIM TF, some of the Si-O-Si networking bonds (Q_2) are broken (concentration decreases) to form orthosilicate ions (Q_0) (concentration increases). Previously, it has been reported that Si-O-Si networking bonds can be broken in the presence of water molecules [54]. Based on the hydrophilic nature of EMIM TF, it may be interpreted that Q_2 bonds are broken due to the water molecules absorbed by the ionic liquid. Hence, increasing the concentration of ionic liquid, hydrolysis of Si-O-Si bonds increases, i.e., Q_2 concentration decreases. Another interpretation is that ionic liquids are effective in breaking some of the Si-O-Si bonds, that there exists a second plasticization mechanism, in which Si-O-Si bonds are broken.

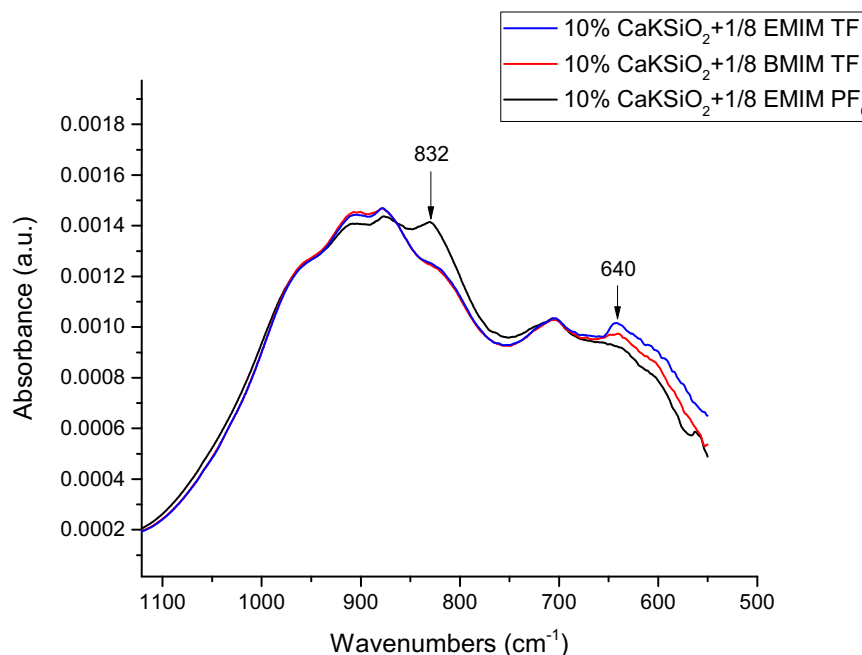


Figure 5.12 Room temperature FTIR spectra of inorganic polymers made of 10 % CaKSiO_2 and 1/8 mole ratios of different ionic liquids: EMIM TF (blue), BMIM TF (red), EMIM PF_6 (black).

Figure 5.12 compares the effect of different ionic liquids on peaks at 832 and 640 cm^{-1} . EMIM TF and BMIM TF show similar behavior at 832 cm^{-1} , whereas the intensity increases significantly for EMIM PF_6 . On the contrary, intensity is the lowest at 640 cm^{-1} for EMIM PF_6 . This indicates that EMIM PF_6 affects the hydrolysis of Si-O-Si bond but does not dissociate well enough to form $\text{O}^- \cdots {}^+\text{EMIM}$ interactions. Poor dissociation of EMIM PF_6 can be explained by its higher melting point compared to EMIM TF and BMIM TF. The FTIR data given above were taken at room temperature at which EMIM PF_6 is in solid state (T_m : 58.9 $^\circ\text{C}$) [55]. This means that, at room temperature, EMIM PF_6 does not dissociate to interact with the silicate glass. Thus, $\text{O}^- \cdots {}^+\text{EMIM}$ interactions do not occur and therefore the peak intensity at 640 cm^{-1} does not increase. DSC data shows that EMIM PF_6 is not as efficient as EMIM TF in decreasing the T_g . Considering that T_g decreases as a result of an increase in the free

volume due to cation exchange, it may be concluded that, at room temperature, the cations of EMIM PF₆ are not favored to interact with non-bridging oxygens and, as a result, EMIM PF₆ becomes a poor plasticizer for silicate glasses.

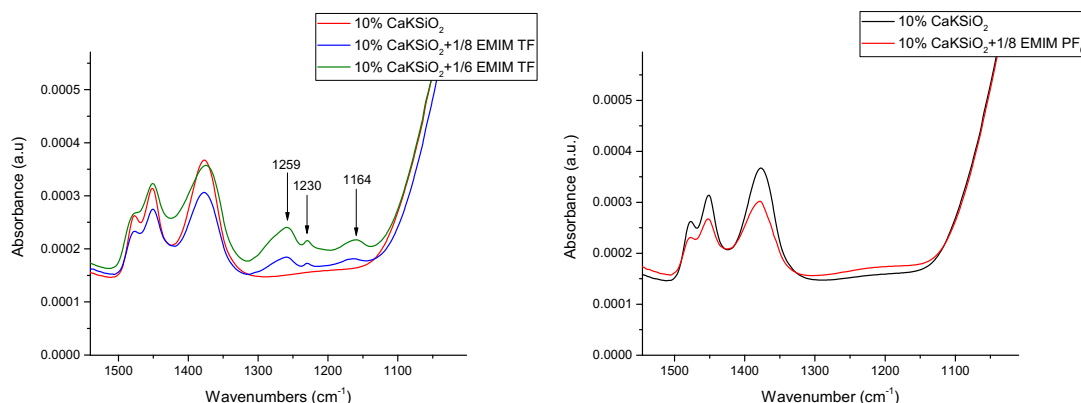


Figure 5.13 Effect of ionic liquid amount (left): room temperature FTIR spectra of 10 % CaKSiO₂ glass (red) and inorganic polymers made of 10 % CaKSiO₂ and EMIM TF with mole ratios of 1/8 (blue) and 1/6 (green). Effect of ionic liquid type (right): room temperature FTIR spectra of 10 % CaKSiO₂ glass (black) and inorganic polymer made of 10 % CaKSiO₂ and 1/8 mole ratio of EMIM PF₆ (red).

In Figure 5.13 (left) bands at 1164, 1230, and 1259 cm⁻¹ are assigned to R-SO stretching vibrations of trifluoromethane sulfonate (TF⁻) anion [51-53]. Starting with 10 % CaKSiO₂, peaks are formed once the ionic liquid is added to the structure. As expected, higher concentrations of ionic liquid show more intense peaks.

Figure 5.13 (right) compares 10 % CaKSiO₂ glass with the sample made of 10 % CaKSiO₂ and 1/8 mole ratio of EMIM PF₆. It is seen that no peaks occur at positions 1164, 1230, and 1259 cm⁻¹, due to absence of TF⁻ anions.

5.2.b. FTIR spectra at higher temperatures

Systems behave differently as they approach their glass transition temperatures. To define T_g in terms of free volume, it is important to study the response of specific bonds to temperature change to obtain insights into glass transition mechanism. It is

known that average kinetic energy increases with increased temperature, resulting in increased free volume [57]. Thus, the response of bonds which are involved in glass transition will give different spectra as the temperature is increased. Previously it has been reported that T_g can be determined by tracing the peak changes in FTIR spectra at different temperatures [58]. As the system approaches the T_g , the intensity of a certain peak will either increase or decrease depending on the glass transition mechanism and, by plotting the change in relative intensities against temperature, T_g is determined as the inflection point [59].

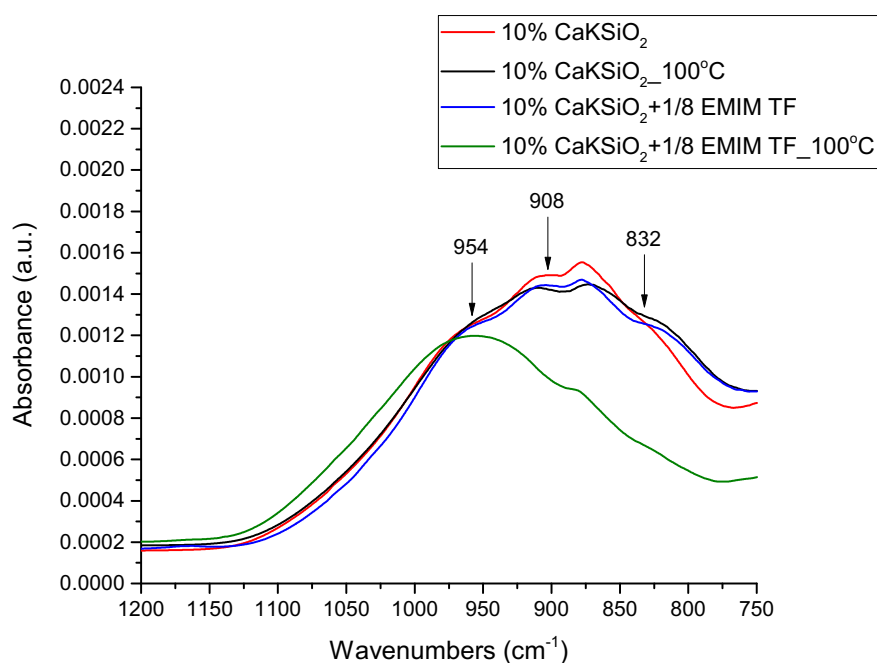


Figure 5.14 FTIR spectra of 10 % CaKSiO₂ glass at room temperature (red) and 100 °C (black) compared with that of inorganic polymer made of 10 % CaKSiO₂ and 1/8 mole ratio of EMIM TF at room temperature (blue) and 100 °C (green).

It is confirmed by our DSC measurements that ionic liquids decrease the T_g of silicate glasses. In other words, they increase the free volume and shift the system towards glass transition (note that we are discussing the system that is at the temperature lower than T_g). FTIR spectra are collected at elevated temperatures to bring the samples

closer to glass transition and investigate the role of ionic liquids on glass transition mechanism. Figure 5.14 compares 10 % CaKSiO₂ glass with its corresponding inorganic polymer prepared with 1/8 mole ratio of EMIM TF at room temperature and at 100 °C. It is observed that the peak at 908 cm⁻¹ due to Si-O⁻ stretching mode in 10 % CaKSiO₂ glass becomes slightly weaker when temperature is increased (red → black), whereas for inorganic polymer, i.e., with addition of ionic liquid and increased temperature, this weakening is significant (blue → green). This may be explained for both samples by the movement of K⁺ ions away from Si-O⁻ bonds as a result of increased average kinetic energy. However, the reason for the difference in the degree of change may be explained as follows. As used for the explanation of the drop of the 908 cm⁻¹ peak intensity in Figure 5.10, the drop may be due to the replacement of K⁺ cations with EMIM⁺ cations; dipole moment (change) of the Si-O⁻ bond decreases as a result of the change from Si-O⁻ ... ⁺K to Si-O⁻ ... ⁺EMIM, since EMIM⁺ attracts electrons less than K⁺, leading to smaller dipole moment of the Si-O⁻ bond. This drop is more pronounced at higher temperatures, because dipole moment is larger at higher temperatures due to higher kinetic energy. Thus, the drop of the peak intensity is more significant at higher temperatures.

In addition to this observation, another valuable interpretation can be made by comparing 10 % CaKSiO₂ glass at 100 °C (black) with its inorganic polymer at room temperature prepared with 1/8 mole ratio of EMIM TF (blue). The intensities at 908 cm⁻¹ are very close for these two samples. This suggests that the free volume gained due to increased temperature (by 75 °C) can also be obtained by addition of ionic liquid at room temperature. In other words, addition of ionic liquid moves the system towards glass transition that occurs at lower temperatures.

Si-O-Si network structure changes as the temperature is increased. Band at 832 cm^{-1} decreases significantly, while 954 cm^{-1} remains the same. This indicates that upon increase in temperature, water is removed from the system and Q_0 bonds go through condensation reaction reforming bridging oxygens.

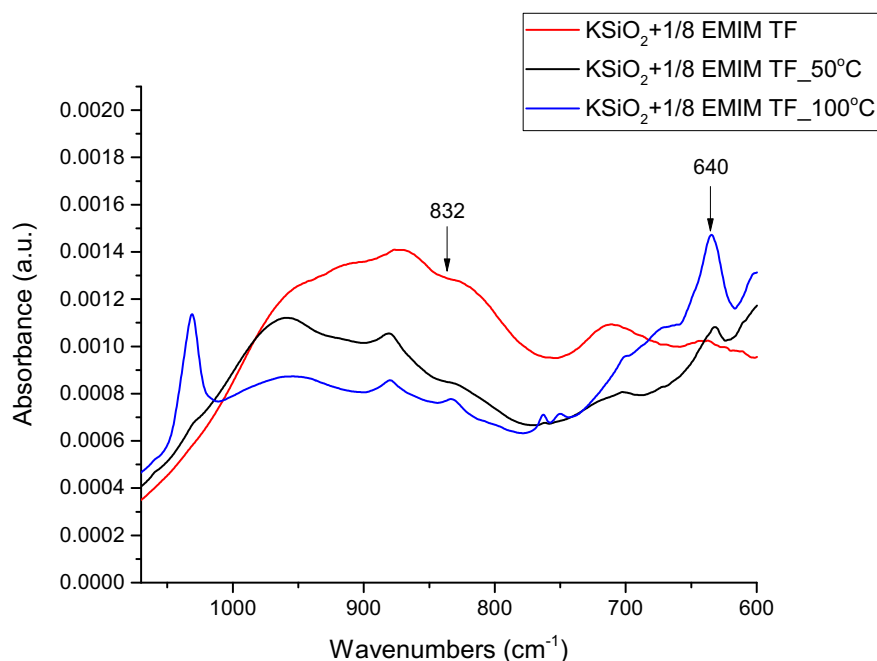


Figure 5.15 FTIR spectra of inorganic polymer made of KSiO_2 and 1/8 mole ratio of EMIM TF at room temperature (red), $50\text{ }^\circ\text{C}$ (black), and $100\text{ }^\circ\text{C}$ (blue).

Spectra for KSiO_2 glass system is collected as a reference to simplify the structure in question. By increasing the temperature, it is intended to eliminate the effect of water and obtain more information on the role of ionic liquids in glass transition mechanism. In Figure 5.15, FTIR spectrum at room temperature is compared to the spectra at $50\text{ }^\circ\text{C}$ and $100\text{ }^\circ\text{C}$ for inorganic polymers with 1/8 mole ratio of EMIM TF. Comparison shows that, at higher temperatures, Q_0 (832 cm^{-1}) concentration becomes smaller. This again suggests condensation of Q_0 bonds to more connective structures ($Q_{n>0}$).

The intensity at 640 cm^{-1} increases with increasing temperature. This may be explained in terms of dipole moments as a function of temperature. Due to the increase in temperature, kinetic energy increases; thus cation-motion vibration of the $\text{Si-O}^- \cdots {}^+\text{EMIM}$ group is increased. This means larger change in the dipole moment, leading to larger peak heights, (Figure 5.15). Another possible explanation is that, more replacement of K^+ ions with EMIM^+ ions occur when temperature is increased; $\text{Si-O}^- \cdots {}^+\text{EMIM}$ concentration (640 cm^{-1}) becomes larger (Figure 5.15). This may be explained thermodynamically as follows: $\text{O}^- \cdots {}^+\text{K}$ bonds are stronger than $\text{O}^- \cdots {}^+\text{EMIM}$ bonds, since K^+ is smaller than EMIM^+ and thus forms stronger bonds with O^- . Therefore, in the reaction, $\text{O}^- \cdots {}^+\text{K} + \text{EMIM}^+\text{TF}^- \rightarrow \text{O}^- \cdots {}^+\text{EMIM} + \text{K}^+\text{TF}^-$, $\Delta H > 0$. On the other hand, $\Delta S > 0$, since K^+TF^- is smaller than EMIM^+TF^- and easier to move around, leading to higher entropy. Because $\Delta G = \Delta H - T\Delta S$, the effect of entropy becomes more important when T becomes higher. The higher the T , the larger the thermodynamic driving force for such a reaction. The replacement of smaller cations (K^+) with larger ones (EMIM^+) is previously reported for plasticization of polyelectrolyte complexes by ionic liquids [60] and is also seen for inorganic polymers here.

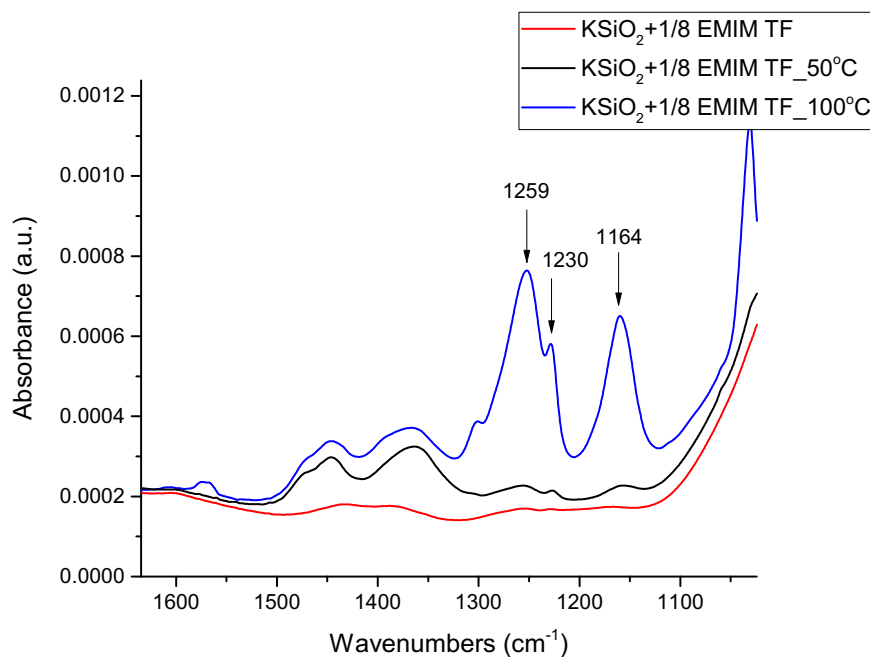


Figure 5.16 FTIR spectra of inorganic polymer made of KSiO₂ and 1/8 mole ratio of EMIM TF at room temperature (red), 50 °C (black), and 100 °C (blue).

Figure 5.16 represents the bands at 1164, 1230, and 1259 cm⁻¹ for the same samples as those in Figure 5.15. As mentioned above, these peaks are assigned to R-SO stretching vibrations of TF⁻ anion. The intensities of these peaks increase as the temperature increases from room temperature, to 50 °C, and to 100 °C. Since a peak intensity is proportional to the change in the polarity (i.e., dipole moment) of the bonds involved and since increased temperature leads to larger dipole moments, peak intensity increases with temperature, as seen in Figure 5.16.

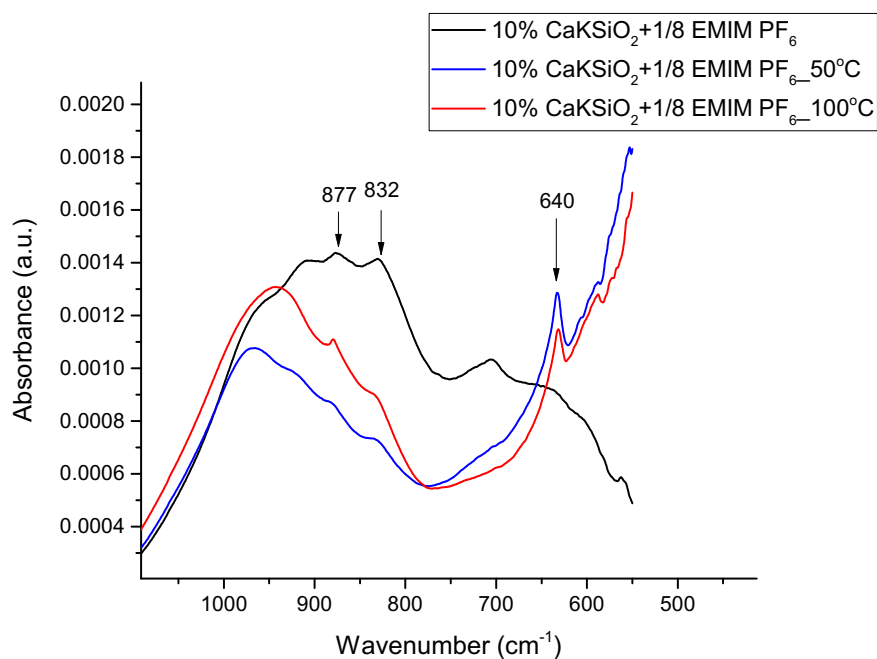


Figure 5.17 FTIR spectra of inorganic polymer made of 10 % CaKSiO_2 and 1/8 mole ratio of EMIM PF_6 at room temperature (black), 50 °C (blue), and 100 °C (red).

The interactions can be further confirmed by changing the ionic liquid from EMIM TF to EMIM PF_6 (Figure 5.17). Having a melting point above room temperature, this sample showed negligible interactions at 640 cm^{-1} band. However, at elevated temperatures which are close to and even higher than T_m of EMIM PF_6 , the interactions increase and become comparable to EMIM TF systems (Figure 5.18). This reveals the importance of ionic liquid selection according to application purposes.

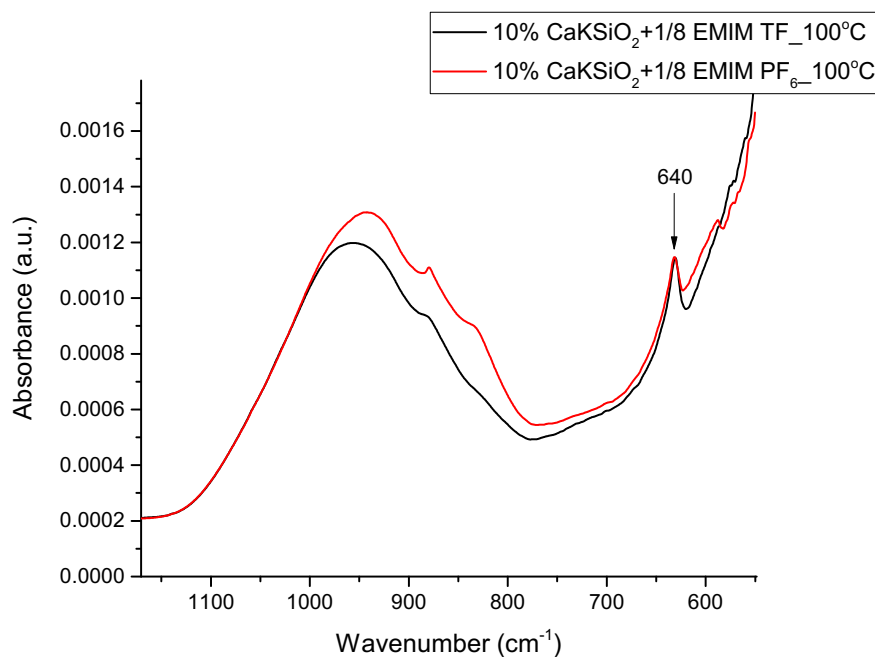


Figure 5.18 FTIR spectra of inorganic polymers made of 10 % CaKSiO₂ and 1/8 mole ratios of EMIM TF (black) and EMIM PF₆ (red) at 100 °C.

5.3. Mechanical Properties of CaKSiO₂-based Inorganic Polymers

Compressive data of inorganic polymers were collected according to ASTM standards (D695-15) [18]. Figure 5.19 gives the stress-strain curve for the two identical 5 % CaKSiO₂ based samples prepared with 1/8 mole ratio of EMIM TF and Figure 5.20 compares 5 % CaKSiO₂ system to NaSiO₂ system. Compressive modulus, strength, and toughness were calculated from the plot and are given in Table 5.4. Polystyrene (PS) sample was molded in this laboratory and tested to be used as a reference.

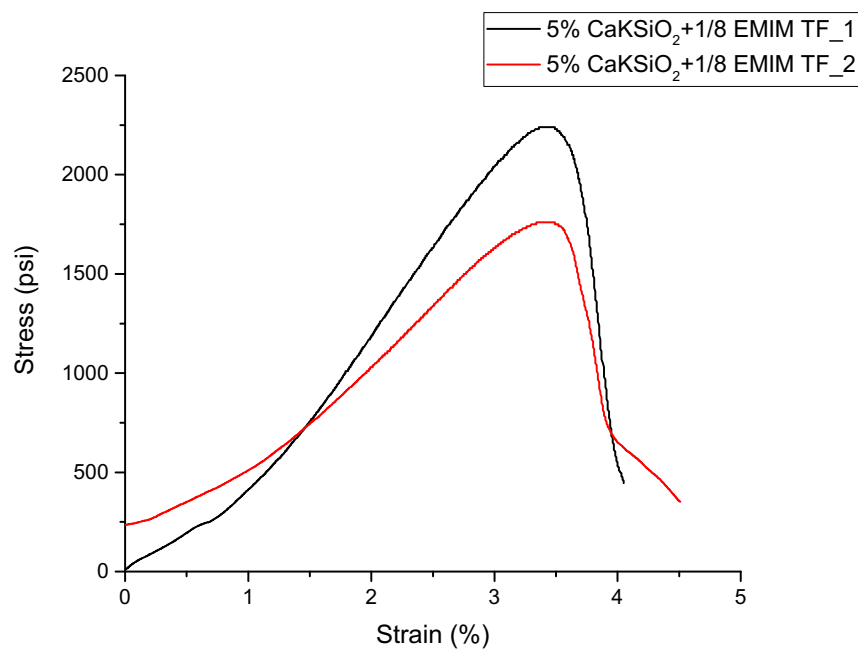


Figure 5.19 Compressive stress-strain curves for samples made of 5 % CaKSiO_2 and 1/8 mole ratio of EMIM TF (compression molded at 180 °C and 1500 psi).

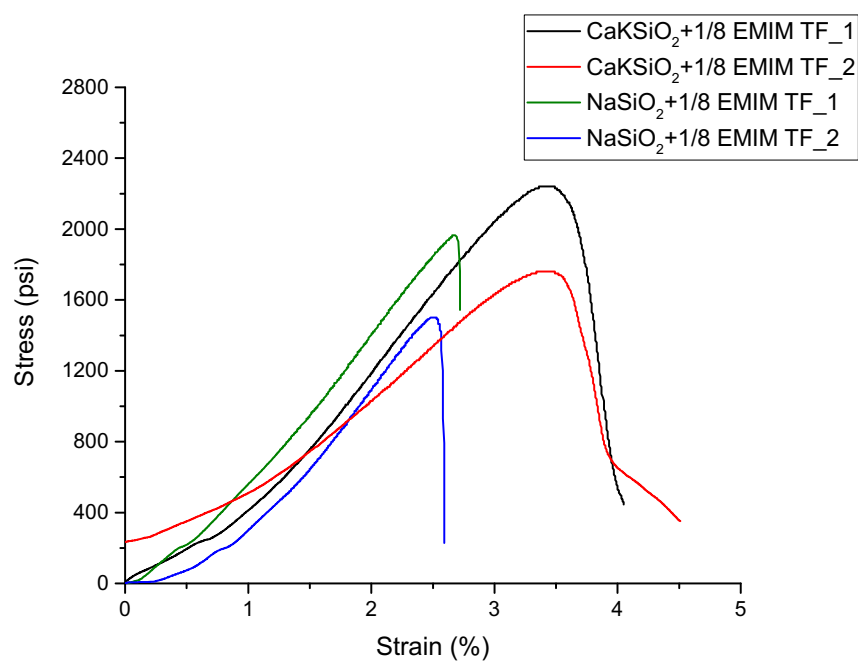


Figure 5.20 Compressive stress-strain curves for samples made of 1/8 mole ratio of EMIM TF and 5 % CaKSiO_2 (black and red) and NaSiO_2 (green and blue).

Results show that mechanical properties of 5 % CaKSiO₂ based samples are reproducible to some extent. The differences in the compressive data may be due to the local inhomogeneities in the sample that can cause premature fracturing (see section 5.4). As seen in Table 5.4, compressive strength values of monovalent (NaSiO₂) and divalent/monovalent (5 % CaKSiO₂) inorganic polymers are comparable. Both systems possess compressive strengths in the range 10-15 MPa, whereas compressive strength for PS is much greater (67.8 MPa). Nevertheless, the modulus values for both inorganic polymers (0.41-0.63 GPa range) are found to be comparable to PS sample (0.63 GPa). The modulus of another widely used conventional polymer, high density polyethylene (HDPE), is reported to be in the range of 0.5-1.4 GPa [61]. These results indicate that even the preliminary modulus data of prototype inorganic polymers are comparable to those of conventional polymers. When synthesis conditions and processing methods are further improved, as has been witnessed in the development of many organic polymers used today, inorganic polymers with better mechanical properties will be produced, which can replace organic polymers for various applications.

Table 5.4 Compressive mechanical properties of SiO₂-based inorganic polymers

Sample Type	Sample Number	Modulus		Toughness		Compressive Strength	
		(ksi)	(GPa)	(psi)	(MPa)	(psi)	(MPa)
NaSiO ₂	1	85.8	0.59	24.3	0.17	1964	13.5
	2	92.0	0.63	15.5	0.11	1500	10.3
CaKSiO ₂	1	87.6	0.60	45.0	0.31	2240	15.4
	2	59.9	0.41	41.6	0.29	1760	12.1
Polystyrene (PS) ^{††}		91.7	0.63	541.7	3.73	9830	67.8

^{††} measured values by using the PS sample of the same size and using the same instrument

Finally, toughness value of 5 % CaKSiO₂ based sample is doubled compared with that of NaSiO₂. Increased compressive properties by using divalent ions are well known. For example, in dentistry, divalent ions such as Ca²⁺ and Zn²⁺ are incorporated into polycarboxylates (e.g., polyacrylic acid) and form the cement whose compressive properties are increased significantly [62]. On the other hand, as in the case of compressive strength, the toughness values are much smaller for inorganic polymers than for PS sample. Organic polymers are generally more ductile than silicate based inorganic polymers produced to date in this laboratory.

After all, it should also be noted that when plasticized with ionic liquid, the mechanical properties of silicate glass are shifted towards those of conventional polymers. Ceramics in general are brittle materials: they possess high mechanical strength and high modulus, as opposed to ductile organic polymers [27, 28]. Hereby, the most significant difference between the two materials is their stiffness (elasticity), quantified by modulus. The modulus of a typical silicate glass (e.g., soda lime glass) is 71.6 GPa at room temperature as compared to that of PS at 0.63 GPa, whereas the strain is only 0.1-0.2 % [63]. Geopolymers, covalently bonded inorganic amorphous materials, behave similar to silicate glasses; they show high modulus and strength, but very low strain [64]. Herein, inorganic polymers proposed in this work carry characteristics of organic polymers rather than typical silicate glasses or geopolymers.

As is well known, polymers are more ductile than ceramics, or amorphous polymers are more ductile than amorphous glass. This is because polymers can develop energy-absorbing mechanisms, such as crazing and shear deformation, when force is applied [19]. By contrast, only cracks are formed under loading without forming any energy-absorbing mechanisms for glass. So, they are in general very brittle. At molecular level, this is related to the (local) molecular motion. For polymers made of

linear chains or very lightly cross-linked chains, relatively large molecular mobility allows the formation of crazes or shear deformation zones [65, 66]. By contrast, glass is usually highly cross-linked, making molecular motion difficult. Thus, formation of crazes or shear deformation zones cannot be possible. We intended to achieve such structure for our inorganic polymers by using ionic liquid as a plasticizer such that molecular motion is enhanced and thus formation of crazes/shear zones may be possible. Although we have not tried to observe craze/shear deformation structures by using a TEM technique [66-68], the observation of such structures can be another strong evidence for our claim that polymers can be made from glass by adding ionic liquid.

5.4. TEM / SEM

TEM pictures were taken for inorganic polymer made of 10 % CaKSiO_2 and 1/10 mole ratio of EMIM TF. The sample was compression molded at 190 °C and 1500 psi. Electron diffraction pattern is composed of concentric rings with no reflections of any ordered (crystal) structure (Figure 5.21, left). This proves that synthesized inorganic polymers possess no long-range order, indicating amorphous structure.

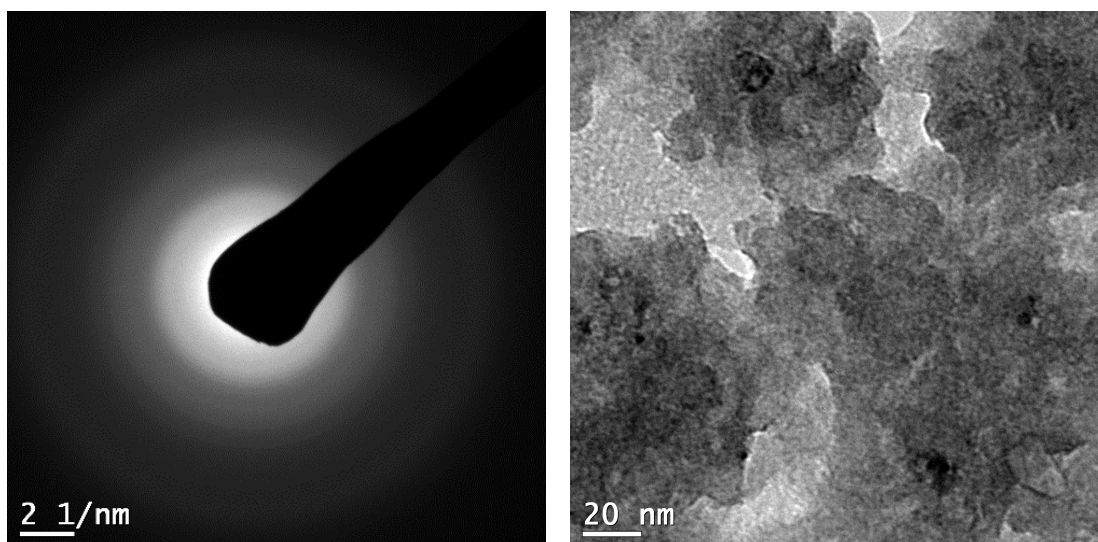


Figure 5.21 Electron diffraction pattern (left) and TEM picture of inorganic polymer made of 10 % CaKSiO_2 and 1/10 mole ratio of EMIM TF (right).

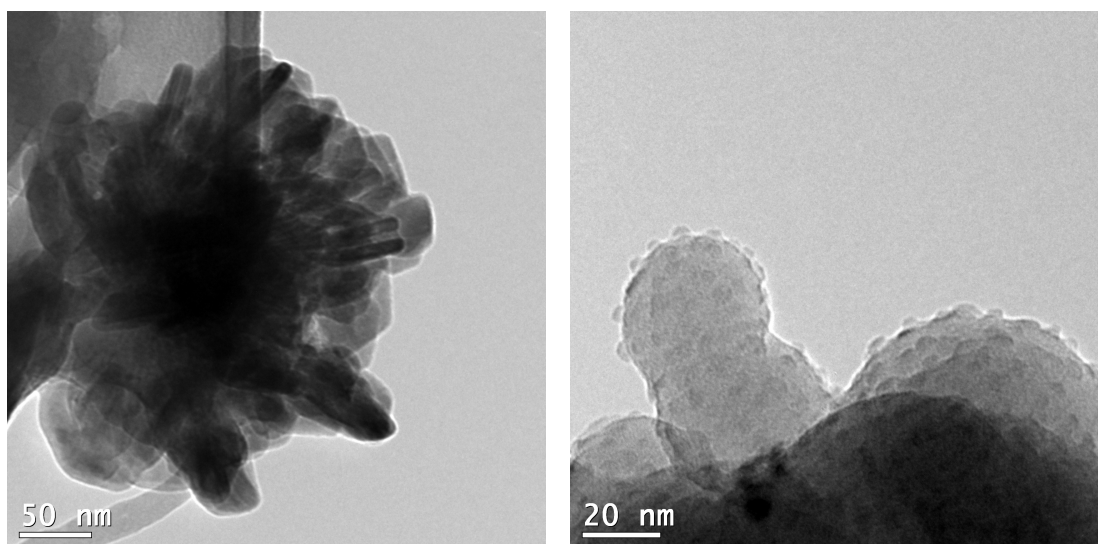


Figure 5.22 TEM pictures of inorganic polymer made of 10 % CaKSiO_2 and 1/10 mole ratio of EMIM TF.

Locally this sample is heterogeneous with clusters formed at about size of 60 nm, but overall it is homogeneous (Figure 5.21, right). Similar structures were reported for silicates with nano-clusters and silica [69-71]. Although these are preliminary data, some unique structures are found by TEM. Figure 5.22 shows the formation of unique structure which is formed by the assembly of nano-sized structures, i.e., rod-like structures (Figure 5.22, left) and spherical structures (Figure 5.22, right).

SEM and EDS images were collected for the sample with 30 % SrRbSiO_2 and 1/8 mole ratio EMIM TF to obtain information on sample topography and elemental distribution (Figure 5.23). EDS images show that ionic liquid is distributed homogeneously throughout the sample; however, local heterogeneity exists in nanometer scale. As expected, the majority of elements consist of silicon (pink dots) and oxygen (red dots). At around 100 nm, clusters of green, yellow, and blue dots are recognized, which stand for carbon, sulfur, and rubidium, respectively. This confirms the presence of rubidium triflate nano-crystals in the structure. Hence, SEM and EDS images are in agreement with TEM pictures. Additionally, they confirm the XRD data collected for the sample with 50 % SrRbSiO_2 and 1/12 mole of EMIM TF (Figure 6.5).

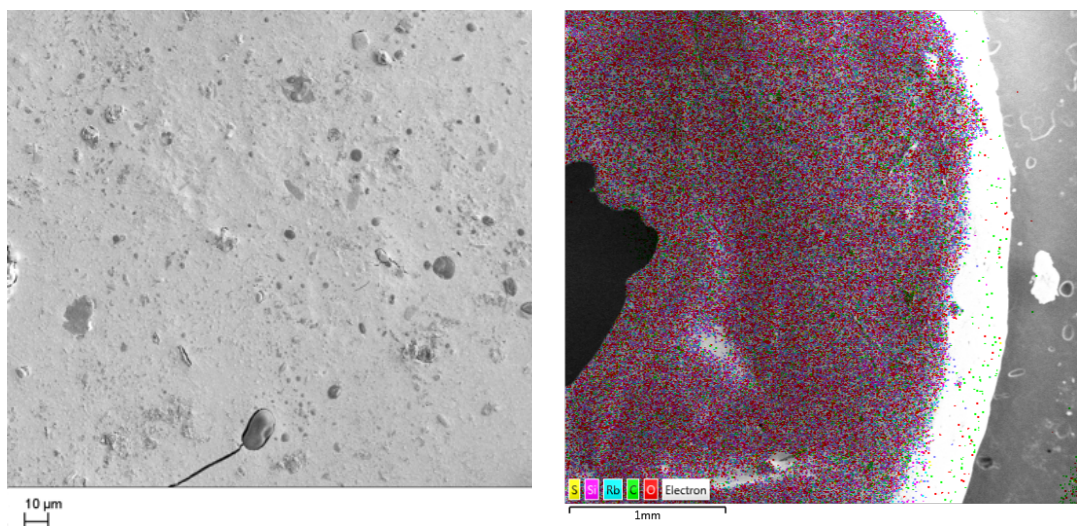


Figure 5.23 SEM (left) and EDS (right) images of the sample prepared with 30 % SrRbSiO_2 and 1/8 mole ratio EMIM TF compression molded at 95 °C and 1000 psi.

Chapter 6

RESULTS: DIVALENT/MONOVALENT SYSTEM

(SrRbSiO₂)

6.1. Effect of Ionic Liquid Addition on Glass Transition Temperature, T_g

6.1.a. *Effect of glass structure*

Ionic liquid works as a plasticizer. Addition of EMIM TF decreases the T_g of SrRbSiO₂ (modified silicate) glass. In Figure 6.1 DSC thermograms of two different inorganic polymers are shown. The top curve (black) shows the scan for 10 % SrRbSiO₂ silicate glass and the bottom curve (red) for 30 % SrRbSiO₂ silicate glass. Both are mixed with 1/12 ratio of EMIM TF and compression molded at 150 °C and 1000 psi. The T_g values of modified silicate glasses decrease to 233.5 °C and 284.3 °C for 10 % and 30 % alkali ratios, respectively.

The T_g value of the silicate glass/ionic liquid system depends on the T_g value of the pure glass (i.e., in the absence of ionic liquid). For example, 10 % SrRbSiO₂ glass shows a T_g at 373.1 °C. Addition of ionic liquid expands the ring structure of silicate glass, creating additional free volume for local molecular motion. Consequently, glass transition temperature (i.e., processing temperature) decreases to 233. 5 °C. On the other hand, 30 % SrRbSiO₂ silicate glass does not show a T_g up to 450 °C. However, once ionic liquid is added to the system, it works as a plasticizer and the T_g appears at 284.3 °C. The difference in these two systems show that, although ionic liquid works

as a plasticizer, the original structure of modified silicate glass has a great effect on the final properties (e.g., glass transition temperature) of inorganic polymers.

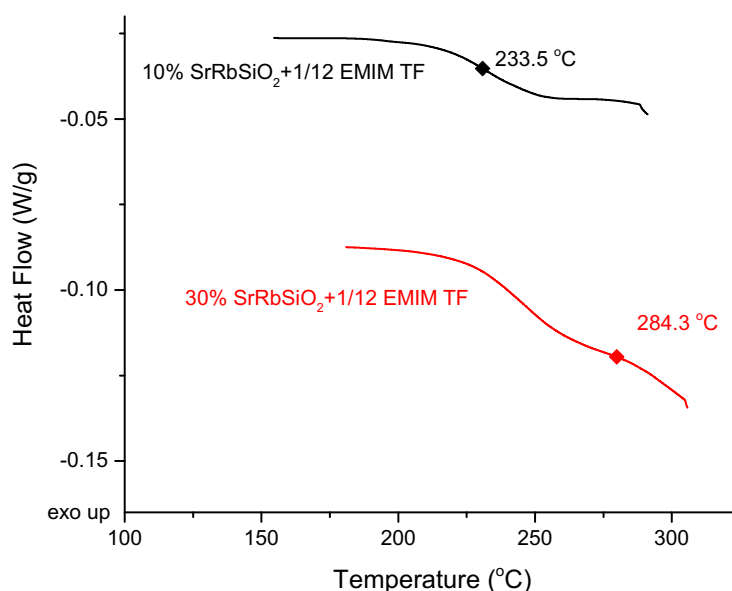


Figure 6.1 Effect of divalent ion ratio: DSC thermograms of inorganic polymers made of 1/12 mole ratio of EMIM TF and 10 % SrRbSiO₂ (black) and 30 % SrRbSiO₂ (red).

6.1.b. Effect of the type of ionic liquid

In addition to the (original) structure of silicate glass, the type of ionic liquid has a great effect on properties of inorganic polymers. Here, different ionic liquids, i.e. EMIM TF (red), EMIM ES (blue), and EMIM BF₄ (green), were mixed with 30 % SrRbSiO₂ glass. The inorganic polymers were made by compression molding at 150 °C and 1000 psi. Figure 6.2 shows the DSC thermograms of these inorganic polymers. The T_g of the inorganic polymer prepared with EMIM TF is 284.3 °C, whereas when prepared with EMIM ES, the T_g is 341.9 °C. Obviously, EMIM TF is a better plasticizer than EMIM ES.

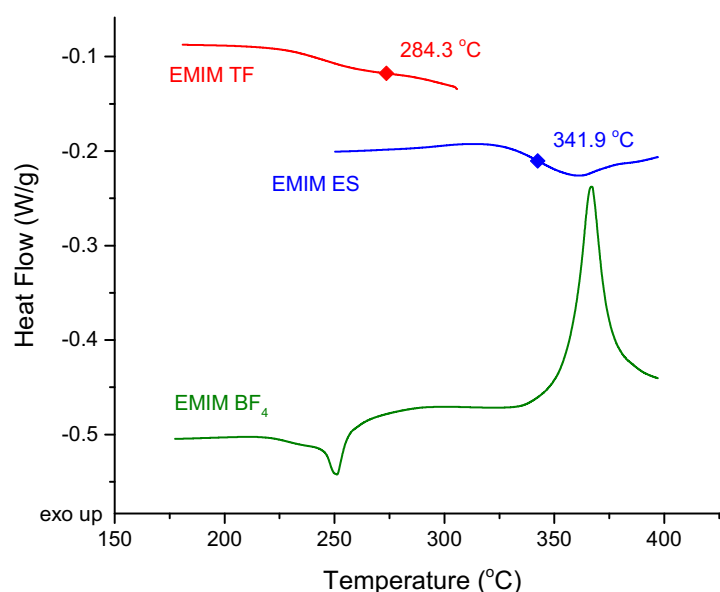


Figure 6.2 Effect of the type of ionic liquid: DSC thermograms of inorganic polymers made of 30 % SrRbSiO₂ and 1/12 mole ratio of EMIM TF (red), EMIM ES (blue), and EMIM BF₄ (green).

Figure 6.2 also shows that not all ionic liquids work effectively as a plasticizer. Depending on the structure of ionic liquid and its interactions with silicate glass, inorganic polymer samples may show crystallization. For example, when prepared with EMIM BF₄, 30 % SrRbSiO₂ glass shows crystal formation. T_g of this inorganic polymer could not be detected in the thermogram. In addition to the possibility that EMIM BF₄ did not work as a plasticizer, another scenario is that T_g of silicate glass is overlapped with crystallization and melting peaks of newly formed crystals (most likely small molecular crystals) so that T_g cannot be identified. However, this does not mean that EMIM BF₄ cannot be used as a plasticizer for silicate glasses. This specific ionic liquid may work effectively for other ratios of SrRbSiO₂ or other glasses modified with different alkali ions, such as Ca and K.

6.1.c. *Effect of synthesis (processing) conditions*

Synthesis conditions affect the properties of inorganic polymers. It is observed that pressure has a significant effect on T_g values. Figure 6.3 illustrates the DSC curves for two samples that were prepared with 10 % SrRbSiO₂ glass and 1/12 EMIM TF. The samples were compression molded at 150 °C, and at 1000 psi (green curve) and at 1500 psi (red curve). Glass transition temperatures (T_g) are 292.6 °C and 231.5 °C, respectively for these inorganic polymers. This result seems contradicting to the result in section 5.1, where it was observed that applying a pressure of 1500 psi at room temperature lead to higher values of T_g . In the current set of experiments (SrRbSiO₂ system), samples were molded between aluminum foils, so that ionic liquid remained in the structure even at high temperatures. In the case of CaKSiO₂ system (in Chapter 5), samples were compression molded in a cylindrical mold, where ionic liquid easily leaked and left the system with less amount of ionic liquid remaining at high temperatures. This leads to higher T_g than expected. Therefore, apparent contradiction on the effect of applied pressure between the current experiment and previous experiment is a result of difference in the retention of ionic liquid during molding.

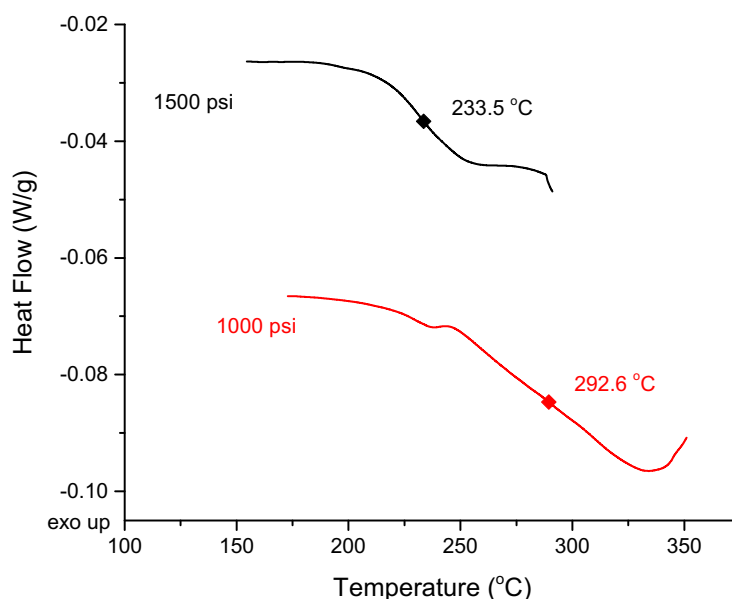


Figure 6.3 DSC second heating curves for samples made of 10 % SrRbSiO₂ glass and 1/12 EMIM TF. Compression molding conditions are 150 °C and 1500 psi (black curve) and 1000 psi (red curve).

To explore the effect of pressure further, another inorganic polymer was synthesized, but during molding no pressure was applied, keeping the other conditions the same. DSC data for these samples show that crystallization is highly promoted when no pressure is applied (Figure 6.4). It is concluded that increasing pressure decreases T_g due to increased mixing. When no pressure is applied, ionic liquid cannot penetrate into the ring structure of SrRbSiO₂ glass (Figure 3.15) and only reacts with the cations on the surface of the ring (i.e., Rb⁺). XRD data for the sample made of 50 % SrRbSiO₂ glass and 1/12 EMIM TF confirms the presence of rubidium-triflate (RbTF) crystals in the structure (Figure 6.5). It is also expected that higher divalent ion ratio increases the tendency for crystallization, as divalent ions bind to NBOs stronger than monovalent ions do, blocking the ionic liquids from going into the silicate ring structure.

Figure 6.5 XRD data for the sample made of 50 % SrRbSiO₂ glass and 1/12 EMIM TF. Literature data for RbTF (red curve) matches the sample data (black curve) very well.

The reactions of SrRbSiO_2 glass with ionic liquid depend on the ionic liquid structure. Due to different mechanisms, samples prepared with different ionic liquids show different thermal behavior and properties. Inorganic polymers prepared with EMIM TF are found to have higher tendency for crystallization, whereas when prepared with EMIM ES they decompose at lower temperatures, thus crystallization, if any, cannot be observed.

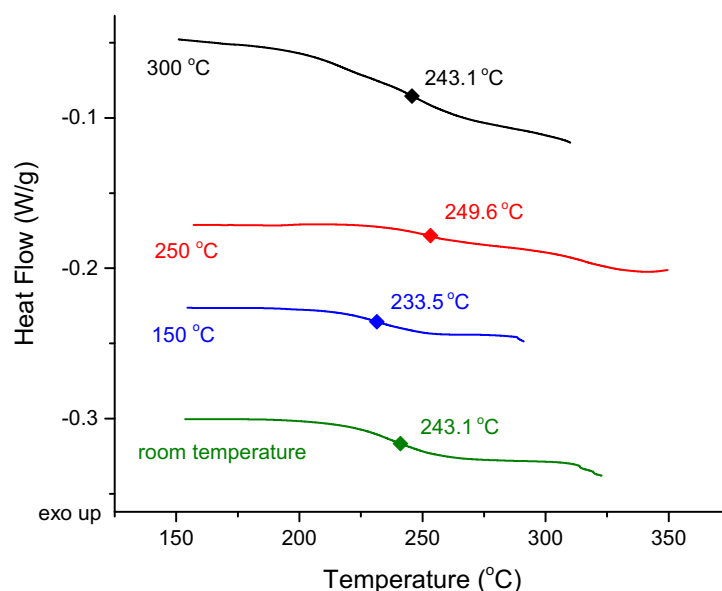


Figure 6.6 Effect of heating: DSC second heating curves for inorganic polymers made of 10 % SrRbSiO_2 and 1/12 EMIM TF under 1500 psi. The compression molding temperatures are 300 °C (black), 250 °C (red), 150 °C (blue) and room temperature (green).

Table 6.1 T_g of inorganic polymers made of 10 % SrRbSiO₂ and 1/12 EMIM TF, compression molded under 1500 psi and at different temperatures.

Compression molding temperature (°C)	Glass transition temperature (°C)
25	243.1
150	233.5
250	249.6
300	243.1

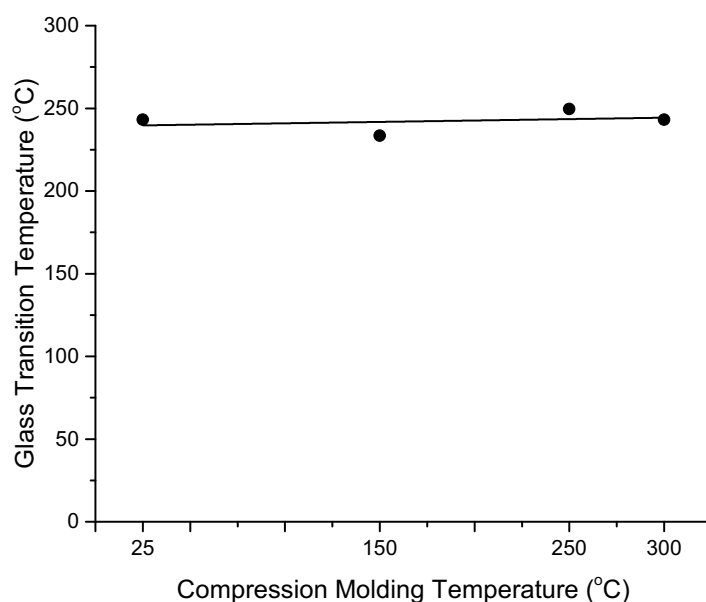


Figure 6.7 Effect of compression molding temperature on T_g for the inorganic polymer made of 10 % SrRbSiO₂ and 1/12 mole ratio of EMIM TF.

Heat applied during compression molding has little effect on T_g . A set of four samples was prepared using 10 % SrRbSiO₂ and 1/12 EMIM TF. The composition was kept constant and the temperature of compression molding was changed. It was observed that changing the processing temperature did not affect the T_g (Figure 6.7). However, special attention should still be paid to the temperature due to decomposition of ionic liquid above 300 °C. DSC data for all the samples show an endothermic peak

at a temperature above 300 °C, which is attributed to the decomposition of ionic liquid in inorganic polymer structure.

6.2. Effect of Water on Inorganic Polymer Properties

Previously it has been reported that water molecules penetrate into silicate glass structure and react [54]. Water acts like a plasticizer and affects the thermal properties of glasses [72, 73]. To minimize water absorption by inorganic polymers and hence its effects on properties, divalent ions are added to the system. It has been observed that addition of divalent ions decreases water absorption significantly but cannot eliminate it completely.

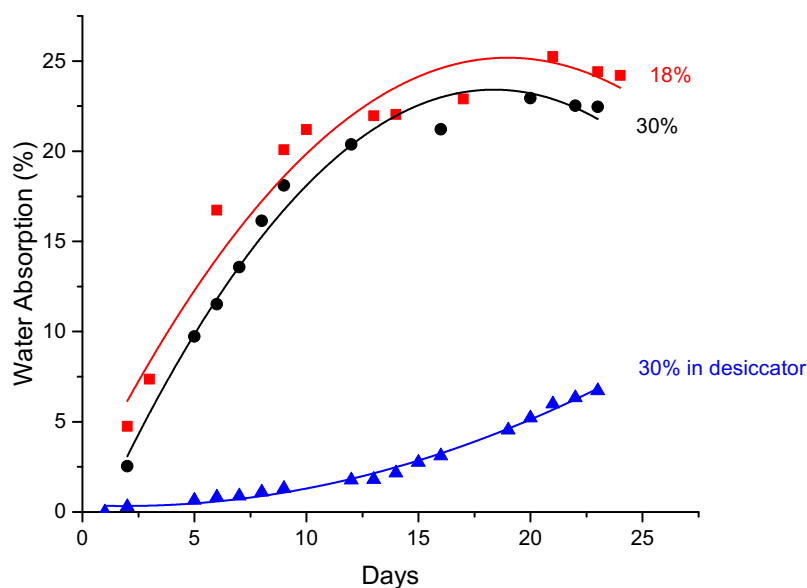


Figure 6.8 Water absorption of samples made of 18 % and 30 % $\text{SrRbSiO}_2 + 1/3$ mole ratio of EMIM TF.

Figure 6.8 compares water absorption of samples prepared with 30 % SrRbSiO_2 and 18 % SrRbSiO_2 using $1/3$ mole ratio of EMIM TF. These samples, left on lab bench

and exposed to air, were compared to the sample (made of 30 % SrRbSiO₂ and 1/3 mole ratio EMIM TF) left in a desiccator.

As expected, the more divalent ions are present in the structure, the less is the water absorption by the sample. Percent water absorption stays higher for 18 % SrRbSiO₂ sample than for 30 % SrRbSiO₂ sample at all times. For both samples, absorption rate (i.e., the slope of the curve) is high in the first 15 days and reaches a plateau of around 25 wt.% absorption. In contrast, the sample left in a desiccator shows significantly low absorption rates compared to the other samples. Water absorption reaches only 6.73 wt.% after 23 days.

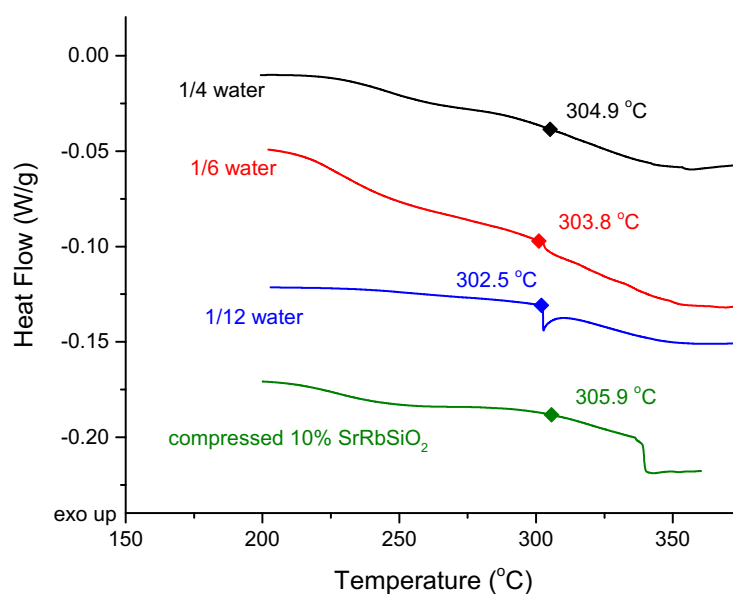


Figure 6.9 Effect of water concentration on T_g: DSC thermograms of samples made of 10 % SrRbSiO₂ with different mole ratios of water; 1/4 (black), 1/6 (red), 1/12 (blue). Compressed 10 % SrRbSiO₂ is used as a reference (green).

Since some water absorption is unavoidable for inorganic polymers, potential plasticization effects on inorganic polymer samples were investigated through a series of experiments. Water was intentionally added to 10 % SrRbSiO₂ glass and

compression molded at 150 °C under 1500 psi. The DSC thermograms in Figure 6.9 show the second heating curves of water added samples. The concentration of water in 10 % SrRbSiO₂ glass is increased up to 1/4 mole ratio and as a reference, pure 10 % SrRbSiO₂ glass is compression molded without addition of water. It is obvious from DSC thermograms that water has a plasticizing effect on silicate glass. However, it is important to note that water can only decrease the T_g up to a certain point. No matter how much of water is added to the system, T_g is only decreased to around 300 °C. It is also seen that T_g for the reference sample also decreases although no water was added. T_g for 10 % SrRbSiO₂ decreases from 373.1 °C to 305.9 °C when compression molded. This finding is associated with the effect of absorbed water by 10 % SrRbSiO₂ glass.

Table 6.2 T_g of samples made of 10 % SrRbSiO₂ and different concentrations of water.

Concentration of water (mol/mol)	Glass transition temperature (°C)
0	305.9
1/12	302.5
1/6	303.8
1/4	304.9

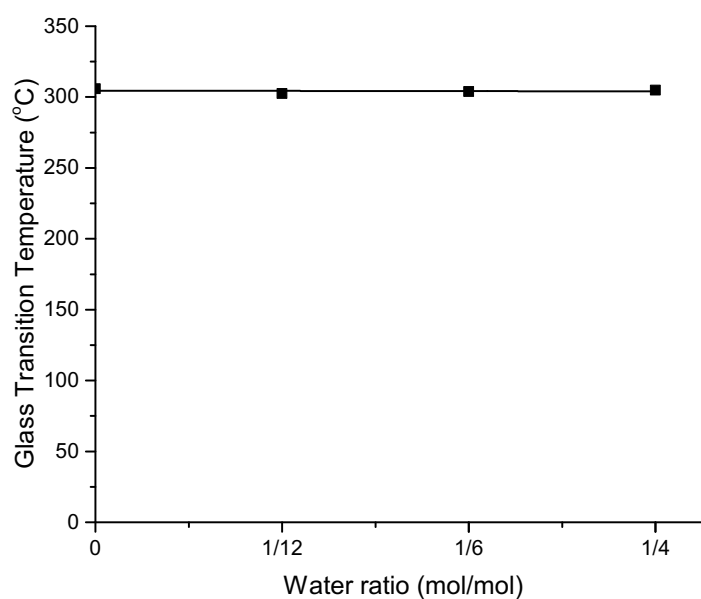


Figure 6.10 The change in T_g as a function of water concentration.

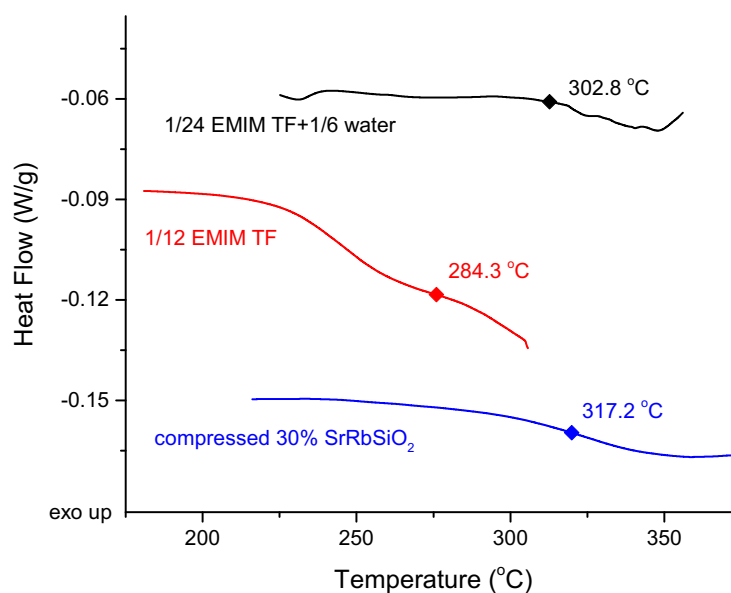


Figure 6.11 Effect of water and ionic liquid: DSC thermograms of inorganic polymers made of 30 % SrRbSiO₂ and 1/24 EMIM TF together with 1/6 water (black), 1/12 EMIM TF (red). Inorganic polymers are compared to the compressed 30 % SrRbSiO₂ glass as a reference.

To investigate the plasticization effect of water further, another series of experiments are conducted on 30 % SrRbSiO₂ glass mixed with different combinations of water and EMIM TF. First, pure 30 % SrRbSiO₂ glass is pressed at 150 °C under 1500 psi to be used as a reference. Note that pure glass could not be compression molded, but it is pressed at elevated temperatures to be used as a reference.

The T_g of heat-pressed 30 % SrRbSiO₂ is found to be 317.2 °C, as opposed to a T_g of pure 30 % SrRbSiO₂ glass whose T_g is higher than 450 °C (T_g could not be detected up to 450 °C). This drop in T_g is due to water absorbed by the modified silicate glass. 30 % SrRbSiO₂ is then mixed with 1/24 EMIM TF and 1/6 water. T_g of this system is found to be 302.8 °C. Considering the fact that the T_g is independent of water concentration, the additional 15 °C drop in T_g can be attributed to the effect of ionic liquid in the system. When prepared with higher concentrations of ionic liquid, T_g decreases further down to 244.7 °C for a molar ratio of 1/12. Thus, once again it is concluded that the T_g is independent of the concentration of water, and that, in the systems with ionic liquid, any T_g value below the reference T_g should be attributed to the contribution from ionic liquid. This shows that ionic liquid is a main plasticizer of modified silicate glasses.

6.3. Investigation of Reaction Mechanism via XPS

Our hypothesis for the formation of rubidium-triflate (RbTF) crystals is that, because the interaction between a divalent ion (Sr²⁺) and an NBO is stronger than the interaction between monovalent ion (Rb⁺) and an NBO, ionic liquid reacts easier with Rb⁺ ion and forms the crystal. Additionally, it is suggested that a reaction between the cation of the ionic liquid and the vicinal silanol of the silicate glass surface occurs [74-

76]. To test this hypothesis and understand the reaction mechanism, XPS measurement is conducted for the sample made of 30 % SrRbSiO₂ glass and 1/3 BMIM PF₆, compression molded at 150 °C and 1000 psi, along with the ionic liquid (BMIM PF₆) and 30 % SrRbSiO₂ glass as two references. High-resolution peaks are obtained by Gaussian curve fitting.

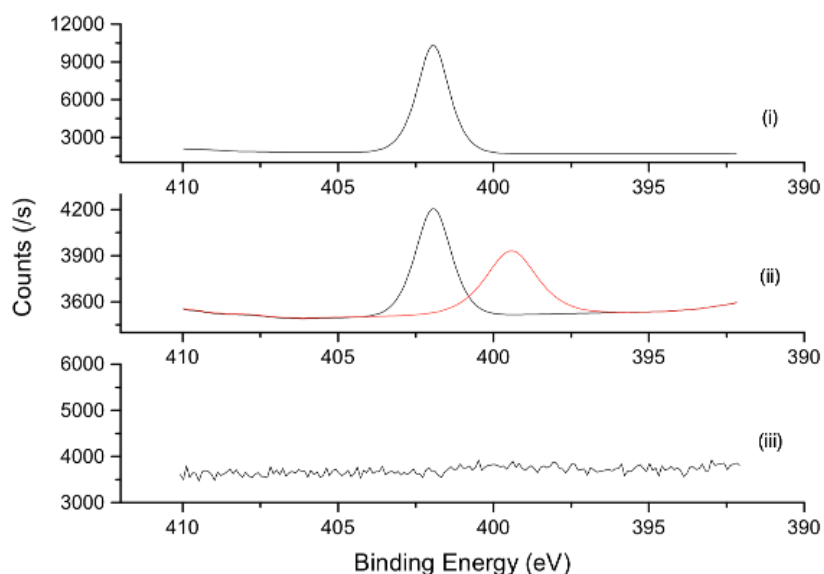


Figure 6.12 High-resolution XPS spectra at N1s orbital binding energy for: (i) BMIM PF₆; (ii) inorganic polymer made of 30 % SrRbSiO₂ glass and 1/3 BMIM PF₆ compression molded at 150 °C and 1000 psi; (iii) 30 % SrRbSiO₂ glass.

The purpose of the XPS measurement is to track the reaction occurring in the system. Figure 6.12 compares N1s orbital photoelectron spectra of the sample with two references. BMIM PF₆ shows a single peak at a binding energy of 401.98 eV (Figure 6.12 (i)), which corresponds to the single position of nitrogen in ionic liquid structure, i.e. imidazole ring. Because no nitrogen is present in the glass structure, 30 % SrRbSiO₂ glass does not show any peaks (Figure 6.12 (iii)), meaning any additional peaks in the inorganic polymer photoelectron spectrum should arise from the reaction between the imidazolium cation and the SrRbSiO₂ glass. Formation of a new peak is observed for

the photoelectron spectrum of inorganic polymer at a binding energy of 399.43 eV (Figure 6.12 (ii)). This supports the finding that ionic liquid and silicate glass interact with each other.

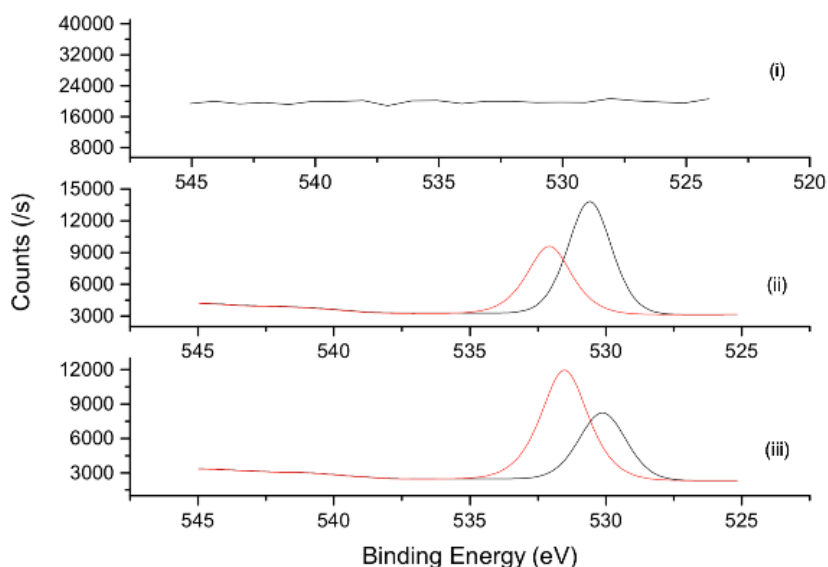


Figure 6.13 High-resolution XPS spectra at O1s orbital binding energy for: (i) BMIM PF₆; (ii) inorganic polymer made of 30 % SrRbSiO₂ glass and 1/3 BMIM PF₆, compression molded at 150 °C and 1000 psi; (iii) 30 % SrRbSiO₂ glass.

Figure 6.13 shows O1s orbital photoelectron spectra of the same system. As expected, with no oxygen in its structure, BMIM PF₆ does not show any peaks (Figure 6.13 (i)). 30 % SrRbSiO₂ shows two different peaks, each arising from NBOs and BOs present in the structure (Figure 6.13 (iii)). The binding energies for NBOs and BOs are 530.12 eV and 531.52 eV, respectively [77]. However, the most valuable observation is that, for inorganic polymer (Figure 6.13 (ii)), NBO and BO peaks change in intensities and shift to 530.59 eV and 532.08 eV, respectively. This supports the idea that a new structure is formed [77, 78].

6.4. Inorganic Polymers Aged in Desiccator

Some samples were left in a desiccator for a while after the initial failing attempt of molding. Figure 6.14 left shows bending of a specimen and Figure 6.14 middle shows fibril formation, both at temperatures above T_g . These samples are flexible above T_g and return to their glassy states at room temperature. Finally, Figure 6.14 right shows the flow of a sample: cylindrical shape is deformed due to flow under the gravitational field. These visual observations confirm that synthesized inorganic polymers possess properties similar to those of organic polymers.



Figure 6.14 Synthesized inorganic polymers showing characteristics of conventional polymers: bending (left), fibril formation (middle), and flow (right).

CONCLUSION

An overarching goal of this laboratory is to convert minerals, which are readily available in nature, directly into inorganic polymers with a minimum number of synthesis steps. This thesis work specifically focuses on plasticization of modified silicate glasses with known chemical structures with the aim to convert glasses to inorganic polymers. The experimental plan allows us to extract the information about the plasticization mechanism between Si-O bond and ionic liquid without any influence of other elements, which are commonly found in minerals (such as network-forming aluminum (Al^{3+})).

Results show that modified silicate glasses can be plasticized, i.e., processing temperature of silicate glass can be reduced significantly, by introduction of ionic liquid in the structure. Beginning with the already reduced T_g of alkali silicates, T_g is decreased by another 250 °C via addition of ionic liquids to enable these new materials to be fabricated by the methods commonly used for polymers. The small amount of ionic liquid used enables the materials to retain their inorganic character, while thermal and mechanical test results show that they possess properties closer to organic polymers rather than ceramics. Introduction of ionic liquid into the structure results in more ductile materials than ceramics.

Apart from thermal and mechanical analysis, spectroscopic measurements are conducted to gain knowledge on reaction mechanism. Based on the XRD data obtained, a plasticization mechanism of inorganic polymers is suggested. According to this model, the cation of ionic liquid attacks the NBOs and replaces the monovalent ions (in this case, K^+ or Rb^+). The monovalent ion may then react with the anion of ionic liquid. It is also suggested that, in the case of divalent/monovalent systems, ionic liquid can

attack the NBOs of divalent ions (in this case, Ca^{2+} or Sr^{2+}). The latter hypothesis is based on the DSC data obtained, in which divalent/monovalent system showed greater drop in T_g as compared to its monovalent counterpart. The suggested plasticization mechanism of silicate glasses is aimed to be confirmed with FTIR and XPS measurements. The interactions involving ionic liquid and silicate glass were generally confirmed by FTIR and XPS; however more systematic studies need to be conducted to elucidate the detailed plasticization mechanism.

Overall, the data shows that plasticization of silicate glasses with ionic liquids is highly promising to obtain inorganic polymers. It is an important step to prove that minerals, which are readily found in nature, could be converted to polymeric structures. This new class of inorganic polymers would overcome the disadvantages of its “relatives” (such as polysiloxanes and geopolymers) by retaining its inorganic character and exhibiting thermal and mechanical properties which are shifted towards those of conventional polymers from those of ceramics and glasses.

FUTURE WORK

This thesis has demonstrated that the idea of plasticization of minerals by ionic liquid is highly promising to synthesize inorganic polymers. Although significant advancement is achieved in the synthesis of these materials, there are still many problems to be resolved.

First, with the aim of improving the thermal analysis, Modulated Differential Scanning Calorimetry (MDSC) can be conducted. The advantage of MDSC is that T_g of a sample can be determined even when it is suppressed by melting or decomposition peaks. Overlapped phenomena (e.g., glass transition and melting/crystallization) can be separated with increased resolution. It is based on the same principle as DSC, except that a changing heating/cooling rate is applied on the sample. Non-constant heating/cooling rate helps to distinguish between the fast and slow responding phenomena [79].

Another problem to be overcome would be to decrease the affinity of inorganic polymers with water. Although switching from monovalent system to divalent/monovalent system suppressed the hygroscopic nature of inorganic polymers significantly, they still show poor mechanical properties as compared to their organic counterparts partly because of water absorbed. This problem could be solved by choosing better modifiers (alkali and alkaline earth ions) of silicate glass. Studies have shown that silicate glasses with lithium ions (Li^+) develop different behavior than those with sodium (Na^+) and potassium (K^+) ions. In general, presence of NBOs affects the BO strength [80, 81]. In the case of Li-silicate (LiSiO_2) glasses, the Si-O bond strength increases with increasing the amount of alkali ions, whereas it is the opposite for Na- and K-silicate glasses [46]. Strengthened Si-O-Si bonds allow the silicate structure to

possess properties closer to silica, while alkali modified regions (NBOs) show characteristics of silicate glasses. Thus, by switching to LiSiO_2 glasses, we can retain characteristics of both silica (such as high connectivity, which reduces hygroscopicity significantly) and silicate glasses (such as an open structure, which is highly reactive towards plasticization by ionic liquids).

The synthesis conditions can still be improved by conducting each step of synthesis in a glove box to eliminate the effect of water. In this way, ionic liquid can work with silicate glass more effectively and a more accurate analysis can be performed without considering the effect of water. In addition, the problem of opacity of inorganic polymers could be resolved by modifying the synthesis procedure. Now, samples are quenched from 180 °C to the room temperature when preset molding time is passed. To eliminate possible crystal formation, samples could be quenched to lower temperatures (e.g., ice water at 0 °C or dry ice at -79 °C). Hence, a sample with increased purity could be obtained, so that transparent samples may be synthesized.

Finally, a detailed FTIR analysis should be performed to gain better insights into plasticization mechanism at the molecular level. Raman spectroscopy may also be used to complement the FTIR analysis.

Appendix A

In this work, most of the samples were made by simple mixing. Simple mixing is the method by which silicate glass and ionic liquid are mixed using a mortar and pestle, followed by compression molding, as explained in section 3.2. However, near the end of the work, different mixing methods were also tried to improve properties of inorganic polymers.

Ball mixing set-up is shown in Figure A.1 left. This consists of a tumbler, 10 aluminum balls, a glove bag, and a nitrogen cylinder. The tumbler with the sample mixture (silicate glass and ionic liquid) was placed in the glove bag filled with nitrogen gas. The mixture of silicate glass and ionic liquid was mixed for 4 hours, followed by the standard procedure of compression molding. In this method, it was aimed to eliminate the effect of water absorption on sample properties during mixing.

Melt mixing, shown in Figure A.1 right, is the method by which silicate glass and the ionic liquid are mixed in a 2-neck round bottom flask with the help of a mechanical rotator. In this method, the species were heated to 150 °C in a mantle heater during mixing. The temperature was then kept constant at 150 °C for 10 minutes, followed by sample collection and standard procedure of compression molding.

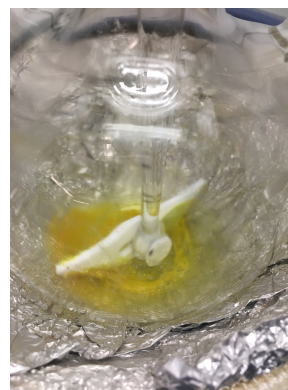


Figure A.1 Set-ups for ball mixing (left) and melt mixing (right).

In solution mixing, the silicate glass was first dissolved in water with a concentration of 0.1 g/mL and then mixed with ionic liquid. The solution was transferred into a petri dish for evaporation of water. The sample was compression molded after it was dried overnight in a vacuum oven.

Finally, precipitation mixing started with dissolution of silicate glass in water and addition of ionic liquid. Differently from solution mixing, the solution of silicate glass and ionic liquid was precipitated with methanol of a 1:20 solution to methanol ratio. The collected sample was dried in a vacuum oven and compression molded.

Figure A.2 gives the DSC thermograms for samples made of 5 % CaKSiO_2 and 1/10 mole ratio of EMIM TF. The samples were mixed by different methods, but not compression molded. As recognized, all mixing methods give similar thermal properties except the solution mixing method. This may be a result of Si-O bond breakage due to addition of water [54] for the sample made by solution mixing.

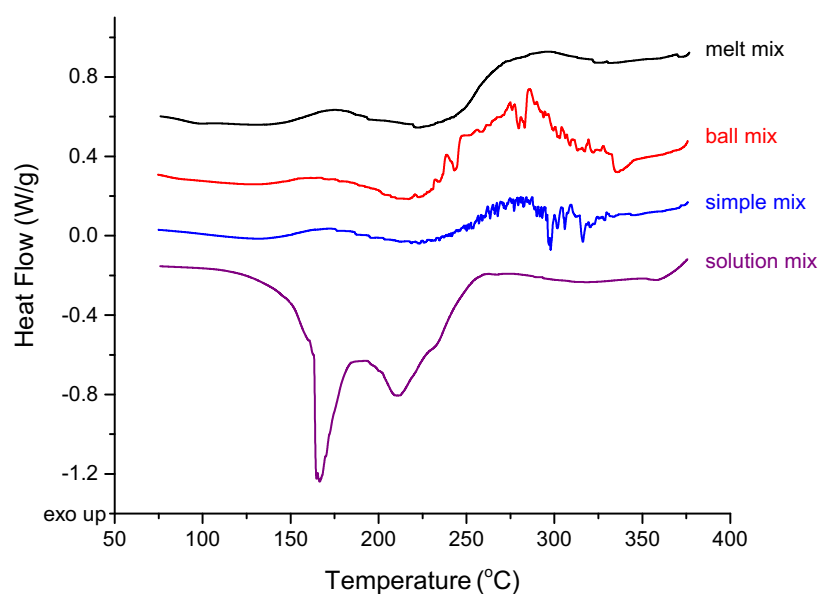


Figure A.2 Effect of mixing: DSC thermograms of samples made of 5 % CaKSiO_2 and 1/10 mole ratio of EMIM TF. The samples were prepared by different mixing methods, but not compression molded.

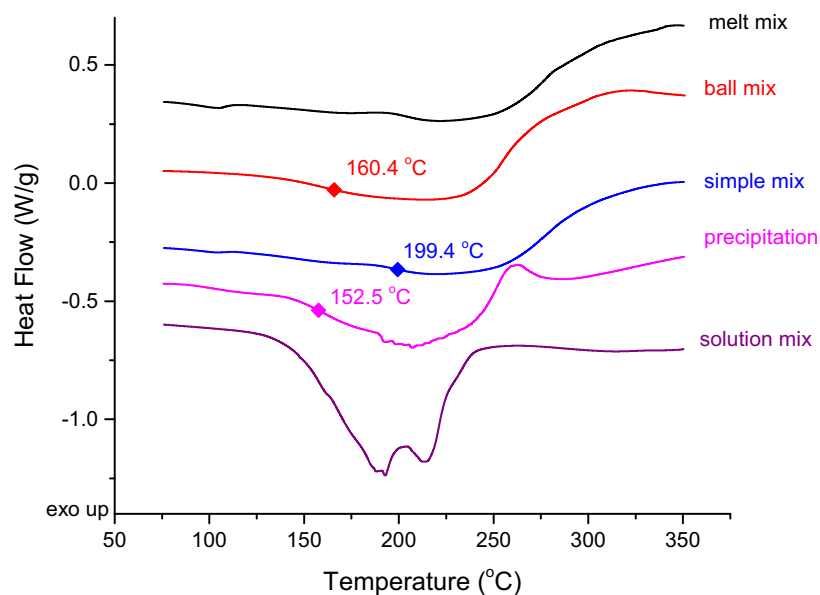


Figure A.3 Effect of mixing: DSC thermograms of samples made of 5 % CaKSiO_2 and 1/10 mole ratio of EMIM TF. The samples, prepared by different mixing methods, were compression molded at 180 °C and 1500 psi.

The DSC thermograms of the same samples, but with compression molding, are given in Figure A.3. Unlike the samples without compression molding, T_g points can be determined for some of the compression molded samples and some valuable observations are made. For example, the T_g values for samples made by simple and ball mixings are 199.4 °C and 160.4 °C, respectively. Based on this result and from physical appearances (Figure A.4 left and middle), it can be suggested that ball mixing produces more homogeneous samples with lower T_g as compared with simple mixing. Additionally, the lighter color of ball-mixed sample suggests that this sample is thermally more stable than simple-mixed sample. This may be a result of better incorporation of ionic liquid into the silicate glass structure. The darker color is usually observed when the ionic liquid is not retained in the glass structure and leaked out of the mold. It is also observed that ball-mixed samples can form a thin film, exhibiting characteristics of organic polymers (Figure A.4 right).

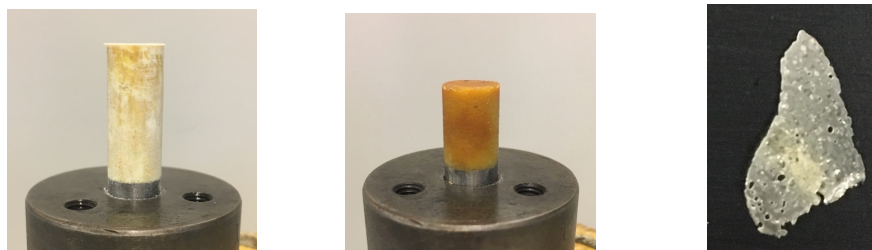


Figure A.4 Pictures of samples prepared by ball mixing (left) and simple mixing (middle). The samples are made of 5 % CaKSiO_2 and 1/10 mole ratio of EMIM TF. Ball-mixed sample showing thin film formation is given on the right.

Appendix B

A separate set of experiments were conducted where typical organic plasticizers were used to plasticize silicate glass. Commercially available sodium metasilicate glass (NaSiO_2) was plasticized with dioctyl phthalate (DOP), as shown in Figure B.1.

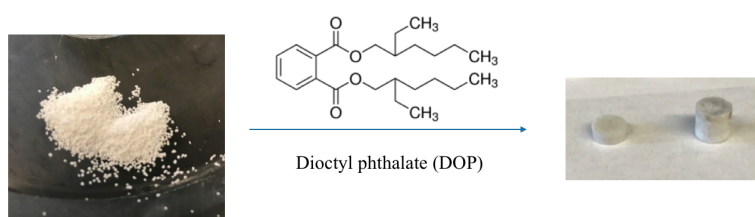


Figure B.1 Plasticization of NaSiO_2 with DOP. Pure NaSiO_2 is shown on the left and the compression molded sample is shown on the right.

The DSC thermograms of the samples made of NaSiO_2 and DOP are given in Figure B.2. As in the case of ionic liquids, DOP plasticized NaSiO_2 glasses. The T_g of NaSiO_2 dropped from $384.2\text{ }^\circ\text{C}$ to $307.3\text{ }^\circ\text{C}$ and $271.9\text{ }^\circ\text{C}$ with addition of 10 wt.% and 22 wt.% DOP.

In addition to NaSiO_2 , 5 % CaKSiO_2 glass was also plasticized with DOP. The DSC thermograms (Figure B.3) showed that the T_g of 5 % CaKSiO_2 glass dropped from $370.9\text{ }^\circ\text{C}$ to $222.5\text{ }^\circ\text{C}$, $216.7\text{ }^\circ\text{C}$, and $264.7\text{ }^\circ\text{C}$ with addition of 5 wt.%, 10 wt.%, and 20 wt.% DOP. Although it is expected that T_g value decreases with increasing the DOP concentration, 20 wt.% DOP shows the highest (not the lowest) T_g value. This anti-plasticization effect may be explained as follows. One possible explanation is based on the formation of Ca-containing bonds. Ca-containing system (i.e., 5 % CaKSiO_2 glass) showed the anti-plasticization effect, but Na-containing system (i.e., NaSiO_2 glass) did not. Ca ions are known to form coordination bonds with carboxylate groups [82]; thus,

Ca ions can form strong bonds with COO groups in DOP. Instead of replacing Ca ions with plasticizer (DOP), DOP may form coordination bonds with Ca ions that already form ionic bonds with silicates (through NBOs). If such bonding is formed between different molecules, resulting intermolecular bonds can strengthen the structure, which leads to higher T_g , as shown in this work. This occurs only at moderate concentrations of DOP (20 wt.%) where enough number of DOP molecules are dispersed such that intermolecular bonds can be formed.

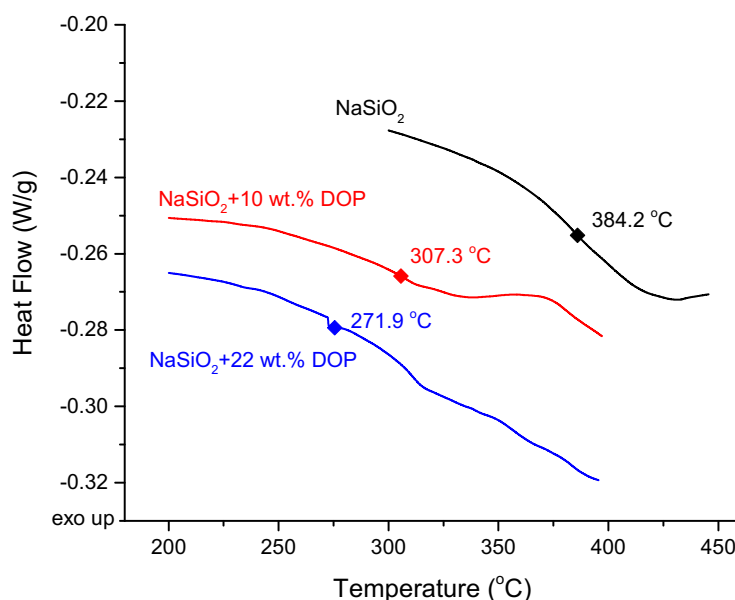


Figure B.2 DSC thermograms of NaSiO_2 glasses plasticized with 10 wt.% (red) and 22 wt.% (blue) DOP. DSC thermogram of NaSiO_2 glass is given as a reference (black).

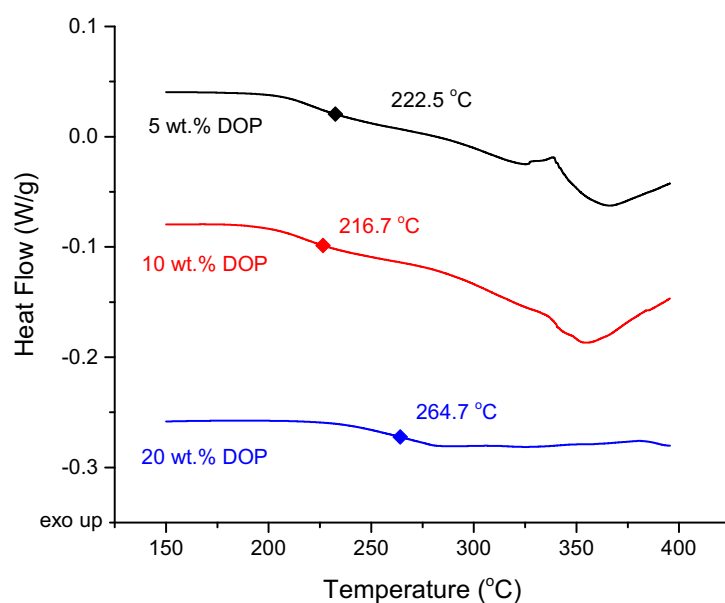


Figure B.3 DSC thermograms of samples made of 5 % CaKSiO₂ and 5 wt.% (black), 10 wt.% (red), and 20 wt.% (blue) DOP.

Additionally, it was concluded that DOP was not as effective as ionic liquids to plasticize the silicate glass. When ionic liquid was used as a plasticizer, the drop in T_g was greater than in the case of organic plasticizer (DOP). Because silicate have many ionic groups along the chain, their interactions with ionic groups of ionic liquid are preferable to their interactions with electric dipoles of DOP.

REFERENCES

1. Wulfsberg, G., *Inorganic chemistry*. 2000, Sausalito, Calif.: University Science Books. xix, 978 p.
2. House, J., *Inorganic Chemistry*. 2012, Academic Press Imprint, Elsevier Science & Technology Books.: San Diego. p. 848 pages.
3. Singh, D.N., *Basic Concepts of Inorganic Chemistry*. 2011: Pearson Education India.
4. Mark, J.E., H.R. Allcock, and R. West, *Inorganic Polymers*. 2005: Oxford University Press.
5. Welton, T., *Room-Temperature Ionic Liquids. Solvents for Synthesis and Catalysis*. Chemical Reviews, 1999. **99**(8): p. 2071-2084.
6. Plechkova, N.V. and K.R. Seddon, *Applications of ionic liquids in the chemical industry*. Chemical Society Reviews, 2008. **37**(1): p. 123-150.
7. Zhang, S., et al., *Structures and interactions of ionic liquids*. Vol. 151. 2013: Springer.
8. Shimano, S., H. Zhou, and I. Honma, *Preparation of nanohybrid solid-state electrolytes with liquidlike mobilities by solidifying ionic liquids with silica particles*. Chemistry of Materials, 2007. **19**(22): p. 5216-5221.
9. Néouze, M.-A., et al., *Ionogels, new materials arising from the confinement of ionic liquids within silica-derived networks*. Chemistry of Materials, 2006. **18**(17): p. 3931-3936.
10. Viau, L., et al., *Ionogels as drug delivery system: one-step sol-gel synthesis using imidazolium ibuprofenate ionic liquid*. Chemical Communications, 2010. **46**(2): p. 228-230.
11. Masanori Hara, R.L., *Inorganic Ionomers Made from Minerals*. Sep. 19, 2017.
12. Paul, A., *Chemistry of Glasses*. 2012: Springer Netherlands.
13. Höhne, G.W.H., W. Hemminger, and H.-J. Flammersheim, *Theoretical fundamentals of differential scanning calorimeters*, in *Differential Scanning Calorimetry*. 1996, Springer. p. 21-40.
14. Waseda, Y., E. Matsubara, and K. Shinoda, *X-ray diffraction crystallography: introduction, examples and solved problems*. 2011: Springer Science & Business Media.
15. Skoog, D.A., F.J. Holler, and T.A. Nieman, *Principles of instrumental analysis*. 1998, Philadelphia; Orlando, Fla.: Saunders College Pub. ; Harcourt Brace College Publishers.
16. Bower, D.I. and W.F. Maddams, *The Vibrational Spectroscopy of Polymers*. 1992: Cambridge University Press.
17. Kuo, J., *Electron Microscopy: Methods and Protocols*. 2007: Humana Press.
18. *ASTM Standard D695-15, 2015 "Standard test method for compressive properties of rigid plastics," ASTM International, West Conshohocken, PA, 2015, DOI: 10.1520/D0695-15, www.astm.org.*
19. Kinloch, A., *Young RJ, Fracture Behavior of Polymers*. Applied Science: London, 1983: p. 236.
20. Bonhote, P., et al., *Hydrophobic, highly conductive ambient-temperature molten salts*. Inorganic chemistry, 1996. **35**(5): p. 1168-1178.
21. Holbrey, J.D., et al., *Efficient, halide free synthesis of new, low cost ionic liquids: 1, 3-dialkylimidazolium salts containing methyl-and ethyl-sulfate anions*. Green Chemistry, 2002. **4**(5): p. 407-413.
22. Ngo, H.L., et al., *Thermal properties of imidazolium ionic liquids*. Thermochemica Acta, 2000. **357**: p. 97-102.
23. Huddleston, J.G., et al., *Characterization and comparison of hydrophilic and hydrophobic room temperature ionic liquids incorporating the imidazolium cation*. Green chemistry, 2001. **3**(4): p. 156-164.

24. Fernandez, A., et al., *Thermophysical properties of 1-ethyl-3-methylimidazolium ethylsulfate and 1-butyl-3-methylimidazolium methylsulfate ionic liquids*. Journal of Chemical & Engineering Data, 2007. **52**(5): p. 1979-1983.
25. Berthod, A. and S. Carda-Broch, *Uses of ionic liquids in analytical chemistry. reactions*, 2004. **1**: p. 6.
26. Vogel, W., N.J. Kreidl, and E. Lense, *Chemistry of glass*. 1985: American Ceramic Society.
27. Ashby, M.F. and D.R.H. Jones, *Engineering Materials 2: An Introduction to Microstructures, Processing and Design*. 2014: Elsevier Science.
28. Callister, W.D., *Materials Science And Engineering: An Introduction*. 2007: John Wiley & Sons.
29. Guloyan, Y.A., *Chemical Reactions Between Components in the Production of Glass-Forming Melt*. Glass and Ceramics, 2003. **60**(7): p. 233-235.
30. Avramov, I., T. Vassilev, and I. Penkov, *The glass transition temperature of silicate and borate glasses*. Journal of non-crystalline solids, 2005. **351**(6-7): p. 472-476.
31. Mysen, B.O. and P. Richet, *Silicate Glasses and Melts: Properties and Structure*. 2005: Elsevier Science.
32. Pauling, L., *General Chemistry*. 2014: Dover Publications.
33. Jones, D.R.H. and M.F. Ashby, *Engineering materials 2: an introduction to microstructures and processing*. 2012: Butterworth-Heinemann.
34. Thomas, L., *Interpreting unexpected events and transitions in DSC results*. Technical publication TA-039, TA Instruments, 2010.
35. Nesbitt, H.W., et al., *Bridging, non-bridging and free (O²⁻) oxygen in Na₂O-SiO₂ glasses: An X-ray Photoelectron Spectroscopic (XPS) and Nuclear Magnetic Resonance (NMR) study*. Journal of Non-Crystalline Solids, 2011. **357**(1): p. 170-180.
36. Bauer, H.H., G.D. Christian, and O.R. E., *Instrumental Analysis*. 1978, Boston, Massachusetts: Allyn and Bacon, Inc.
37. Willard, H.H., et al., *Instrumental methods of analysis*. 1988.
38. *TA Instruments (2012) Thermal Analysis Brochure*.
39. Ewing, G.W., *Instrumental Methods of Chemical Analysis*. 1985: McGraw-Hill.
40. Warren, B.E., *X-Ray Diffraction*. 2012: Dover Publications.
41. Khursheed, A., *Scanning Electron Microscope Optics and Spectrometers*. 2011: World Scientific.
42. Hawkes, P.W. and L. Reimer, *Scanning Electron Microscopy: Physics of Image Formation and Microanalysis*. 2013: Springer Berlin Heidelberg.
43. Chait, R., et al., *Compression Testing of Homogeneous Materials and Composites: A Symposium*. 1983: ASTM.
44. Platzer, N.A., *Plasticization and plasticizer processes*. 1965: American Chemical Society.
45. Fernandes, A.M., et al., *Evaluation of cation– anion interaction strength in ionic liquids*. The Journal of Physical Chemistry B, 2011. **115**(14): p. 4033-4041.
46. Ferraro, J.R. and M.H. Manghnani, *Infrared absorption spectra of sodium silicate glasses at high pressures*. Journal of Applied Physics, 1972. **43**(11): p. 4595-4599.
47. Ferraro, J.R., M.H. Manghnani, and L.J. Basile, *Infrared absorption spectra of lithium and potassium silicate glasses at high pressure*. Journal of Applied Physics, 1973. **44**(12): p. 5391-5396.
48. Jialiang, Y., *Further studies on the IR spectra of silicate glasses*. Journal of Non-Crystalline Solids, 1986. **84**(1-3): p. 114-119.
49. Serra, J., et al., *FTIR and XPS studies of bioactive silica based glasses*. Journal of Non-Crystalline Solids, 2003. **332**(1-3): p. 20-27.
50. VERWEIJ, H. and W.L. KONIJNENDIJK, *Structural Units in K₂O-PbO-SiO₂ Glasses by Raman Spectroscopy*. Journal of the American Ceramic Society, 1976. **59**(11-12): p. 517-521.
51. Akai, N., A. Kawai, and K. Shibuya, *Ion-pair structure of vaporized ionic liquid studied by matrix-isolation FTIR spectroscopy with DFT calculations: A case of 1-*

- ethyl-3-methylimidazolium trifluoromethanesulfonate*. The Journal of Physical Chemistry A, 2010. **114**(48): p. 12662-12666.
52. Singh, D.K., et al., *Molecular structure and interactions in the ionic liquid 1-ethyl-3-methylimidazolium trifluoromethanesulfonate*. The Journal of Physical Chemistry A, 2016. **120**(31): p. 6274-6286.
 53. Göbel, R., et al., *Surprisingly high, bulk liquid-like mobility of silica-confined ionic liquids*. Physical Chemistry Chemical Physics, 2009. **11**(19): p. 3653-3662.
 54. Bunker, B., *Molecular mechanisms for corrosion of silica and silicate glasses*. Journal of Non-Crystalline Solids, 1994. **179**: p. 300-308.
 55. Domańska, U. and A. Marciniak, *Solubility of 1-alkyl-3-methylimidazolium hexafluorophosphate in hydrocarbons*. Journal of Chemical & Engineering Data, 2003. **48**(3): p. 451-456.
 56. Shi, F. and Y. Deng, *Abnormal FT-IR and FTRaman spectra of ionic liquids confined in nano-porous silica gel*. Spectrochimica Acta Part A: Molecular and Biomolecular Spectroscopy, 2005. **62**(1-3): p. 239-244.
 57. Hiemenz, P.C. and T.P. Lodge, *Polymer Chemistry, Second Edition*. 2007: CRC Press.
 58. Eisenberg, A. and J.S. Kim, *Introduction to Ionomers*. 1998: Wiley.
 59. Ogura, K., H. Sobue, and S. Nakamura, *Infrared spectroscopic studies of polymer transitions. III. Effects of sodium ion on glass transitions in styrene-based ionomers*. Journal of Polymer Science: Polymer Physics Edition, 1973. **11**(10): p. 2079-2088.
 60. Zhang, B., D.A. Hoagland, and Z. Su, *Ionic Liquids as Plasticizers for Polyelectrolyte Complexes*. The Journal of Physical Chemistry B, 2015. **119**(8): p. 3603-3607.
 61. Nakai, K. and T. Yokoyama, *Uniaxial compressive response and constitutive modeling of selected polymers over a wide range of strain rates*. Journal of Dynamic Behavior of Materials, 2015. **1**(1): p. 15-27.
 62. Wilson, A. and S. Crisp, *Rigid highly carboxylated ionic polymers*. IN: *Ionic Polymers. L. Holiday*. 1975, Chapman and Hall, New York.
 63. Shen, J., et al., *Stress relaxation of a soda lime silicate glass below the glass transition temperature*. Journal of non-crystalline solids, 2003. **324**(3): p. 277-288.
 64. Hardjito, D. and B.V. Rangan, *Development and properties of low-calcium fly ash-based geopolymer concrete*. 2005.
 65. Kramer, E.J., *Microscopic and molecular fundamentals of crazing*, in *Crazing in polymers*. 1983, Springer. p. 1-56.
 66. Kramer, E.J. and L.L. Berger, *Fundamental processes of craze growth and fracture*, in *Crazing in Polymers Vol. 2*. 1990, Springer. p. 1-68.
 67. Hara, M. and P.Y. Jar, *Deformation and fracture of ionomers under simple tension. 1. Sulfonated polystyrene film from THF solution*. Macromolecules, 1988. **21**(11): p. 3187-3190.
 68. Ma, X., J. Sauer, and M. Hara, *Poly (methyl methacrylate) ionomers. 2. Deformation modes under simple tension*. Macromolecules, 1995. **28**(16): p. 5526-5534.
 69. Musić, S., N. Filipović-Vinceković, and L. Sekovanić, *Precipitation of amorphous SiO₂ particles and their properties*. Brazilian journal of chemical engineering, 2011. **28**(1): p. 89-94.
 70. Liu, Y., et al., *Immobilization and melting point depression of imidazolium ionic liquids on the surface of nano-SiO₂ particles*. Dalton Transactions, 2010. **39**(13): p. 3190-3194.
 71. Boccaccini, A.R., et al., *Sintering, crystallisation and biodegradation behaviour of Bioglass®-derived glass-ceramics*. Faraday discussions, 2007. **136**: p. 27-44.
 72. Tomozawa, M., et al., *Thermal properties of Na₂O-3SiO₂ glasses with high water content*. Journal of Non-Crystalline Solids, 1983. **56**(1): p. 343-348.
 73. Rudd, G.I., et al., *Atomic Force Microscopy and X-ray Photoelectron Spectroscopy Investigation of the Onset of Reactions on Alkali Silicate Glass Surfaces*. Journal of the American Ceramic Society, 1993. **76**(10): p. 2555-2560.
 74. Brinker, C.J., et al., *Surface structure and chemistry of high surface area silica gels*. Journal of Non-Crystalline Solids, 1990. **120**(1): p. 26-33.

75. Palacio, M. and B. Bhushan, *A review of ionic liquids for green molecular lubrication in nanotechnology*. Tribology Letters, 2010. **40**(2): p. 247-268.
76. Amarasekara, A.S. and O.S. Owereh, *Synthesis of a sulfonic acid functionalized acidic ionic liquid modified silica catalyst and applications in the hydrolysis of cellulose*. Catalysis Communications, 2010. **11**(13): p. 1072-1075.
77. Sawyer, R., H. Nesbitt, and R. Secco, *High resolution X-ray Photoelectron Spectroscopy (XPS) study of K₂O–SiO₂ glasses: Evidence for three types of O and at least two types of Si*. Journal of Non-Crystalline Solids, 2012. **358**(2): p. 290-302.
78. Sharma, A., H. Jain, and A. Miller, *Surface modification of a silicate glass during XPS experiments*. Surface and Interface Analysis: An International Journal devoted to the development and application of techniques for the analysis of surfaces, interfaces and thin films, 2001. **31**(5): p. 369-374.
79. Reading, M., A. Luget, and R. Wilson, *Modulated differential scanning calorimetry*. Thermochimica Acta, 1994. **238**: p. 295-307.
80. Smets, B. and T. Lommen, *Incorporation of aluminum oxide and boron oxide in sodium silicate glasses, studied by X-ray photoelectron spectroscopy*. Physics and Chemistry of Glasses, 1981. **22**: p. 158-62.
81. Bruckner, R., H.-U. Chun, and H. Goretzki, *Photoelectron spectroscopy (ESCA) on alkali silicate-and soda aluminosilicate glasses*. Glastechn. Ber, 1978. **51**(1): p. 1-7.
82. Einspahr, H. and C.E. Bugg, *The geometry of calcium carboxylate interactions in crystalline complexes*. Acta Crystallographica Section B, 1981. **37**(5): p. 1044-1052.